UNIVERSITY OF CALIFORNIA, MERCED

Assessments of Biofuel Sustainability: Air Pollution and Health Impacts

DISSERTATION

submitted in partial satisfaction of the requirements
for the degree of

DOCTOR OF PHILOSOPHY

in Environmental Systems

by

Chi-Chung Tsao

Dissertation Committee:
Associate Professor Carlos Coimbra, Chair
Assistant Professor Elliott Campbell
Associate Professor Yihsu Chen
Assistant Professor Marcelo Mena

2012

DEDICATION

To

my father, Ho-Fen Tsao

I will never finish a degree without his encouragements and endless love.

TABLE OF CONTENTS

LIST OF FIGURES

LIST OF TABLES

ACKNOWLEDGMENTS

CURRICULUM VITAE

Chi-Chung Tsao

1998	B.S. in Environmental Engineering, National Cheng Kung University, Tainan, Taiwan
2000	M.S. in Environmental Engineering, National Cheng Kung University, Tainan, Taiwan
2000-02	Mandatory military service, Ministry of National Defense, Taiwan
2002-06	Associate Researcher, Industrial Technology Research Institute, Hsinchu, Taiwan
2008	M.S. in Environmental Science, Policy and Management, Lund University, Lund, Sweden
2008-10	Teaching Assistant, School of Engineering, University of California, Merced, USA
2008-12	Research Assistant, School of Engineering, University of California, Merced, USA
2012	Ph.D. in Environmental Systems, University of California, Merced, USA

FIELD OF STUDY

Sustainable energy, Energy and Environmental Policy Analysis, Air Quality Management

PUBLICATIONS

1. **C.-C. Tsao**, J.E. Campbell, M. Mena-Carrasco, S.N. Spak, G.R. Carmichael and Y. Chen (2012) "Increased estimates of air pollution emissions from Brazilian sugarcane ethanol," Nature Climate Change, 2, (1): 53-57; DOI 10.1038/nclimate1325.
2. **C.-C. Tsao**, J.E. Campbell, and Y. Chen (2011) "When renewable portfolio standards meet cap-and-trade regulations in the electricity sector: Market interactions, profits implications, and policy redundancy," *Energy Policy*, 39(7): 3966-3974; DOI 10.1016/j.enpol.2011.01.030.
3. Marcelo Mena-Carrasco, Estefania Oliva, Pablo Saide, Scott Spak, Cristóbal de la Maza, Mauricio Osses, Sebastián Tolvett, J. Elliott Campbell, **Chi-Chung Tsao**, Luisa T. Molina (2012) "Estimating the health benefits from natural gas use in transport and heating in Santiago, Chile," *Science of the Total Environment*, 429: 257-265.

ABSTRACT OF THE DISSERTATION

Assessments of Biofuel Sustainability: Air Pollution and Health Impacts

By

Chi-Chung Tsao

Doctor of Philosophy in Environmental Systems

University of California, Merced, 2012

Professor Carlos Coimbra, Chair

Accelerating biofuel production has been promoted as an opportunity to enhance energy security, offset greenhouse gas emissions and support rural economies. However, large uncertainties remain in the impacts of biofuels, particularly, on air quality and human health. Sugarcane ethanol is one of the most widely used biofuels, and Brazil is its largest producer. Here a systematic framework, including emission modeling, air quality simulation, and health impact assessment was developed to quantify direct and indirect air-pollution and health impacts throughout the life-cycle of Brazilian biofuel. It was found Brazilian biofuel with dominant effects of pre-harvesting burning and indirect land-use change has increasing life-cycle emissions (non-GHG) due to expanding sugarcane areas. Current satellite-based approaches may not account for sugarcane burning emissions due to the small scale of these fires relative to satellite resolution and assumptions regarding fuel loadings. Results also suggest that Brazilian ethanol would cause greater health impacts than US conventional gasoline and cellulosic ethanol if current practices of sugarcane harvesting and land-use change management remain. Effective controls of deforestation, better management of pre-harvesting burning practices, and utilization

of agricultural residues, e.g. sugarcane trash and bagasse, would be possible solutions to improve air quality. However, the cost and the maturity of technologies might be the issues. The research framework may assist the future determination on the sustainability of other advanced fuels.

Chapter 1 Introduction

1.1 Background

Since the industrial revolution, the demand of energy has continued to grow due to a boost of production and consumption. The rapid increases of energy use accelerate the depletion of fossil fuel resources and accompany with degraded environment. In particular, burning fossil fuels with consequences of dominant greenhouse gas (GHG) emissions would influence global and regional climate that might damage ecological systems and human economy. Searching for economically feasible, clean, and renewable energy sources becomes desperate.

In recent decades, governments over the world encourage the use of renewable energy through measures including economic instruments and the development of innovative technology. Economic instruments, a common policy tool, are usually applied to level the playing field of less polluting-intensive pathways, like renewable energy, by either direct subsidy or tax on polluting resources such as conventional fossil energy. For example, Renewable Portfolio Standard (RPS), which requires a certain percentage of electricity to be generated from renewable sources, is established to expedite the market penetration of renewable generation. Emission trading (or cap-and-trade) is a market-based approach which encourages the reduction of GHG emissions by providing economic incentives to facilities with green production or using clean energy (e.g. renewable). Further analysis of policy implications for RPS and cap-and-trade regulations refers to Appendix A.

Scientists and engineers have explored methods to extract energy from renewable resources through different pathways and applications. Currently, eight major types of renewable resources including geothermal, tides, waves, ocean currents, hydropower, solar radiation, wind, and biomass, are applied in various energy-conversions with outputs like electricity or transportation liquid fuels [1]. However, economic and environmental impacts from innovative pathways and applications of renewable resources in a large scale have not been thoroughly examined. Detailed examination on the sustainability issues and potential effects is essential.

Biomass energy as one of renewable energy sources have been developed in recent decades in order to enhance energy security, mitigate global warming due to excessive greenhouse gases (GHGs) emissions by fossil fuels, and support rural economies [2-5]. One of several pathways is to convert energy from biomass photosynthesis into liquid biofuels. Several types of liquid biofuels, such as biodiesel, ethanol, biogas, biomenthanol, bio-dimethylether, could be broadly used as vehicle fuels. Currently, ethanol produced from various biomass sources through hydrolysis and fermentation processes is the most widely used biofuel. The demand and supply of bio-ethanol are projected to grow due to current market penetration of flexible fuel vehicles (FFVs) and a mandatory blend of biofuels. Ethanol from sugarcane in Brazil may provide higher annual life-cycle GHG reductions than other conventional biofuels. However, land use impacts may result in greater life-cycle GHG emissions for biofuels than for fossil fuels [6, 7].

Ethanol production and combustion has significant impacts on air pollution [8-11]. Niven [11] concludes that the use of E10 may result in greater tropospheric ozone pollution, and lead to greater air toxicity due to high evaporative losses relative to gasoline. Hill et al. [9] monetize the life-cycle health effects of fine particulate matter emissions (PM2.5) and found that corn ethanol has higher health costs than gasoline while cellulosic ethanol may reduce costs. Jacobson [10] further examines the health consequences due to a large-scale conversion from gasoline to E85, and finds enhanced health risks due to increased tropospheric ozone concentration resulting from vehicle emissions. These studies imply not only the importance of the air pollution from biofuels, but the consideration of spatial or temporal analysis for future research on biofuels sustainability.

Brazilian sugarcane ethanol has potentially large life-cycle air pollution emissions [12]. The cradle-to-grave life-cycle of sugarcane ethanol includes cultivation, transportation to refinery plants, refinery processes, product distribution, and fuel use phases [12, 13]. Sugarcane cultivation requires a tropical or subtropical climate, and can be planted up to twice a year [14]. During the cultivation phase, pesticides and fertilizers are the essential input, and exhaust from farming machines also appears in this phase. Before harvesting, farmers burn sugarcane crops to reduce the amount of leafy extraneous material, including stalk tops [14-16]. Sugarcane field burning might remove soil organic matter, resulting in a change of soil structure, increased soil erosion [16], and considerable air pollution. To mitigate the air impacts, some regional governments, e.g. the Sao Paulo State government, have started to encourage local farmers to gradually end practices of pre-harvesting burning [13].

Air pollution from Brazilian sugarcane has been investigated by several studies. Ometto et al. examine environmental impacts of fuel ethanol from sugarcane in Brazil through life-cycle assessment (LCA), and find contributions to photochemical-ozone-formation and greenhouse gas emissions associated with harvesting [12]. Pozza et al. [17] confirmed significant PM10 and PM2.5 emissions associated with the burning of sugarcane by detecting significant amounts of Cl and K, the tracers of sugarcane foliage burning, in samples of PM10 and PM2.5. Goldemberg et al. [16] indicate that besides air emissions from the burning phase such as CO, VOC and PM, the smog from burning also impacts the operation of railway and highway systems. Analysis of nitrogen compounds in the ambient air and dissolved organic carbon (DOC) of rainwater, suggests significant air pollution during harvest season [18, 19]. For the refinery phase, Turn et al. profile the emissions of ethanol refinery boilers using different types of fuel including coal, fuel oil, bagasse, and fiber cane, and indicate that cofiring high-moisture biomass with fossil fuels can produce higher emissions when compared with firing coal alone [20].

Direct and indirect land-use changes (LUC) due to a large-scale expansion of sugarcane croplands may also cause significant air pollution. Air pollution emissions from LUC are due to open burning practices for land clearing, e.g. slash-and-burn [21]. Recent analyses of global biomass burning found that deforestation and degradation fire are the dominant sources of biomass burning emissions in South America [22]. These land clearing emissions continue to grow rapidly because deforestation (cropland and rangeland expansion) has shifted towards areas with higher biomass density in Amazonia [23]. However, burning practices are not limited to deforestation. In the Brazilian

Amazon area, local farmers use fires as a conventional and cost-effective way to remove aboveground biomass on Cerrado savanna to prepare land for agricultural use [24, 25].

Exposure to air pollution causing health impacts during harvesting season in Brazil is another issue which has been widely discussed. Polycyclic Aromatic Hydrocarbons (PAHs), a carcinogen, emitted along with PM emission from the burning phase have significant health impacts [26-28]. Health risks such as respiratory disease, e.g. asthma, caused by air pollution are also addressed in several epidemiological studies [15, 29-33]. Arbex et al. found that an increase of 11.6% in asthma hospital admissions in São Paulo State from 2003 to 2004 was associated with an increase in the total suspended particle concentration due to sugarcane harvesting [15].

Air pollution, which largely depends on spatial and temporal varying emissions, is a crucial issue to biofuel sustainability, particularly sugarcane ethanol. LCA studies have indicated the importance of spatial and temporal variation in the evaluation of environmental burdens including air and health impacts [34-37]. Brazil is a potential target to evaluate air pollution impacts because it is the largest producer of sugarcane ethanol and may rapidly expand production to meet the energy demand of developed countries [38, 39]. Although many studies discuss the air pollution from each life-cycle phase of biofuel, rare studies evaluate its overall air pollution impacts with the consideration of spatial and temporal variation. This dissertation aims to provide an appropriate framework to examine air pollution impacts and better understand biofuel sustainability.

1.2 Overview and Objectives

The objective of this study is to access the information of biofuels sustainability, particularly air pollution and health impacts. In this dissertation, I use a Brazilian case to answer a research question: How might the increase in production, distribution, and use of biofuels affect air pollution and human health? The hypothesis of my study is that an increase in production, distribution, and use of Brazilian sugarcane ethanol exacerbate air pollution and health impacts in central-southern Brazil. I applied a systematic framework including various models to answer this research question in this dissertation. In Chapter 2, I established a spatially and temporally explicit emission model for the entire life-cycle phases of Brazilian sugarcane ethanol. In Chapter 3, I further examined indirect effects of land-use change due to the future expansion of sugarcane cropland from incremental biofuels supply. In Chapter 4, I applied emissions models established in previous chapters and integrate air quality simulation and health risk assessment to access the human health impacts of air emissions from Brazilian sugarcane ethanol.

1.3 Summary of Contributions

As the worldwide demand and supply of biofuels grow rapidly, significant air pollution emissions from all phases in the life-cycle would potentially affect the air quality. The public has increasing concerns on assessments of biofuel sustainability. Identifying spatial and temporal variation of those emissions also becomes an essential task to manage the air quality and determine potential health risks. Brazil, as the largest ethanol producer in the world, has been indicated in many studies that significant air pollution and associated health impacts occurs during the life-cycle phases of sugarcane ethanol. However, most studies are unable to explicit quantifies spatially and temporally specific air emissions and potential health impacts. This study aims to establish an appropriate method to estimate spatially and temporally explicit life-cycle emissions of sugarcane ethanol including LUC phase, and analyze its spatial and temporal variation. Later, by using these spatially and temporally emission data, a health risk assessment is conducted to determine the health impacts due to the expansion of ethanol production and consumption in Brazil. The outcome of this study assists to access the effects of incremental Brazilian sugarcane ethanol on air pollution and health impacts, and provide an insight on the sustainability of sugarcane ethanol. The outcome also benefits USEPA for the policy analysis on future Renewable Fuel Standard (RFS).

Reference

1. Hoffert, M. I.; Caldeira, K.; Benford, G.; Criswell, D. R.; Green, C.; Herzog, H.; Jain, A. K.; Kheshgi, H. S.; Lackner, K. S.; Lewis, J. S.; Lightfoot, H. D.; Manheimer, W.; Mankins, J. C.; Mauel, M. E.; Perkins, L. J.; Schlesinger, M. E.; Volk, T.; Wigley, T. M. L., Advanced technology paths to global climate stability: Energy for a greenhouse planet. *Science* 2002, *298*, (5595), 981-987.
2. Farrell, A. E.; Plevin, R. J.; Turner, B. T.; Jones, A. D.; O'Hare, M.; Kammen, D. M., Ethanol can contribute to energy and environmental goals. *Science* 2006, *311*, (5760), 506-508.
3. Hill, J.; Nelson, E.; Tilman, D.; Polasky, S.; Tiffany, D., Environmental, economic, and energetic costs and benefits of biodiesel and ethanol biofuels. *Proc. Natl. Acad. Sci. U. S. A.* 2006, *103*, (30), 11206-11210.
4. Schneider, U. A.; McCarl, B. A., Economic potential of biomass based fuels for greenhouse gas emission mitigation. *Environ. Resour. Econ.* 2003, *24*, (4), 291-312.
5. Sheehan, J.; Aden, A.; Paustian, K.; Killian, K.; Brenner, J.; Walsh, M.; Nelson, R., Energy and environmental aspects of using corn stover for fuel ethanol. *Journal of Industrial Ecology* 2003, *7*, (3-4), 117-146.
6. Fargione, J.; Hill, J.; Tilman, D.; Polasky, S.; Hawthorne, P., Land clearing and the biofuel carbon debt. *Science* 2008, *319*, (5867), 1235-1238.
7. Searchinger, T.; Heimlich, R.; Houghton, R. A.; Dong, F. X.; Elobeid, A.; Fabiosa, J.; Tokgoz, S.; Hayes, D.; Yu, T. H., Use of US croplands for biofuels increases greenhouse gases through emissions from land-use change. *Science* 2008, *319*, (5867), 1238-1240.
8. *Renewable Fuel Standard Program (RFS2) Regulatory Impact Analysis*; EPA-420-R-10-006; USEPA: 2010; p 1119.
9. Hill, J.; Polasky, S.; Nelson, E.; Tilman, D.; Huo, H.; Ludwig, L.; Neumann, J.; Zheng, H. C.; Bonta, D., Climate change and health costs of air emissions from biofuels and gasoline. *Proc. Natl. Acad. Sci. U. S. A.* 2009, *106*, (6), 2077-2082.
10. Jacobson, M. Z., Effects of ethanol (E85) versus gasoline vehicles on cancer and mortality in the United States. *Environmental Science & Technology* 2007, *41*, (11), 4150-4157.
11. Niven, R. K., Ethanol in gasoline: environmental impacts and sustainability review article. *Renewable & Sustainable Energy Reviews* 2005, *9*, (6), 535-555.
12. Ometto, A. R.; Hauschild, M. Z.; Roma, W. N. L., Lifecycle assessment of fuel ethanol from sugarcane in Brazil. *International Journal of Life Cycle Assessment* 2009, *14*, (3), 236-247.
13. Macedo, I. C.; Seabra, J. E. A.; Silva, J., Green house gases emissions in the production and use of ethanol from sugarcane in Brazil: The 2005/2006 averages and a prediction for 2020. *Biomass & Bioenergy* 2008, *32*, (7), 582-595.

14. Yadava, R. L., *Agronomy of Sugarcane : Principles and Practice* 1st ed.; International Book Distributing Co., Publishing Division: Lucknow, U.P., India, 1993; p 375.

15. Arbex, M. A.; Martins, L. C.; de Oliveira, R. C.; Pereira, L. A. A.; Arbex, F. F.; Cancado, J. E. D.; Saldiva, P. H. N.; Braga, A. L. F., Air pollution from biomass burning and asthma hospital admissions in a sugar cane plantation area in Brazil. *Journal of Epidemiology and Community Health* 2007, *61*, (5), 395-400.

16. Goldemberg, J.; Coelho, S. T.; Guardabassi, P., The sustainability of ethanol production from sugarcane. *Energy Policy* 2008, *36*, (6), 2086-2097.

17. Pozza, S. A.; Bruno, R. L.; Tazinassi, M. G.; Goncalves, J. A. S.; Do Nascimento, V. F.; Barrozo, M. A. S.; Coury, J. R., Sources of particulate matter: emission profile of biomass burning. *International Journal of Environment and Pollution* 2009, *36*, (1-3), 276-286.

18. Coelho, C. H.; Francisco, J. G.; Nogueira, R. F. P.; Campos, M., Dissolved organic carbon in rainwater from areas heavily impacted by sugar cane burning. *Atmospheric Environment* 2008, *42*, (30), 7115-7121.

19. Machado, C. M. D.; Cardoso, A. A.; Allen, A. G., Atmospheric emission of reactive nitrogen during biofuel ethanol production. *Environmental Science & Technology* 2008, *42*, (2), 381-385.

20. Turn, S. Q.; Jenkins, B. M.; Jakeway, L. A.; Blevins, L. G.; Williams, R. B.; Rubenstein, G.; Kinoshita, C. M., Test results from sugar cane bagasse and high fiber cane co-fired with fossil fuels. *Biomass & Bioenergy* 2006, *30*, (6), 565-574.

21. Ward, D. E.; Susott, R. A.; Kauffman, J. B.; Babbitt, R. E.; Cummings, D. L.; Dias, B.; Holben, B. N.; Kaufman, Y. J.; Rasmussen, R. A.; Setzer, A. W., Smoke and fire characteristics for cerrado and deforestation burns in Brazil - Base-B experiment. *J. Geophys. Res.-Atmos.* 1992, *97*, (D13), 14601-14619.

22. van der Werf, G. R.; Randerson, J. T.; Giglio, L.; Collatz, G. J.; Mu, M.; Kasibhatla, P. S.; Morton, D. C.; DeFries, R. S.; Jin, Y.; van Leeuwen, T. T., Global fire emissions and the contribution of deforestation, savanna, forest, agricultural, and peat fires (1997-2009). *Atmos. Chem. Phys.* 2010, *10*, (23), 11707-11735.

23. Loarie, S. R.; Asner, G. P.; Field, C. B., Boosted carbon emissions from Amazon deforestation. *Geophysical Research Letters* 2009, *36*, (14), L14810 (5 pp.)-L14810 (5 pp.).

24. Carvalho, J. L. N.; Cerri, C. E. P.; Feigl, B. J.; Piccolo, M. D.; Godinho, V. D.; Herpin, U.; Cerri, C. C., Conversion of cerrado into agricultural land in the south-western amazon: Carbon stocks and soil fertility. *Sci. Agric.* 2009, *66*, (2), 233-241.

25. Levine, J. S.; Cofer, W. R.; Cahoon, D. R.; Winstead, E. L., Biomass burning - A driver for global change. *Environmental Science & Technology* 1995, *29*, (3), A120-A125.

26. Mazzoli-Rocha, F.; Magalhaes, C. B.; Malm, O.; Saldiva, P. H. N.; Zin, W. A.; Faffe, D. S., Comparative respiratory toxicity of particles produced by traffic and sugar cane burning. *Environmental Research* 2008, *108*, (1), 35-41.

27. Tfouni, S. A. V.; De Souza, N. G.; Neto, M. B.; Loredo, I. S. D.; Leme, F. M.; Furlani, R. P. Z., Polycyclic aromatic hydrocarbons in sugar cane juice from the city of Ribeirao Preto-SP, Brazil. *Toxicology Letters* 2008, *180*, S75-S75.

28. Umbuzeiro, G. D.; Franco, A.; Magalhaes, D.; de Castro, F. J. V.; Kummrow, F.; Rech, C. M.; de Carvalho, L. R. F.; Vasconcellos, P. D., A preliminary characterization of the mutagenicity of atmospheric particulate matter collected during sugar cane harvesting using the Salmonella/microsome microsuspension assay. *Environmental and Molecular Mutagenesis* 2008, *49*, (4), 249-255.

29. Allen, A. G.; Cardoso, A. A.; da Rocha, G. O., Influence of sugar cane burning on aerosol soluble ion composition in Southeastern Brazil. *Atmospheric Environment* 2004, *38*, (30), 5025-5038.

30. Arbex, M. A.; Bohm, G. M.; Saldiva, P. H. N.; Conceicao, G. M. S.; Pope, A. C.; Braga, A. L. F., Assessment of the effects of sugar cane plantation burning on daily counts of inhalation therapy. *Journal of the Air & Waste Management Association* 2000, *50*, (10), 1745-1749.

31. Cancado, J. E.; Saldiva, P. H. N.; Pereira, L. A. A.; Lara, L.; Artaxo, P.; Martinelli, L. A.; Arbex, M. A.; Zanobetti, A.; Braga, A. L. F., The impact of sugar cane-burning emissions on the respiratory system of children and the elderly. *Environmental Health Perspectives* 2006, *114*, (5), 725-729.

32. Ribeiro, H., Sugar cane burning in Brazil: respiratory health effects. *Revista De Saude Publica* 2008, *42*, (2).

33. Uriarte, M.; Yackulic, C. B.; Cooper, T.; Flynn, D.; Cortes, M.; Crk, T.; Cullman, G.; McGinty, M.; Sircely, J., Expansion of sugarcane production in Sao Paulo, Brazil: Implications for fire occurrence and respiratory health. *Agriculture Ecosystems & Environment* 2009, *132*, (1-2), 48-56.

34. de Haes, H. A. U.; Heijungs, R.; Suh, S.; Huppes, G., Three strategies to overcome the limitations of life-cycle assessment. *Journal of Industrial Ecology* 2004, *8*, (3), 19-32.

35. Owens, J. W., Life-cycle assessment in relation to risk assessment: An evolving perspective. *Risk Analysis* 1997, *17*, (3), 359-365.

36. Ross, S.; Evans, D., Excluding site-specific data from the LCA inventory: How this affects Life Cycle impact Assessment. *International Journal of Life Cycle Assessment* 2002, *7*, (3), 141-150.

37. Yellishetty, M.; Ranjith, P. G.; Tharumarajah, A.; Bhosale, S., Life cycle assessment in the minerals and metals sector: a critical review of selected issues and challenges. *International Journal of Life Cycle Assessment* 2009, *14*, (3), 257-267.

38. 2008 World Fuel Ethanol Production. http://www.ethanolrfa.org/industry/statistics/#C (Dec. 1),
39. International Trade Statistics 2009. In World Trade Organization: Geneva, Switzerland, 2009.

Chapter 2 Life-cycle Emissions of Brazilian Ethanol

2.1 Introduction

Bioenergy resources have been developed in recent decades in order to enhance energy security, offset the greenhouse gas (GHG) emissions from fossil fuels, and support rural economies [1-3]. Several types of biofuels, such as biodiesel, ethanol, biogas, menthanol, and bio-dimethylether, could be broadly used as vehicle fuels. Currently, ethanol produced from various biomass sources through fermentation processes is the most widely used biofuel, and its demand and supply are projected to grow. Ethanol from sugarcane in Brazil may provide higher annual life-cycle GHG reductions than other conventional biofuels [4]. However, land use impacts may result in greater life-cycle GHG emissions for biofuels than for fossil fuels [5-7].

Biofuel production and combustion can also have significant impacts on air pollution [8-11]. The relative impact of ethanol and gasoline on mobile vehicle emissions (evaporative and exhaust) are debatable with the potential for ethanol to increase ozone levels [11]. The health consequences of mobile emissions due to a large-scale conversion from gasoline to E85 may result in enhanced health risks due to increased tropospheric ozone concentrations resulting from E85 vehicle emissions [10]. Monetizing the health impacts of life-cycle ethanol emissions (fuel production and vehicle emissions) of fine particulate matter emissions ($PM_{2.5}$) suggests that corn ethanol has higher health costs than gasoline while cellulosic ethanol may reduce costs [9]. These studies imply not only the importance of the air pollution from biofuels, but the consideration of spatial and

temporal analysis of emissions for future research on biofuels sustainability, as this is relevant to estimate exposure, and consequently health effects.

Brazilian sugarcane ethanol has potentially large life-cycle air pollution emissions [12]. The cradle-to-grave life-cycle of sugarcane ethanol includes cultivation, transportation to refinery plants, refinery processes, product distribution, and fuel use phases [12, 13]. During the cultivation phase, pesticides and fertilizers are the essential inputs, and exhaust from farming machines also appears in this phase. Before harvesting, many farmers burn sugarcane crops [14-16], resulting in a loss of soil organic matter, change in the soil structure, increase in soil erosion, and enhancement of atmospheric emissions [15]. To mitigate the air impacts, some regional governments, e.g. the São Paulo State government, have started to encourage local farmers to gradually end sugarcane pre-harvesting burning [17].

Air pollution from Brazilian sugarcane has been investigated by several studies. Ometto et al. examine environmental impacts of sugarcane ethanol in Brazil through life-cycle assessment (LCA), and find contributions to photochemical-ozone-formation and greenhouse gas emissions associated with harvesting [12]. Pozza et al. confirmed significant PM_{10} and $PM_{2.5}$ emissions associated with the burning of sugarcane by detecting significant amounts of Cl and K, the tracers of sugarcane foliage burning in samples of PM_{10} and $PM_{2.5}$ [18]. Goldemberg et al. indicate that besides air emissions from the burning phase such as carbon monoxide (CO), volatile organic compounds (VOC), and particulate matter (PM), the smog from burning also impacts the operation of railway and highway conditions [15]. Analysis of nitrogen compounds in the ambient air

and dissolved organic carbon (DOC) of rainwater, suggests significant air pollution during the harvest season [19, 20]. For the refinery phase, Turn et al. profile the emissions of ethanol refinery boilers using different types of fuel including coal, fuel oil, bagasse, and fiber cane, and indicate that co-firing high-moisture biomass with fossil fuels can produce higher emissions when compared with firing coal alone [21].

Exposure to air pollution during the harvesting season in Brazil is another issue which has been widely discussed. Polycyclic Aromatic Hydrocarbons (PAHs), which are carcinogenic, emitted along with PM emission from the burning phase have significant health impacts [22-24]. Health risks such as respiratory disease caused by air pollution are also addressed in several epidemiological studies [14, 25-29]. Arbex et al. found that an increase of 11.6% in asthma hospital admissions in São Paulo State from 2003 to 2004 was associated with an increase in the total suspended particle concentrations due to sugarcane harvesting [14].

Air pollution, which largely depends on spatial and temporal varying emissions, is a crucial issue to sugarcane ethanol sustainability. It is sometimes overseen or oversimplified in other studies because of its complexity. LCA studies have indicated the importance of spatial and temporal variation in the evaluation of environmental burdens including air and health impacts [30-33]. Brazil is a potential target to evaluate air pollution impacts because it is the largest producer of sugarcane ethanol and may rapidly expand production to meet the energy demand of developed countries [34, 35]. Herein, spatially and temporally explicit emissions from the life-cycle of sugarcane ethanol in Brazil are estimated using agriculture survey data, emissions factors, and life-cycle

assessment of the farming, field burning, refinery, transportation and distribution, and vehicle use phases. Burning phase results are of particular importance given the high magnitude of this phase in the overall life-cycle and these emissions are compared with remote sensing approaches to estimating biomass burning emissions [36, 37].

2.2 Methodology

Spatially and temporally explicit emissions from Brazilian sugarcane ethanol were estimated by integrating emission factors and activity rates associated with emissions in different life-cycle phases. The emissions, $E_{i,s,m}$, of regulated pollutant i at location s during the month m is determined by aggregating the emissions from p phases, where p represents farming ($p=f$), field burning ($p=b$), refinery ($p=r$), and transportation/distribution (T/D) ($p=t$) as follows,

$$E_{i,s,m} = \sum_p E_p = \sum_p \left(A_{s,p} \times MAF_{m,p} \times AR \times EF_{i,p} \right), \ \forall p = f, b, r, t \qquad (1)$$

where $A_{s,p}$ is the activity rate associated with emissions at location s in phase p including sugarcane production and ethanol production. $MAF_{m,p}$ represents the monthly allocation factor which converts annual emissions to a monthly basis. It is derived from the monthly intensity of emission activities for each phase, i.e. the monthly ratio of cultivation, harvest, ethanol production, distributed ethanol, or ethanol consumption. AR is the fraction of sugarcane production used for producing ethanol since not all sugarcane crops in Brazil contribute to ethanol production (e.g. around 60% of sugarcane crops were converted into ethanol products in 2008) [38]. $EF_{i,p}$ is the emission factor of pollutant i in the phase p.

In the farming and field burning phases, $MAF_{m,f}$ is the monthly cultivation ratio of sugarcane crops, which is calculated by dividing the average sugarcane harvest in the next ten months by the total production due to the average 10-month-growth period of sugarcane. The monthly quantity of sugarcane harvested and crushed in Brazil is obtained from the USDA FAS [38]. The activities of the burning and refinery phases follow the

same temporal scaling. $MAF_{m,t}$, the monthly ratio of ethanol distributed, is assumed to be evenly allocated over the 12 months in a year due to year-round demand.

Since activity rates in the above four phases are associated with spatially explicit sugarcane production, the estimation of life-cycle emissions can be further expressed by the following formula:

$$E_{i,s,m} = \sum_p \left[(Y_s \times CA_s \times CF_p) \times MAF_{m,p} \times AR \times EF_{i,p} \right], \ \forall\, p = f, b, r, t \quad (2)$$

where Y_s represents the spatial dataset of annual sugarcane yield (MT/ha·yr), CA_s denotes the sugarcane crop area (ha) at location *s*, and CF_p denotes conversion factors (24 gal ethanol/MT sugarcane). The sugarcane crop area, CA_s, is determined by the fraction of cropland in a grid cell (ha cropland / ha grid cell) and the area of a grid cell. Monfreda et al. [39] produced datasets of global cropland in 2000 including yield (MT sugarcane/ha cropland/y) and the fraction of cropland (ha cropland / ha grid cell) by spatially disaggregating agricultural inventory data at the political unit level and redistributing to grid cells in relation to remotely sensed land cover (resolution 5 arcmin × 5 arcmin). Given the expansion of sugarcane production from 2000 to 2008, we scale the production data for the year 2000 to the more recent production year based on state-level data. The sugarcane production in São Paulo state has increased by 81% from 2000 to 2008 due to an increase in area and yield [38]. We evaluate this assumption by comparing our map of sugarcane production with a map of sugarcane production based on 2008 Landsat data [40].

Emission factors ($EF_{i,p}$) of 6 regulated air pollutants in each phase of the sugarcane ethanol life-cycle are obtained from the Greenhouse Gases, Regulated Emissions, and Energy Use in Transportation (GREET) model [41].The formulation of emission factors (per Mg sugarcane yield) for the field burning phase in the GREET model are based on emission factors of biomass burning (per kg dried matter burned) synthesized from IPCC and Andreae et al.'s work, and the estimation of sugarcane residue yield in an official report of sugarcane ethanol assessment prepared for Brazilian government [42]. The residue yield is 0.140 Mg dried matter of trash per Mg sugarcane produced with 80% of cane burned (resulting in 0.112 Mg dried matter burned per Mg sugarcane). Mechanized harvesting of sugarcane in São Paulo state has allowed for a reduction in burning. Both agriculture survey data and Landsat studies for São Paulo state suggest that the use of burning as a management practice has been reduced to 50% of sugarcane cropland area in 2008 [4, 40]. We apply the survey data for the burning practice rates in São Paulo state and assume 100% of the areas are burned in other states.

While the focus of this study is on production phase emissions, we also develop a simple vehicle phase emission estimate. It is assumed that the spatial distribution of ethanol consumption for vehicles follows the distribution of population in Brazil, and ethanol is evenly consumed within 12 months in a year. Although distributing vehicle emissions by population is a rough first approximation, this approach has been found to be useful in previous air quality studies of the region [43]. The vehicle emission factors are taken from GREET and the spatial distribution of population is obtained from LandScan, a global population database with a 30 arcsec × 30 arcsec resolution which is available for 2008 conditions [44].

We compare the field burning emissions estimated from our approach with global inventories of biomass burning emissions. The Global Fire Emissions Database version (GFEDv2.1) provides open biomass burning emissions at a global scale by combining 500m MODIS burned areas, the Carnegie-Ames-Stanford Approach (CASA) biogeochemical model, and emissions factors [37, 45]. The 1° x 1° gridded, 8-day time step, fire emissions are available from 1999 to 2008 (GFEFv2) [46] and at a monthly time step in a more recent release (GFEDv3.1) [37]. Wiedinmyer et al. applied a related approach of integrating fuel loadings and MODIS fire observations to estimate fire emission in the Fire INventory from NCAR (FINN) [36],[47]. FINN uses 1-km daily fire data identified by the MODIS Thermal Anomalies product. Except burned area data, another important difference between those two studies is the data sources used for fuel loadings and combustion completeness. The GFED approach estimates fuel loadings as a function of the net primary production modeled by the CASA biogeochemical model and the value of combustion completeness is determined by fuel types. Wiedinmyer et al. assign the value of fuel loading for each grid cell by combining the Global Land Cover Dataset for 2000 (GLC2000), the MODIS Vegetation Continuous Field (VCF), and the Fuel Characteristic Classification System (FCCS).

2.3 Results

The estimated life-cycle emissions per unit energy of sugarcane ethanol produced are shown in Figure 2.1, together with life-cycle emissions from conventional gasoline and diesel. The field burning phase is the dominant source of emissions for all species except SO_X. In São Paulo state, the occurrence of burning is thought to have been reduced to half of the sugarcane cropland areas which results in NO_X and SO_X emissions from field burning that are the same order of magnitude as the emissions from the other life-cycle stages while the field burning emissions remain dominant for the other species. In contrast to air pollution emissions, there has been extensive work on estimating life-cycle CO_2 emissions from Brazilian ethanol and the GREET results for CO_2 emissions are shown in Figure 2.1 for comparison.

State-level estimates are shown for 2008 in Table 2.1. Over 40% of the total emissions from biofuels in Brazil occur in São Paulo state. The life-cycle emissions of ethanol in Brazil for crop years 2000 through 2008 are shown in Figure 2.2. Despite reductions in burned area in São Paulo state, the emissions increase in time due to the increased production. Emissions estimates for each life-cycle phase for São Paulo state are shown in Table 2.2. The majority of pollution, i.e. VOC, PM_{10}, $PM_{2.5}$, and CO, occurs during the sugarcane burning phase while most of the SO_X emissions are from the T/D phase.

That spatial variation of these emissions is shown in Figure 2.3 for São Paulo state in January and July, 2008. Concentrated emissions appear near the central region and northern border of São Paulo state due to the high utilization of land for sugarcane

crops in these areas. Emissions of VOC and PM also exhibit high levels of emissions in July. This seasonal variation is associated with the temporal pattern of sugarcane cultivation and harvest, with the peak occurring in July. Figure 2.4 exhibits the emissions by life-cycle phases, and the dominant contribution of emissions is from the sugarcane burning phase.

Next, we compare our estimates of sugarcane field burning with satellite fire detection approaches (GFED and FINN) to estimating biomass burning emissions in the region. This comparison is done for São Paulo state because the GFED and FINN approaches integrate burning from all sources which requires that we compare our sugarcane burning emissions in a region where sugarcane field burning is the dominant source of biomass burning. The emissions for $PM_{2.5}$ for the years 2000 through 2008 are shown for GFEDv2.1, GFEDv3.1, and our approach in Figure 2.5. The satellite-based approaches might be thought to lead to larger emissions than our approach because the GFED emissions include all sources of biomass burning (e.g. forest, cropland, savannah, pastures etc.) in addition to sugarcane burning. However, our emissions in this study are on average 7.3 times the GFEDv2.1 emissions, 1.5 times the GFEDv3.1 total emissions, 3.6 times the GFEDv3.1_Ag (calculated by the burning fraction for agriculture land only), and 3.1 times the FINN emissions. This suggests that sugar cane emissions are underestimated in these widely used burning databases.

The low emissions for the satellite-based approach are in part due to burnt area estimates that are low relative to the area estimates in this study (Table 2.3). One limitation of the GFEDv2.1 approach is that burned area was estimated indirectly by a

regression tree relationship between fire hot spots and burned area [37]. The larger areas in GFEDv3.1 relative to GFEDv2.1 represent an improvement where 90% of the areas were mapped directly from 500 meter MODIS burned area data rather than the regression tree relationship. The GFEDv3.1 burned areas are still only 33% of our estimates 2008 (Table 2.3). The subset of GFEDv3.1 areas on agriculture lands are not reported, but these would be even smaller. The FINN areas are also not reported but may be similar to GFEDv3.1 areas as a similar MODIS-based approach was taken. The top-down underestimate of burned areas in the region may be due to the small size of the sugarcane fires relative to the 500 m resolution for MODIS burned areas used in GFEDv3.1 [48]. However, high resolution remote sensing of burned areas using Landsat has identified sugarcane burning in São Paulo state that is within 13% of our estimate [40].

While the GFEDv3.1 approach has relatively small burned areas, the average fuel loading and average emissions factors are relatively high compared to our approach (Table 2.3). The fuel loadings are likely larger because the GFEDv3.1 land cover map indicates that only 38% of the burned areas in São Paulo state occurred on agriculture land while the rest of the emissions occurred on other lands such as forests that may have high fuel loadings and emissions factors relative to agriculture burning [42].

Some similarities are observed between the temporal and spatial variability of the satellite and life-cycle approaches, suggesting a relationship of drivers between the sugarcane burning from our inventory and the large-scale burning from the top-down approaches. The inter-annual variability of the GFEDv3.1 and our approaches is somewhat consistent as suggested by an r-squared value of 0.67 between the annual

$PM_{2.5}$ emissions for the GFEDv3.1 and our emissions. All emissions estimates in Figure 2.5 show positive trends over the 2000 to 2008 period with regression slopes that are 3%, 6%, and 7% of the average emissions for ours, GFEDv2.1, and GFEDv3.1, respectively. The seasonal variation for all methods have emissions concentrated during the harvesting season, though our emissions have a longer burning season that extends from May to November (Figure 2.6). These peak emissions during the harvest season are consistent with analysis of Advance Very High Resolution Radiometer (AVHRR) fire spot detection for the region and field air quality measurements [49]. The spatial variability is shown in Figures 2.7 for burned areas and in Figure 2.8 for $PM_{2.5}$ emissions. The burned area maps have some similarities with widespread burning in the north-central region where sugarcane is concentrated. The spatial distribution of differences between our and satellite-based emission estimates is largest in the regions of largest sugarcane production due to the overall differences in magnitude of the approaches. However, several anomalous differences are observed for FINN in the southern extent of the domain and for GFEDv3.1 in western São Paulo which may be due to satellite detection of fires that are not sugarcane related (Figure 2.9).

While the FINN burned areas are not specified, the fuel loadings can be compared for the different approaches. The FINN loadings were fixed at 0.5 kg m^{-2} for croplands based on a literature review of agriculture burning while the GFED and our emissions are based on spatially and temporally varying estimates of biomass availability. The average fuel loading in this study is 1.1 kg $m^{-2,}$ more than double the FINN loading, which may reflect the high yields of sugarcane relative to other crops.

Table 2.1: State-level life-cycle emission of ethanol in Brazil, 2008 (Unit: MT yr^{-1})

State	VOC	NO_X	PM_{10}	$PM_{2.5}$	SO_X	CO	CO_2	BC	OC	COS
ACRE	106	87	18	9	1	2,321	229,284	0	0	0
RONDONIA	303	238	122	61	11	5,977	539,784	10	49	1
AMAZONAS	778	608	333	166	31	15,177	1,354,648	29	140	3
PARÁ	1,636	1,279	693	346	64	31,991	2,861,294	61	290	6
TOCANTINS	236	189	77	39	7	4,836	451,353	5	26	1
MARANHÃ O	2,434	1,758	1,930	957	196	39,459	2,809,833	220	1,053	21
PIAUÍ	1,061	776	779	386	78	17,762	1,325,044	87	416	8
CEARÁ	1,403	1,141	317	161	24	29,940	2,899,503	12	57	1
R. G. NORTE	2,505	1,720	2,547	1,260	264	35,537	1,989,515	308	1,472	29
PARAIBA	4,314	2,920	4,653	2,301	485	58,821	3,001,191	569	2,719	54
PERNAMBUCO	13,365	8,969	14,891	7,363	1,555	177,905	8,529,385	1,831	8,755	172
ALAGOAS	17,773	11,700	21,210	10,483	2,225	223,840	9,076,521	2,638	12,617	249
SERGIPE	1,473	1,016	1,470	727	152	21,160	1,216,025	177	846	17
BAHIA	3,888	2,928	2,349	1,168	231	69,694	5,671,979	246	1,174	23
MINAS GERAIS	30,003	20,139	33,389	16,509	3,487	399,715	19,208,958	4,104	19,626	387
ESPIRITO SANTO	3,310	2,255	3,474	1,719	361	45,992	2,455,915	422	2,020	40
RIO DE JANEIRO	5,040	3,717	3,528	1,751	354	85,963	6,574,114	388	1,857	37
SÃ O PAULO	124,383	112,396	156,221	76,555	22,434	1,512,931	91,561,414	16,726	79,994	1,576
PARANÁ	30,034	19,913	34,962	17,282	3,662	386,210	16,753,412	4,331	20,711	408
SANTA CATARINA	950	782	159	82	10	20,773	2,052,291	0	0	0
R. G. SUL	1,733	1,415	362	184	27	37,255	3,629,456	10	50	1
MATO GROSSO	10,134	6,702	11,901	5,883	1,247	129,358	5,483,574	1,476	7,061	139
MATO GROSSO DO SUL	11,815	7,784	14,057	6,948	1,475	149,175	6,101,183	1,748	8,358	165
GOIÁ S	19,971	13,276	23,032	11,386	2,411	258,767	11,487,701	2,848	13,623	268
Brazil (Total)	288,645	223,707	332,472	163,727	40,794	3,760,558	207,263,378	38,245	182,913	3,603

Table 2.2: Summary of emissions and emission ratio from 5 life-cycle phases for São Paulo State, 2008 (Unit: MT yr^{-1})

Unit	Farming		Field Burning		Refinery		T/D		Vehicle		Life-cycle
VOC	2,293	(1.8%)	101,204	(81.4%)	13,384	(10.8%)	1,055	(0.8%)	6,448	(5.2%)	124,383
NO_X	15,449	(13.7%)	36,144	(32.2%)	31,724	(28.2%)	23,772	(21.2%)	5,307	(4.7%)	112,396
PM_{10}	1,466	(0.9%)	112,769	(72.2%)	40,151	(25.7%)	753	(0.5%)	1,081	(0.7%)	156,221
$PM_{2.5}$	744	(1.0%)	56,388	(73.7%)	18,341	(24.0%)	527	(0.7%)	555	(0.7%)	76,555
SO_X	3,676	(16.4%)	5,786	(25.8%)	1,487	(6.6%)	11,415	(50.9%)	69	(0.3%)	22,434
CO	5,577	(0.4%)	1,330,114	(87.9%)	31,724	(2.1%)	4,483	(0.3%)	141,033	(9.3%)	1,512,931

Table 2.3: Comparison of $PM_{2.5}$ emission in 2008, total burned area, and fuel loading in São Paulo state among GFEDv2.1, GFEDv3.1, GFEDv3.1_Ag, FINN, and our approach.

Item	This study[a]	GFEDv2.1	GFEDv3.1	GFEDv3.1_Ag	FINN
Emission (MT yr^{-1})	100,857	16,894	87,703	38,595	32,457
Burned area (ha)	2,222,638	341,682	746,316	NA	NA
Fuel load (MT dm yr^{-1})	25,859,274	3,428,936	12,697,708	4,678,169	NA
Avg. EF (g kg^{-1} dm)[b]	3.9	4.9	6.9	8.3	NA
Avg. fuel load (MT dm ha^{-1} yr^{-1})[c]	11.0	10.0	17.0	NA	NA

[a] Burned area for the our approach is obtained from São Paulo harvest areas for sugarcane cropland areas and then multiplied by the burned fraction (2005, 75%; 2006, 70%; 2007, 70%; 2008, 50%) [40].

[b] The average emission factor is calculated by dividing $PM_{2.5}$ emission by fuel load

[c] The average fuel load is calculated by dividing fuel load by burned area

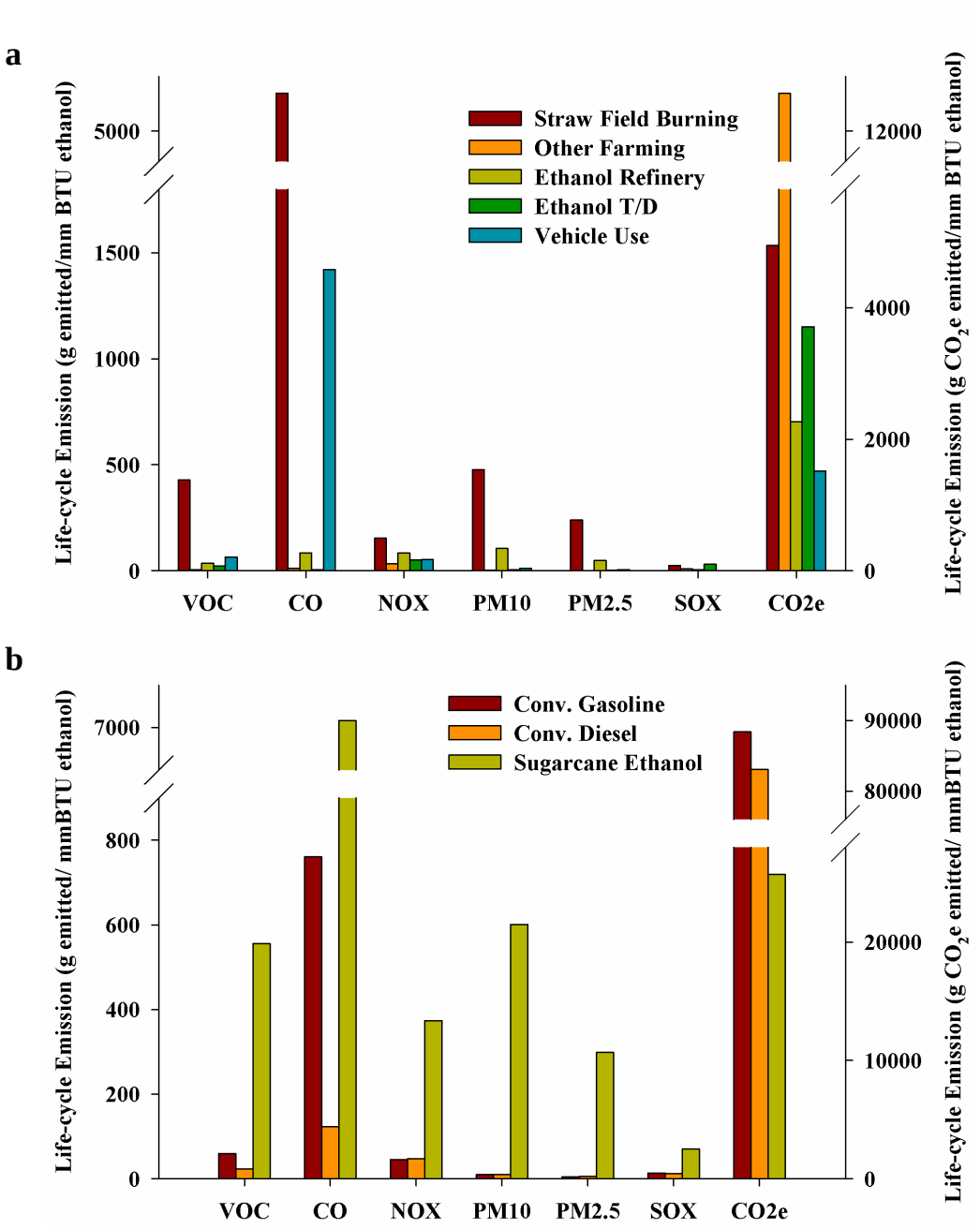

Figure 2.1: Comparisons of life-cycle emissions for sugarcane ethanol in Brazil and conventional liquid fuels. (a) Life-cycle emissions per unit energy of sugarcane ethanol produced within five life-cycle phases. Although our life-cycle emissions account for a mix of sugarcane fields where the burning practice is used and not used, the burning-phase emissions shown here are for ethanol produced from croplands that are burned. (b) Comparisons of life-cycle emissions for conventional gasoline, diesel, and sugarcane ethanol. Estimates from the GREET model include six air pollutants (VOC, CO, NO_X, PM_{10}, $PM_{2.5}$, and SO_X) and GHGs (as CO_2 equivalent, CO_2e). Right axis is for GHG emissions.

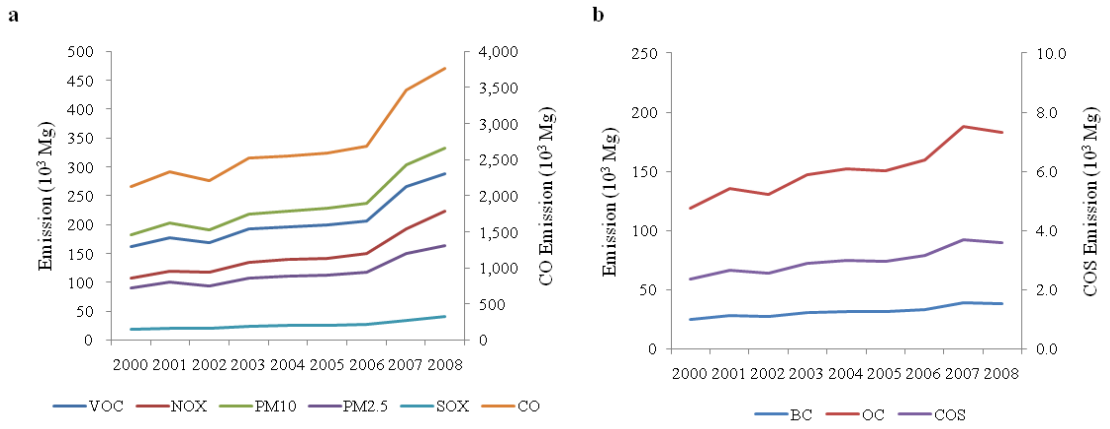

Figure 2.2: Estimated life-cycle emissions of ethanol in Brazil from crop year 2000 through 2008 (crop year is from April to January next year). (a) emissions of VOC, NO_X, PM_{10}, $PM_{2.5}$ SO_X, and CO; (b) emissions of black carbon (BC), organic carbon (OC), and carbonyl sulfide (COS) which are estimated only for the field burning phase.

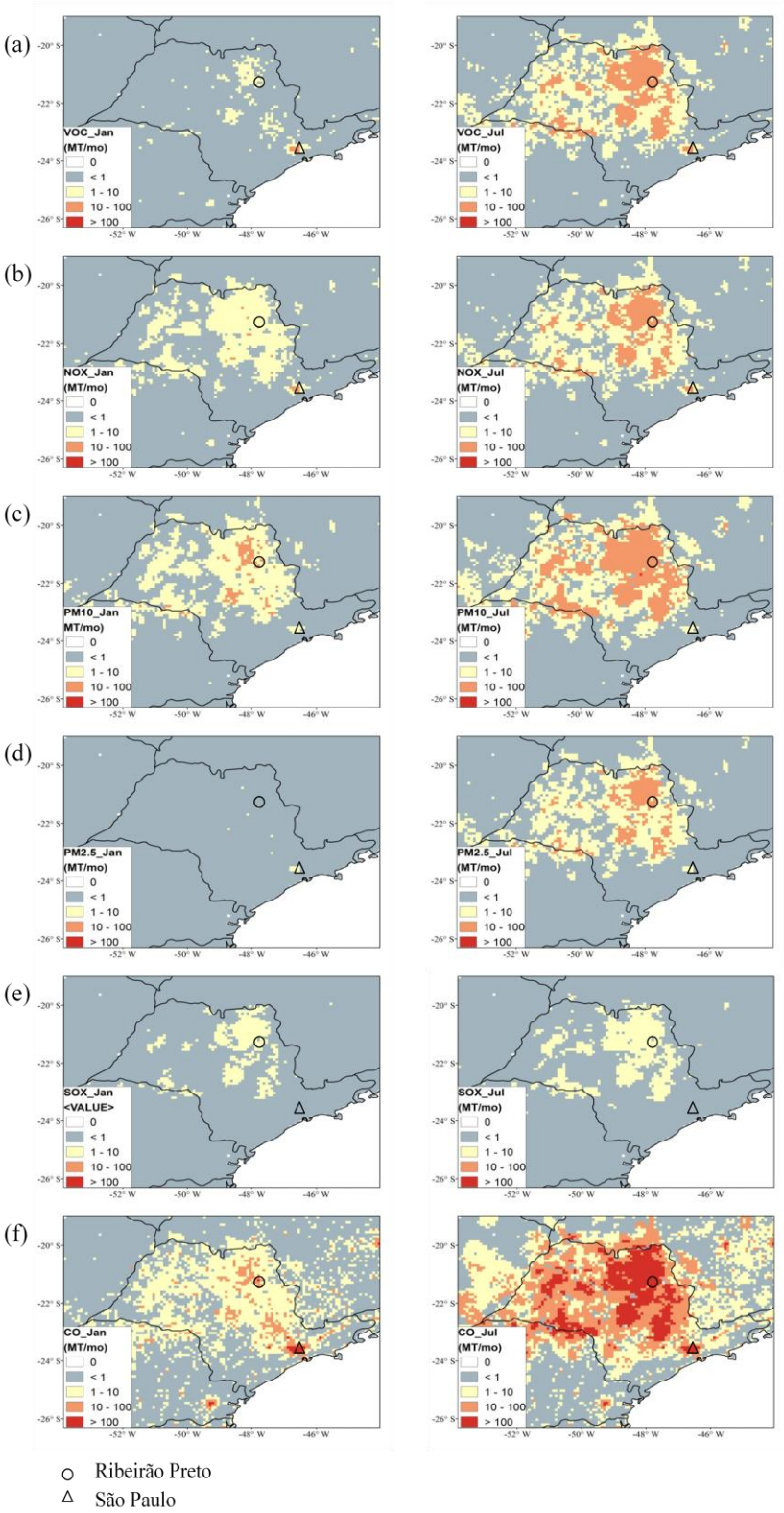

Figure 2.3: Emissions of 5 air pollutants (a) VOC (b) NO_X (c) PM_{10} (d) $PM_{2.5}$ (e) SO_X (f) CO in January and July, 2008.

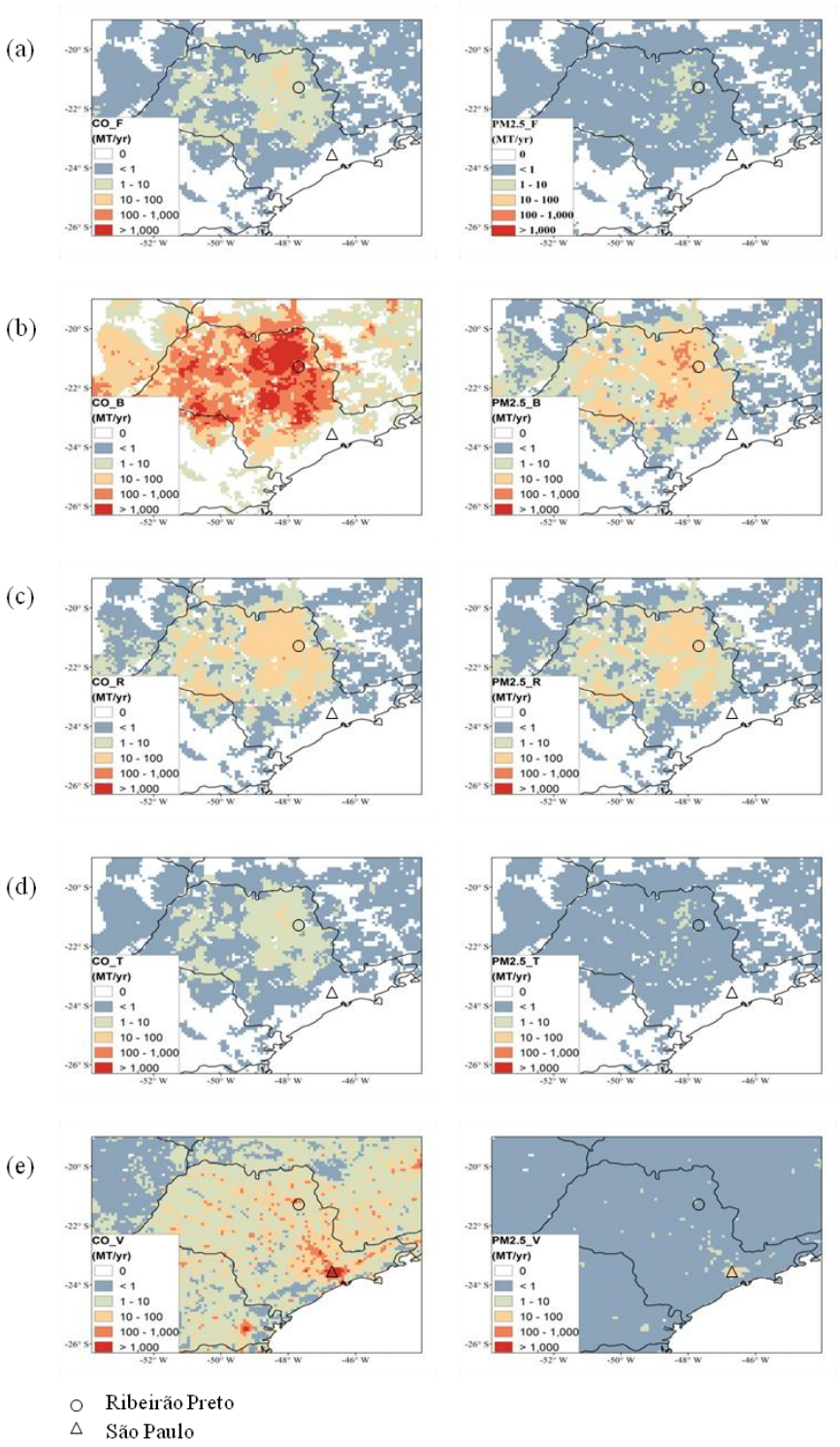

Figure 2.4: Emission of $PM_{2.5}$ and CO in different phases for July 2008 including (a) Field burning (b) Farming (c) Refinery (d) Transportation and distribution (e) Vehicle combustion phase.

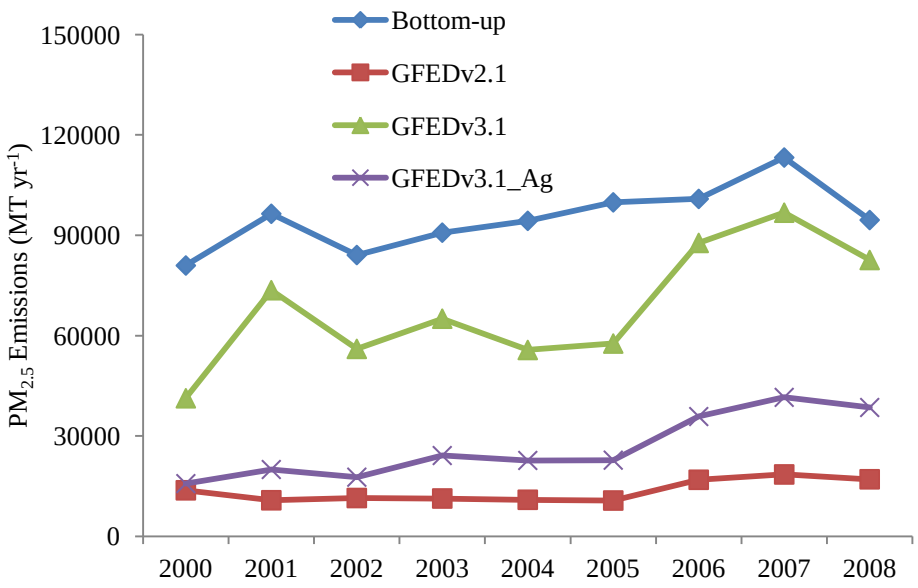

Figure 2.5: Comparison of annual $PM_{2.5}$ emission from sugarcane field burning by GFEDv2.1, GFEDv3.1 and our approach in this study.

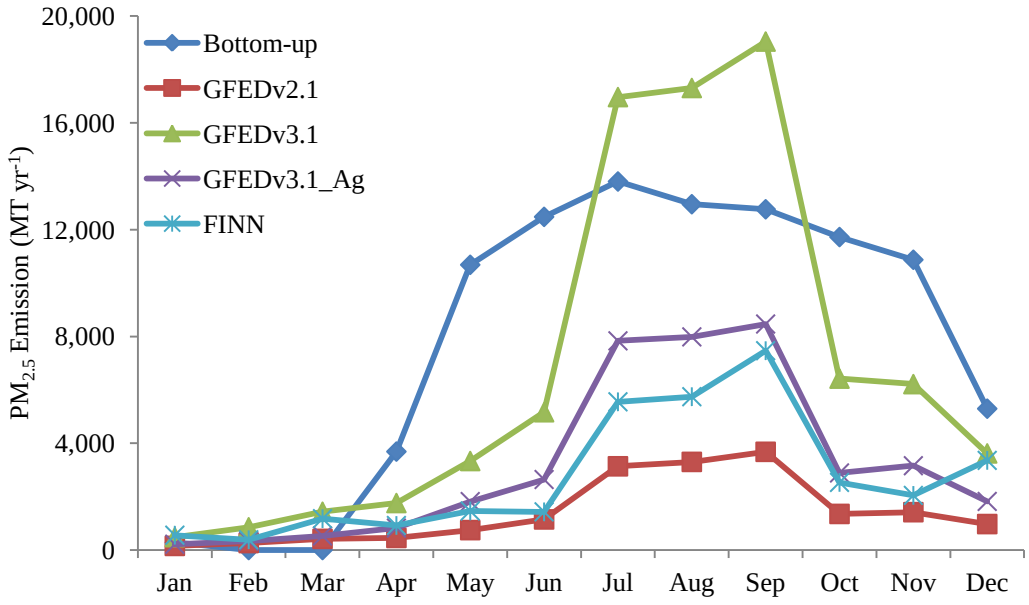

Figure 2.6: Comparison of monthly emissions in São Paulo state of $PM_{2.5}$ from biomass burning in 2008 by GFEDv2.1, GFEDv3.1, FINN and our approach.

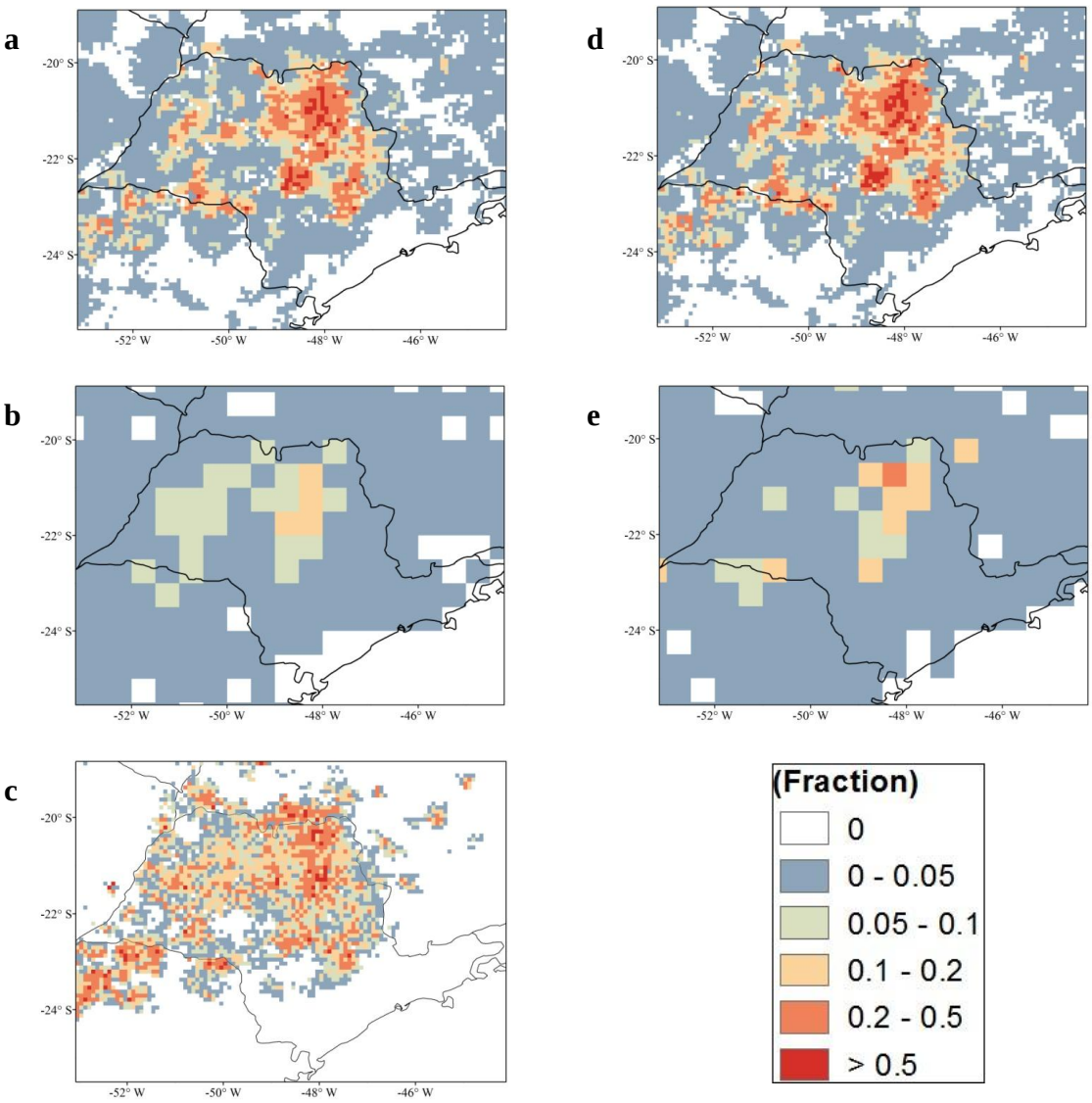

Figure 2.7: Fraction of each grid cell burned by three approaches. (a) Results for year 2008 using the approach in this study (resolution: 5 arcmin×5 arcmin), (b) GFEDv3.1 (resolution: 30 arcmin×30 arcmin), and (c) Landsat-based Canasat fire data (re-gridded to 5 arcmin×5 arcmin). (d) Results for year 2006 using the approach in this study resolution: 5 arcmin×5 arcmin) and (e) GFEDv3.1 (resolution: 30 arcmin×30 arcmin).

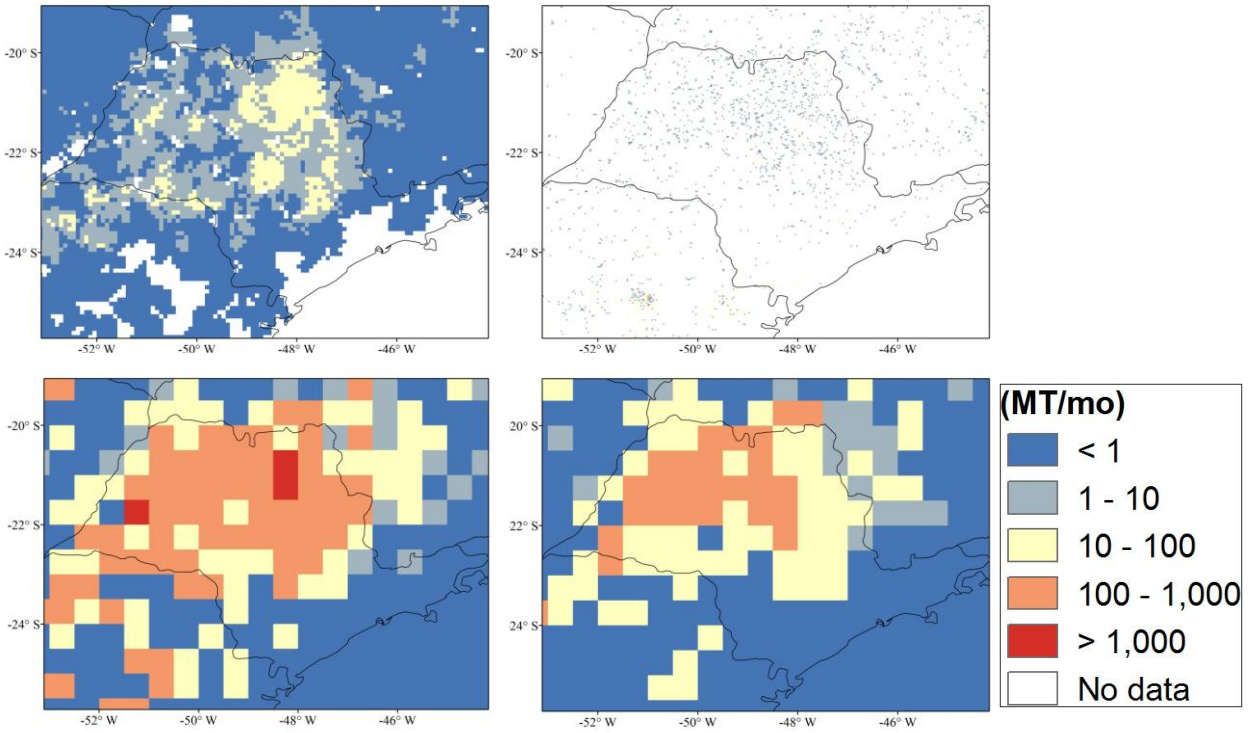

Figure 2.8: Comparison of monthly $PM_{2.5}$ emission in August 2008 (a) Sugarcane field burning emissions estimated by our approach; (b) FINN; (c) GFEDv3.1; and (d) GFEDv3.1_Ag.

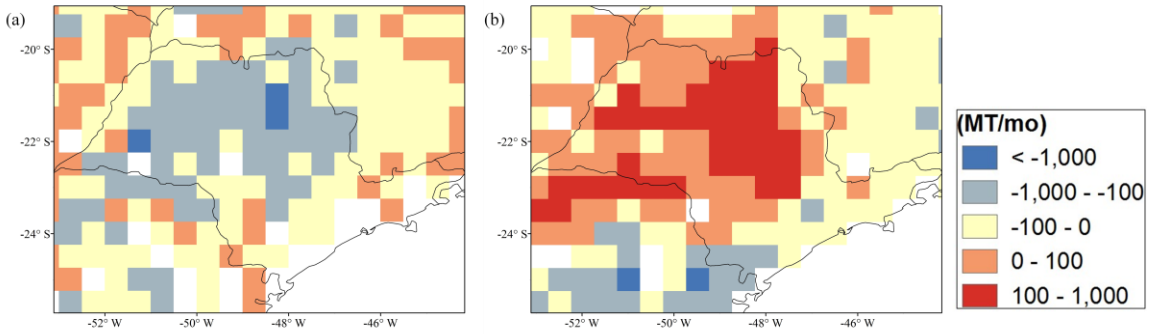

Figure 2.9: Difference of satellite-based and our emission estimates in August 2008: (a) our estimates minus GFEDv3.1; (b) our estimates minus FINN.

2.4 Uncertainty

It is not possible to directly validate emissions from the sugarcane life-cycle due to a lack of direct measurements. However, we have explored the uncertainties in our emissions inventory, particularly with respect to the parameters associated with the dominant burning phase, including fuel loadings, burned area, and emission factors. Our fuel loadings for the open-burning phase are based on a fixed ratio of burned biomass to yields that has been applied in previous work [4, 41]. Agronomic assessment is needed to provide uncertainty estimates for this ratio.

The estimates of burned area are driven by agronomic data for yield and production as well as remote sensing. The scale of our estimates (5 arcmin×5 arcmin, ~9.3 km) differs markedly from the MODIS-based approaches (500 m-1 km) as well as the validation Landsat data (30 m). The coarse resolution of MODIS-based approaches may have resulted in detection problems of sugarcane burning. However, even without these detection problems, the coarse scale could result in challenges in applying these emissions to high-resolution atmospheric models that are used to simulate atmospheric composition and climate forcing.

A range of emission factors for open burning have been reported in the literature, introducing significant uncertainty into the modeling approach. The standard deviations for the emissions factors vary widely on the basis of the emission factors applied in a range of studies (Table 2.4) [37, 42, 47, 50]. The uncertainty is particularly large for $PM_{2.5}$ and CO, at 32% and 46%, respectively. Incorporating crop-specific emissions factors as opposed to those used in GREET and MODIS-based approaches could lead to

improved estimates. Top-down studies of atmospheric composition could provide one approach to validating these emission factors.

Uncertainties in other stages of the life-cycle are not reported in GREET which provides the parameters for the non-burning life-cycle phases. Air pollution control devices on vehicles and sugarcane refineries may vary and lead to different emission factors. Further exploration of available life-cycle data beyond GREET should be used to develop quantitative uncertainty estimates. However, since the burning phase is the dominant source of emissions the errors in the other life-cycle stages may be important regionally but less important to the overall budgets.

Table 2.4: Emission factors (g emitted kg^{-1} dm) of sugarcane or agriculture biomass burning applied in this study and in satellite based approaches.

	This study[a]	Jenkins[b]	Andrea and Merlet.[c]	IPCC	GFEDv3.1 [d]	FINN [e]
CO	92	24.48	92±84	--	94	70
NOx	2.5	2.06	2.5±1.0	2.5±1.0	2.29	2.4
SOx[f]	0.4	0.62	0.4	--	0.4	0.4
PM_{10}[g]	7.8	5.4	13	--	12.4[e]	6.9
$PM_{2.5}$	3.9	5.0	3.9	--	8.25	5.7
VOC	7.0	--	7.0	--	11.19	7.0
OC	3.3	--	3.3	--	3.71	3.3
BC	0.69	--	0.69±0.13	--	0.48	0.69
COS	0.065	--	0.065±0.077	--	--	--

[a]: Emission factors from GREET are based on Andrea et al.
[b]: Emission factors from sugarcane burning experiments[50].
[c]: Emission factors for biomass burning from agriculture open burning [42].
[d]: Based on Andreae and Merlet (2001) and personal communication [37].
[e]: Based on Dennis et al. (2002), Andreae and Merlet (2001), Jenkins (1996), and EPA AP-42 document (1995) [47].
[f]: as SO_2
[g]: as TPM

2.5 Discussion and Conclusion

Life-cycle air pollution emissions were quantified in space and time for production through consumption phases for sugarcane ethanol with the dominant emissions associated with the pre-harvest burning of sugarcane. Even in regions where burning has been eliminated on 50% of the farms, burning continue to be the dominant life-cycle stage for emissions and emissions continue to grow in time due to expanding sugarcane areas.

Some studies with air pollution from corn ethanol in the U.S. have neglected production stage emissions when assessing climate and health impacts because production emissions are distant from population centers while vehicle emissions are concentrated around populations centers [10]. This may be an appropriate assumption for the U.S. domain but the Brazil domain may require inclusion of the production-phase emissions due to the large magnitude of the burning emissions and the distribution of population in rural areas.

Given the significance of the burning phase, these emissions were compared with alternative biomass burning emissions based on GFED and FINN satellite fire detection methods. The GFED and FINN approaches may not account for sugarcane burning emissions due to the small scale of these fires relative to satellite resolution and assumptions regarding fuel loadings. Improvements in the satellite-based methods may be achieved by integrating information from the inventory-based approach applied here or through the use of higher resolution satellite data where available [48]. Because the GFED and FINN data may not account for sugarcane burning, the total burning emissions

for the region may be the sum of our and the satellite-based emissions. This would result in an increase in total $PM_{2.5}$ emissions relative to only using the satellite-based estimates by a factor of 2.1 and 4.1 for the GFEDv3.1 and FINN data, respectively. The burned area for the sum of our estimates and the GFEDv3.1 estimates would be four times greater than the GFEDv3.1 burned area alone.

The rapid expansion of sugarcane ethanol and the changing production methods result in air pollution emissions that are changing in space and time. The impacts of air pollution on health and regional climate forcing are perhaps some of the most uncertain impacts that sugarcane ethanol, but are critical for assessing its sustainability. Further work coupling the spatially and temporally resolved maps from this work with satellite-based methods and atmospheric chemical transport models is needed to better understand these impacts on climate and health.

Reference

1. Farrell, A. E.; Plevin, R. J.; Turner, B. T.; Jones, A. D.; O'Hare, M.; Kammen, D. M., Ethanol can contribute to energy and environmental goals. *Science* 2006, *311*, (5760), 506-508.
2. Field, C. B.; Campbell, J. E.; Lobell, D. B., Biomass energy: the scale of the potential resource. *Trends Ecol. Evol.* 2008, *23*, (2), 65-72.
3. Schneider, U. A.; McCarl, B. A., Economic potential of biomass based fuels for greenhouse gas emission mitigation. *Environ. Resour. Econ.* 2003, *24*, (4), 291-312.
4. Macedo, I. C.; Seabra, J. E. A.; Silva, J., Green house gases emissions in the production and use of ethanol from sugarcane in Brazil: The 2005/2006 averages and a prediction for 2020. *Biomass & Bioenergy* 2008, *32*, (7), 582-595.
5. Fargione, J.; Hill, J.; Tilman, D.; Polasky, S.; Hawthorne, P., Land clearing and the biofuel carbon debt. *Science* 2008, *319*, (5867), 1235-1238.
6. Searchinger, T.; Heimlich, R.; Houghton, R. A.; Dong, F. X.; Elobeid, A.; Fabiosa, J.; Tokgoz, S.; Hayes, D.; Yu, T. H., Use of US croplands for biofuels increases greenhouse gases through emissions from land-use change. *Science* 2008, *319*, (5867), 1238-1240.
7. Lapola, D. M.; Schaldach, R.; Alcamo, J.; Bondeau, A.; Koch, J.; Koelking, C.; Priess, J. A., Indirect land-use changes can overcome carbon savings from biofuels in Brazil. *Proc. Natl. Acad. Sci. U. S. A.* 2010, *107*, (8), 3388-3393.
8. *Renewable Fuel Standard Program (RFS2) Regulatory Impact Analysis*; EPA-420-R-10-006; USEPA: 2010; p 1119.
9. Hill, J.; Polasky, S.; Nelson, E.; Tilman, D.; Huo, H.; Ludwig, L.; Neumann, J.; Zheng, H. C.; Bonta, D., Climate change and health costs of air emissions from biofuels and gasoline. *Proc. Natl. Acad. Sci. U. S. A.* 2009, *106*, (6), 2077-2082.
10. Jacobson, M. Z., Effects of ethanol (E85) versus gasoline vehicles on cancer and mortality in the United States. *Environmental Science & Technology* 2007, *41*, (11), 4150-4157.
11. Niven, R. K., Ethanol in gasoline: environmental impacts and sustainability review article. *Renewable & Sustainable Energy Reviews* 2005, *9*, (6), 535-555.
12. Ometto, A. R.; Hauschild, M. Z.; Roma, W. N. L., Lifecycle assessment of fuel ethanol from sugarcane in Brazil. *International Journal of Life Cycle Assessment* 2009, *14*, (3), 236-247.
13. Fukushima, Y.; Chen, S.-P., A decision support tool for modifications in crop cultivation method based on life cycle assessment: a case study on greenhouse gas emission reduction in Taiwanese sugarcane cultivation. *International Journal of Life Cycle Assessment* 2009, *14*, (7), 639-655.
14. Arbex, M. A.; Martins, L. C.; de Oliveira, R. C.; Pereira, L. A. A.; Arbex, F. F.; Cancado, J. E. D.; Saldiva, P. H. N.; Braga, A. L. F., Air pollution from biomass burning and

asthma hospital admissions in a sugar cane plantation area in Brazil. *Journal of Epidemiology and Community Health* 2007, *61*, (5), 395-400.

15. Goldemberg, J.; Coelho, S. T.; Guardabassi, P., The sustainability of ethanol production from sugarcane. *Energy Policy* 2008, *36*, (6), 2086-2097.
16. Yadava, R. L., *Agronomy of Sugarcane : Principles and Practice* 1st ed.; International Book Distributing Co., Publishing Division: Lucknow, U.P., India, 1993; p 375.
17. Brazil sugarcane mills agree to end burning by '17. http://www.reuters.com/article/idUSN2245768620071022
18. Pozza, S. A.; Bruno, R. L.; Tazinassi, M. G.; Goncalves, J. A. S.; Do Nascimento, V. F.; Barrozo, M. A. S.; Coury, J. R., Sources of particulate matter: emission profile of biomass burning. *International Journal of Environment and Pollution* 2009, *36*, (1-3), 276-286.
19. Coelho, C. H.; Francisco, J. G.; Nogueira, R. F. P.; Campos, M., Dissolved organic carbon in rainwater from areas heavily impacted by sugar cane burning. *Atmospheric Environment* 2008, *42*, (30), 7115-7121.
20. Machado, C. M. D.; Cardoso, A. A.; Allen, A. G., Atmospheric emission of reactive nitrogen during biofuel ethanol production. *Environmental Science & Technology* 2008, *42*, (2), 381-385.
21. Turn, S. Q.; Jenkins, B. M.; Jakeway, L. A.; Blevins, L. G.; Williams, R. B.; Rubenstein, G.; Kinoshita, C. M., Test results from sugar cane bagasse and high fiber cane co-fired with fossil fuels. *Biomass & Bioenergy* 2006, *30*, (6), 565-574.
22. Mazzoli-Rocha, F.; Magalhaes, C. B.; Malm, O.; Saldiva, P. H. N.; Zin, W. A.; Faffe, D. S., Comparative respiratory toxicity of particles produced by traffic and sugar cane burning. *Environmental Research* 2008, *108*, (1), 35-41.
23. Tfouni, S. A. V.; De Souza, N. G.; Neto, M. B.; Loredo, I. S. D.; Leme, F. M.; Furlani, R. P. Z., Polycyclic aromatic hydrocarbons in sugar cane juice from the city of Ribeirao Preto-SP, Brazil. *Toxicology Letters* 2008, *180*, S75-S75.
24. Umbuzeiro, G. D.; Franco, A.; Magalhaes, D.; de Castro, F. J. V.; Kummrow, F.; Rech, C. M.; de Carvalho, L. R. F.; Vasconcellos, P. D., A preliminary characterization of the mutagenicity of atmospheric particulate matter collected during sugar cane harvesting using the Salmonella/microsome microsuspension assay. *Environmental and Molecular Mutagenesis* 2008, *49*, (4), 249-255.
25. Allen, A. G.; Cardoso, A. A.; da Rocha, G. O., Influence of sugar cane burning on aerosol soluble ion composition in Southeastern Brazil. *Atmospheric Environment* 2004, *38*, (30), 5025-5038.
26. Arbex, M. A.; Bohm, G. M.; Saldiva, P. H. N.; Conceicao, G. M. S.; Pope, A. C.; Braga, A. L. F., Assessment of the effects of sugar cane plantation burning on daily counts of inhalation therapy. *Journal of the Air & Waste Management Association* 2000, *50*, (10), 1745-1749.

27. Cancado, J. E.; Saldiva, P. H. N.; Pereira, L. A. A.; Lara, L.; Artaxo, P.; Martinelli, L. A.; Arbex, M. A.; Zanobetti, A.; Braga, A. L. F., The impact of sugar cane-burning emissions on the respiratory system of children and the elderly. *Environmental Health Perspectives* 2006, *114*, (5), 725-729.

28. Ribeiro, H., Sugar cane burning in Brazil: respiratory health effects. *Revista De Saude Publica* 2008, *42*, (2).

29. Uriarte, M.; Yackulic, C. B.; Cooper, T.; Flynn, D.; Cortes, M.; Crk, T.; Cullman, G.; McGinty, M.; Sircely, J., Expansion of sugarcane production in Sao Paulo, Brazil: Implications for fire occurrence and respiratory health. *Agriculture Ecosystems & Environment* 2009, *132*, (1-2), 48-56.

30. de Haes, H. A. U.; Heijungs, R.; Suh, S.; Huppes, G., Three strategies to overcome the limitations of life-cycle assessment. *Journal of Industrial Ecology* 2004, *8*, (3), 19-32.

31. Owens, J. W., Life-cycle assessment in relation to risk assessment: An evolving perspective. *Risk Analysis* 1997, *17*, (3), 359-365.

32. Ross, S.; Evans, D., Excluding site-specific data from the LCA inventory: How this affects Life Cycle impact Assessment. *International Journal of Life Cycle Assessment* 2002, *7*, (3), 141-150.

33. Yellishetty, M.; Ranjith, P. G.; Tharumarajah, A.; Bhosale, S., Life cycle assessment in the minerals and metals sector: a critical review of selected issues and challenges. *International Journal of Life Cycle Assessment* 2009, *14*, (3), 257-267.

34. 2008 World Fuel Ethanol Production. http://www.ethanolrfa.org/industry/statistics/#C (Dec. 1),

35. International Trade Statistics 2009. In World Trade Organization: Geneva, Switzerland, 2009.

36. Wiedinmyer, C.; Quayle, B.; Geron, C.; Belote, A.; McKenzie, D.; Zhang, X. Y.; O'Neill, S.; Wynne, K. K., Estimating emissions from fires in North America for air quality modeling. *Atmospheric Environment* 2006, *40*, (19), 3419-3432.

37. van der Werf, G. R.; Randerson, J. T.; Giglio, L.; Collatz, G. J.; Mu, M.; Kasibhatla, P. S.; Morton, D. C.; DeFries, R. S.; Jin, Y.; van Leeuwen, T. T., Global fire emissions and the contribution of deforestation, savanna, forest, agricultural, and peat fires (1997-2009). *Atmos. Chem. Phys.* 2010, *10*, (23), 11707-11735.

38. Barros, S. *Brazil Sugar Annual 2009*; BR9004; USDA: 4/30/2009, 2009.

39. Monfreda, C.; Ramankutty, N.; Foley, J. A., Farming the planet: 2. Geographic distribution of crop areas, yields, physiological types, and net primary production in the year 2000. *Global Biogeochemical Cycles* 2008, *22*, (1), GB1022.

40. Rudorff, B. F. T.; Aguiar, D. A.; Silva, W. F.; Sugawara, L. M.; Adami, M.; Moreira, M. A., Studies on the rapid expansion of sugarcane for ethanol production in Sao Paulo State (Brazil) using Landsat data. *Remote Sensing* 2010, *2*, (4), 1057-1076.

41. Wang, M.; Wu, M.; Huo, H.; Liu, J. H., Life-cycle energy use and greenhouse gas emission implications of Brazilian sugarcane ethanol simulated with the GREET model. *Int. Sugar J.* 2008, *110*, (1317), 527-545.

42. Andreae, M. O.; Merlet, P., Emission of trace gases and aerosols from biomass burning. *Global Biogeochemical Cycles* 2001, *15*, (4), 955-966.

43. Saide, P. E.; Carmichael, G. R.; Spak, S. N.; Gallardo, L.; Osses, A. E.; Mena-Carrasco, M. A.; Pagowski, M., Forecasting urban PM10 and PM2.5 pollution episodes in very stable nocturnal conditions and complex terrain using WRF–Chem CO tracer model. *Atmospheric Environment* 2011, *45*, 2769-2780.

44. LandScan™ Global Population Database. In Oak Ridge National Laboratory: Oak Ridge, TN, 2008.

45. van der Werf, G. R.; Randerson, J. T.; Giglio, L.; Collatz, G. J.; Kasibhatla, P. S.; Arellano, A. F., Interannual variability in global biomass burning emissions from 1997 to 2004. *Atmos. Chem. Phys.* 2006, *6*, 3423-3441.

46. Randerson, J. T.; Van der Werf, G. R.; Giglio, L.; Collatz, G. J.; Kasibhatla, P. S., Global Fire Emissions Database, Version 2 (GFEDv2.1). In Oak Ridge National Laboratory Distributed Active Archive Center, Oak Ridge, Tennessee, U.S.A: 2007.

47. Wiedinmyer, C.; Akagi, S. K.; Yokelson, R. J.; Emmons, L. K.; Saadi, J. A.; Orlando, J. J.; Soja, A. J., The Fire INventory from NCAR (FINN) – a high resolution global model to estimate the emissions from open burning. *Geosci. Model Dev.* 2011, *4*, (3), 625-641.

48. Schroeder, W.; Csiszar, I.; Giglio, L.; Schmidt, C. C., On the use of fire radiative power, area, and temperature estimates to characterize biomass burning via moderate to coarse spatial resolution remote sensing data in the Brazilian Amazon. *J. Geophys. Res.-Atmos.* 2010, *115*, D21121.

49. Lara, L. L.; Artaxo, P.; Martinelli, L. A.; Camargo, P. B.; Victoria, R. L.; Ferraz, E. S. B., Properties of aerosols from sugar-cane burning emissions in Southeastern Brazil. *Atmospheric Environment* 2005, *39*, (26), 4627-4637.

50. Jenkins, B. M. *Atmospheric pollutant emission factor from open burning of sugar cane by wind tunnel simulations*; University of California, Davis: Davis, CA, 1994.

Chapter 3 Land-use Changes and Air Pollution

3.1 Introduction

Expansions of biofuels production and uses may provide benefits to energy security, GHG reductions, and rural economic development [1-3]. Production of liquid biofuels including ethanol and biodiesel is expected to grow rapidly in the future due to market forces and government mandates for fuel-blending [4, 5]. Expansion in Brazil presents unique opportunities for both liquid fuel and electricity production [6]. Estimates of the life-cycle GHG emissions from biofuels are largely based on regional and global models of the deforestation that may result from land-use change (LUC) impacts from biofuels [4, 7, 8]. Here we consider how these LUC impacts may also be a critical, though overlooked, source of life-cycle air pollution emissions.

Several studies suggest that LUC due to biofuel cropland expansion may offset the potential carbon saving of biofuels. Searchinger et al. [8] found that life-cycle GHG emissions for US corn ethanol are double the emissions of conventional gasoline due to indirect LUC (iLUC) effects. Fargione et al. [9] quantified the carbon debt resulting from direct LUC (dLUC) to produce biofuels, and found payback times of up to 423 years that are primarily driven by the carbon density of the natural land that is converted. Lapola et al. examined both dLUC and iLUC effects of biofuels in Brazil by coupling a spatially explicit land-use model with carbon density maps [4]. The Brazilian iLUC emissions, especially conversion from Amazonian forests to rangelands, offset the carbon savings from biofuels to a much greater extent than dLUC emissions. In addition to carbon emissions, other concerns associated with LUC include competition with food,

biodiversity loss, water quality and quantity degradation, and regional climate change [2, 10-15].

Among the available biofuels on the market, sugarcane ethanol, which is primarily produced in Brazil may result in lower life-cycle GHG emissions than other conventional biofuels such as corn ethanol [16]. However, sugarcane ethanol may be of particular concern with respect to air pollution due to pre-harvest burning of sugarcane fields [17]. An additional driver of life-cycle air pollution emissions from sugarcane ethanol may be the dLUC and iLUC emissions that could be incurred by an expansion of biofuel croplands.

Air pollution emissions from LUC are due to open burning practices for land clearing, e.g. slash-and-burn [15]. Recent analyses of global biomass burning found that deforestation and degradation fire are the dominant sources of biomass burning emissions in South America [18]. These land clearing emissions continue to grow rapidly because deforestation (cropland and rangeland expansion) has shifted towards areas with higher biomass density in Amazonia [19]. However, burning practices are not limited to deforestation. In the Brazilian Amazon area, local farmers use fires as a conventional and cost-effective way to remove aboveground biomass on Cerrado savanna to prepare land for agricultural use [20, 21].

Air pollution from LUC may be a significant problem if biofuel production continues to grow without effective controls on burning practice. Although previous biofuels studies focus on air pollution from other life-cycle phases, air pollution from land-use is in general a significant global emissions source and thus may present an

important impact in the biofuels life-cycle as well. The composition and magnitude of potential emissions from future biofuels LUC remains an important unknown for biofuels sustainability. In this paper, spatially explicit emissions from direct and indirect LUC due to the future expansion of biofuels production in Brazil are estimated using a bottom-up approach incorporating LUC maps, fuel loading, combustion completeness, and emission factors. These emissions are compared with other life-cycle phases and emissions estimates for deforestation in the past.

3.2 Methodology

A bottom-up estimation of dLUC and iLUC emissions based on multiple approaches for estimating non-CO_2 emissions from land-use is applied in this study. Spatially explicit emissions from LUC in Brazil due to incremental biofuels production are estimated by integrating predicted activities of LUC and emission factors. Equation 1 formulates the LUC emissions,

$$E_i^{LUC} = \sum_{j,k,s} \left[A_{js} \times F_{jks} \times CF_{jk} \times EF_{ijk} \right] \quad (1)$$

where E_i^{LUC} (Mg emitted) is the LUC emissions of pollutant *i*. E_i^{LUC} is the aggregation of the emissions from different types of LUC, *j*, including dLUC of forest to biofuel (F2B), cropland to biofuel (C2B), ranchland to biofuel (R2B), wood savanna to biofuel (W2B), and other vegetation to biofuel (O2B), as well as iLUC of forest to ranchland (F2R), cropland to ranchland (C2R), wood savanna to ranchland (W2R), other vegetation to ranchland (O2R), and ranchland to cropland (R2C). A_{js} (ha) is the area for the *j* type LUC at location *s*. F_{jks} (Mg dried matter $\cdot$ ha^{-1}) is the removed biomass as the available fuel loading per area for burning practices due to the *j* type LUC and the *k* type biomass (i.e. aboveground or belowground biomass) at location *s*. CF_{jk} (%) is the fraction of fuel consumption relative to the total available fuel loading for the *j* type LUC and the *k* type biomass. EF_{ijk} (Mg emitted $\cdot$ Mg^{-1} dried matter) is the emission factor of the i^{th} pollutant for different types (i.e. *j* and *k*) of biomass burning.

The following sections (section 3.2.1 to 3.2.4) describe the data sources and application of each parameter in Eq. 1. The parameter estimates for the baseline scenario

and two additional scenarios for future burning controls are introduced in section 3.2.5. We normalize our estimates for LUC emissions using an energy functional unit (mmBTU fuel) in order to allow for comparison with other types of liquid fuels. The method for normalization is addressed in section 3.2.6. The approach to quantifying uncertainty in LUC emissions based on parameter uncertainty is introduced in section 3.2.7.

3.2.1 Projection of LUC Area

The LUC area (A_{js}) summarized in Table 3.1 was based on spatially explicit results from a previous analysis of biofuels LUC in Brazil estimated from the LandSHIFT model [4]. This study used a spatially explicit modeling framework (5 arc-min resolution) to project direct and indirect LUC caused by biofuel cropland expansion, for an incremental biofuel production scenario of 39 billion liters per year (35 billion liters sugarcane ethanol and 4 billion liters soy biodiesel) in the 2003-2020 period. The estimates of production projection are similar to OECD predictions (38.2 billion liters ethanol and 3.1 billion liter biodiesel) [22]. The framework couples the LandSHIFT model with two other models, IMPACT (the International Model for Policy Analysis of Agricultural Commodities and Trade) and LPJ for managed Lands (LPJmL, Lund-Potsdam-Jena managed Land Dynamic Global Vegetation and Water Balance Model) dynamic global vegetation model, to account for future changes in crop yield, population, food demand, and biomass productivity. The LandShift model simulates the interactions between anthropogenic and environmental drivers and their competition for land resources.

Table 3.1: Estimated area of biofuels LUC in Brazil in the 2003-2020 period

	dLUC					iLUC				
Type	**F2B**	**R2B**	**W2B**	**O2B**	**C2B**	**F2R**	**R2C**	**W2R**	**O2R**	**C2R**
LUC (10^3 km^2)	1.84	145.20	1.81	1.56	14.55	119.81	15.58	20.15	21.70	2.27
% of total LUC	0.5	42.2	0.5	0.5	4.2	34.8	4.5	5.9	6.3	0.7

3.2.2 Estimates of Fuel Loading from LUC

Available fuel loading per area, F_{jks}, were derived from the difference of available aboveground and belowground biomass before and after LUC. The component of the removed biomass that was used as products (e.g. logs) rather than burned was subtracted from the fuel loading. In the IPCC approach, fuel loadings are summarized by vegetation type (Tier 1 fire emissions) [23]. An alternative approach by Fargione et al. [9] calculated fuel loading from land clearing based on the evaluation and synthesis of published studies for relevant native habitats and land-uses. Due to the potential spatial and temporal variations in biomass, other studies have applied either remote-sensing techniques, direct measurements, or a combination of these two approaches to access spatially and temporally explicit biomass stocks [18, 24-27]. Carbon stock modeling methods based on CASA (Carnegie Ames Stanford Approach), a satellite-driven biogeochemical model, are commonly used for determining aboveground or belowground biomass [18, 24]. Potter et al. developed a simulation model incorporating CASA and direct biomass measurements to examine monthly fire emissions in terrestrial ecosystems of the Brazilian Amazon and the Cerrado region [24]. The GFED also applied CASA to estimate fuel loadings for use in modeling fire emissions [18]. Saatchi et al. combined remote sensing data with more than 500 plot measurements to determine the spatial distribution of forest biomass in the Amazon area [26].

In our study, we synthesized carbon stocks and fuel loading information from Saatchi et al. and Fargione et al. and developed a spatially explicit dataset of potential fuel loadings for LUC. We used the Saatchi et al. data for forest conversion LUC (F2B

and F2R) and Fargione et al. for non-forest LUC (R2B, R2C, O2B, O2R, C2B, C2R, W2B, and W2R). Table 3.2 summarizes carbon changes for non-forest LUC. We assumed fuel loading consisted of 50% carbon relative to dry biomass. Available fuel loadings for forest LUC (F2B and F2R) were reduced by 14% of the dried matter due to removal for long-lived wood products [9, 23]. For conversion to cropland, we assume all biomass is removed by fires or other agricultural practices or uses. For conversion to rangeland, the available fuel loading is calculated as the difference between the fuel loading of the original land-use and the rangeland land-use. Figure 3.1 shows the spatial distribution of fuel loading for LUC.

Table 3.2: Fuel loading for non-forest LUC (Mg C ha-1).

LUCs	Aboveground Biomass			Belowground Biomass		
	High	**Best Guess**	**Low**	**High**	**Best Guess**	**Low**
R2B	7.14	4.93	2.65	18.04	13.10	8.09
R2C	7.14	4.93	2.65	18.04	13.10	8.09
W2B	44.52	17.53	8.47	30.90	23.20	13.80
W2R	41.87	12.60	1.33	30.90	23.20	13.80
O2B	25.83	11.23	5.56	24.47	18.20	10.95
O2R	23.18	6.30	0	24.47	18.20	10.95

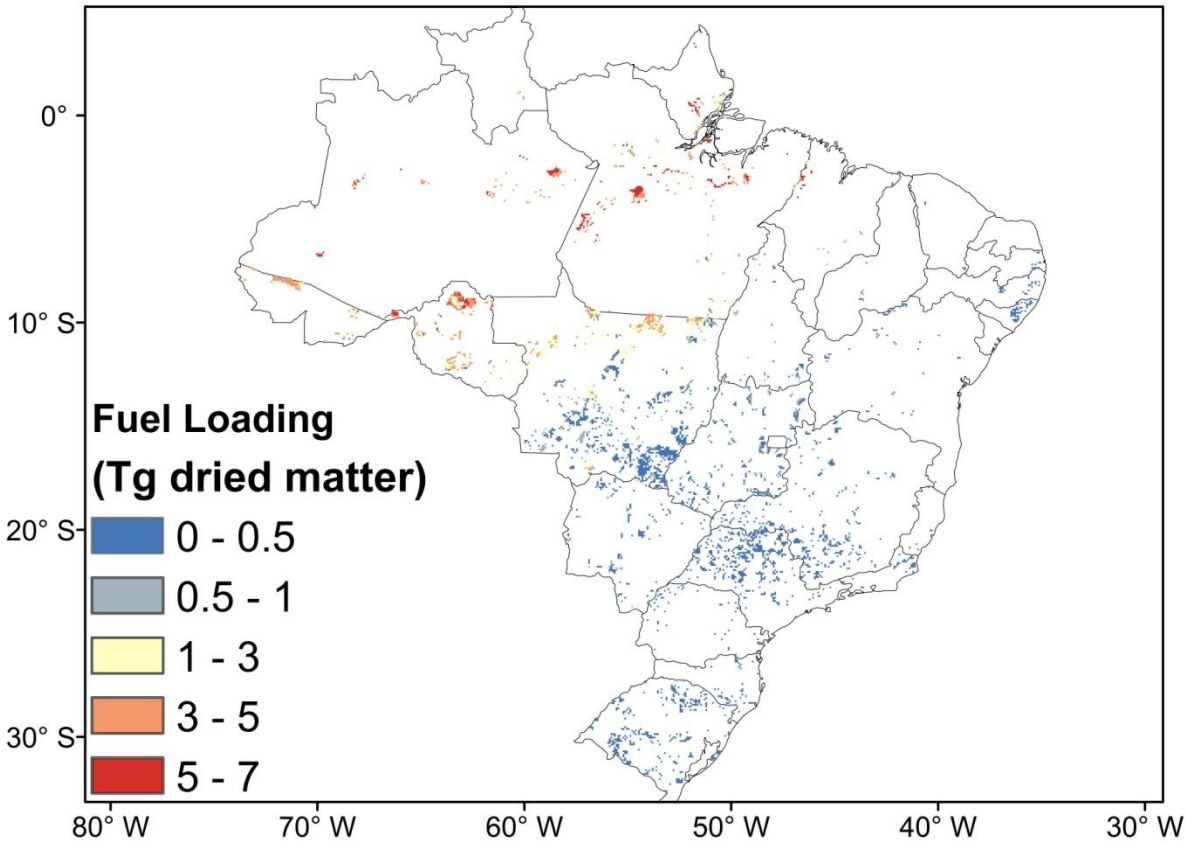

Figure 3.1: Fuel loadings for land-use change due to incremental Brazilian biofuel production of 39 billion liters per year (35 billion liter sugarcane ethanol and 4 billion liter soy biodiesel) in the 2003-2020 period.

3.2.3 Emission Factors of Biomass Burning

Emission factors (EF_{ij}) representing emission intensity per unit fuel burned (g emission / kg dried matter burned) are obtained from the van der Werf et al. [18] and Wiedinmyer et al. [28] studies for biomass fire emissions. These emission factors have been applied in the calculation of fire emissions in the GFED and FINN global fire databases. The GFED and FINN models do not report separate emission factors for aboveground and belowground biomass so we applied the same for both. Table 3.3 compares the emissions factors from these two datasets for eight species and five types of LUC. Emission factors of CO, TPM, and $PM_{2.5}$ within a given LUC type are similar for both data sets (10%, 12%, and 18% average difference , respectively) while larger difference are found for NMHC (42% difference in average).

Table 3.3: Emission factors of biomass burning for each type of land-use (g emitted / kg dried matter burned)

Original land-use	**Sources**	**CO**	**NO_X**	**NMHC**	**SO_2**	**$PM_{2.5}$**	**TPM**	**OC**	**BC**
Cropland[a]	GFED	94	2.29	11.19	0.40	8.25	12.40	3.71	0.48
	FINN	111	3.50	7.00	0.40	5.80	13.00	3.30	0.69
Other Vegetation[b]	GFED	61	2.12	3.41	0.37	4.94	8.50	3.21	0.46
	FINN	59	2.80	3.40	0.48	5.40	8.30	2.60	0.37
Forest[c]	GFED	101	2.26	7.00	0.71	9.05	11.80	4.30	0.57
	FINN	92	2.60	1.70	0.45	9.70	13.00	4.70	0.52
Rangeland[d]	GFED	61	2.12	3.41	0.37	4.94	8.50	3.21	0.46
	FINN	59	2.80	3.40	0.48	5.40	8.30	2.60	0.37
Woody Savana[e]	GFED	81	2.19	5.21	0.54	7.00	10.20	3.76	0.52
	FINN	68	3.90	3.40	0.68	9.30	15.40	6.60	0.50

[a]: GFED: Agricultural waste burning; FINN: cropland
[b]: GFED: Savanna/ grassland; FINN: Sparse shrub/veg. (Avg.)
[c]: GFED: Deforestation fire; FINN: Tropical forest
[d]: GFED: Savanna/ grassland; FINN: Savanna and grasslands
[e]: GFED: Woodland; FINN: Woody savanna/ shrublands

3.2.4 Combustion Completeness

The fraction of fuel consumption relative to the total available fuel loading is the combustion factor (CF), also known as combustion completeness [28, 29]. The IPCC provides combustion completeness for non-GHG emission inventories of wild or prescribed fires, indicating 50% of dried matter is burned for tropical rainforest [23]. Carvalho et al. conducted a forest clearing experiment in the Brazilian Amazon and found an average combustion completeness for land clearing of one-time fire of 20.5% [30]. Houghton et al. synthesized two studies and also found 20% of initial forest biomass is burned during deforestation [31]. Aboveground fire might also result in the burning of belowground biomass which can cause relatively small emissions [32-34]. Two studies, Tufekcioglu et al. [34] and Rau et al. [33], investigate the characteristics of belowground biomass for forest and shrubland after burning. We apply their fractions of biomass burning, for calculating LUC emissions from belowground. Table 3.4 summarizes the range and the mean of CF values for LUC occurring in each type of vegetation. We also assume no burning practices are required for land-use conversion from existing cropland to biofuels cropland.

Table 3.4: The range of CF values for LUC occurring in each type of vegetation

Vegetation	Aboveground Biomass			Belowground Biomass
	High	Mean	Low	Value
Forest	0.50[a]	0.36	0.21[b]	0.08[c]
Rangeland	-	0.74[a]	-	0.23[d]
Woody savanna	-	0.74[a]	-	0.23[d]
Other vegetation	-	0.72[a]	-	0.23[d]

[a] Paustian et al (2006) [23].
[b] Carvalho et al. (1998) [30].
[c] Tufekcioglu et al. (2007) [34] .
[d] Rau et al. (2009) [33].

3.2.5 Scenarios of Future Burning Controls

To project LUC emissions, a baseline estimate is calculated by the mean values and best guess parameter estimates addressed in the previous sections, and compared with different scenarios of burning controls. We assume there are no open burning controls in the baseline case since open-field burning is the most common practices for LUC in Brazil [20, 21, 35]. Due to increasing concerns over air pollution from open biomass burning in several states of Brazil, we expect some actions on burning control might be adopted in the future. For example, pre-harvesting burning practices for sugarcane crops are encouraged to gradually shift to mechanized practices in São Paulo state. Both agriculture survey data and remote sensing studies for São Paulo state suggest that the use of open burning as a management practice has been reduced to 50% of sugarcane cropland area [16, 36]. This measure of control on sugarcane pre-harvesting burning might extend to other types of open-field burning (i.e. LUC fires) or even to the area outside São Paulo state in the future. Therefore, we assume two scenarios of burning control on LUC emissions which are (A) 50% reduction of open burning practices in São Paulo state and (B) 100% reduction of open burning practices in São Paulo state and 50% reduction of burning practices in other states.

3.2.6 Normalization of LUC emissions for Biofuels

LUC emissions as a part of the biofuel life-cycle emissions might be compared with other types of fuel based on the same functional unit, i.e. 1 mmBTU biofuel produced. However, unlike emissions from other life-cycle phases, LUC emissions largely occur in the first year of production and are much smaller in subsequent years. To normalize LUC emissions to the mmBTU functional unit, they must be amortized over the period that biofuels are produced in order to compare the upfront LUC emissions with the annual emissions associated with biofuels production. Thus the amortization is sensitive to the assumed production period. We apply straight-line amortization of the LUC emissions over the biofuel production period. It should be noted that this amortization approach may underestimate the effects of air pollution from LUC emissions because LUC emissions are concentrated in the earlier part of the production period which can result in larger air pollution impacts than emissions that are evenly distributed over time [37]. Equation 2 formulates the amortization of LUC emission,

$$NE_i^{LUC} = \frac{E_i^{LUC} \times 10^{-6}}{\left(\sum_s \sum_{j=dLUC} A_{js} \right) \times FY \times PP} \quad (2)$$

where NE_i^{LUC} is the normalized value of LUC emissions (Mg emitted / mmBTU fuel) for the i^{th} pollutant. NE_i^{LUC} as the average LUC emissions per unit biofuel produced is the baseline LUC emissions divided by the net biofuel yields over the converted lands within the product period. The net biofuel yields are determined by the product of cropland expansion area associated with direct LUC (A, ha), fuel yield (FY, mmBTU fuel/ ha · year), and product period (PP, year). We use the average value of the current (2006) and

future (2020 projection) fuel yield for soy biodiesel (30.9 mmBTU/ ha · year) and sugarcane ethanol (174 mmBTU/ ha · year) based on previous studies [16, 38]. We also follow the assumption of the product period for biofuels from Plevin et al. allowing a range from 15 to 45 years [7].

3.2.7 Sensitivity and Uncertainty Estimates

The uncertainty of emissions estimates was determined by Monte Carlo simulations ($n = 10^6$) given uncertainties of each parameter. We assumed uniformly-distributed input parameter distributions across the range of available estimates. The variation in parameter estimates is also assumed to be independent from each other.

Sensitivity of LUC emissions to individual input variables (i.e. F_{jk}, EF_{ij}, and CF_{jk}) was reported using a sensitivity index for each variable,

$$S_l = \frac{\mathrm{V}\left[\mathrm{E}\left(E^{LUC} \mid X_l\right)\right]}{\mathrm{V}\left(E^{LUC}\right)} \tag{3}$$

where S_l is the sensitivity index for the l^{th} variable, and X_l is the l^{th} variable (i.e. F_{jk}, EF_{ij}, and CF_{jk}). $\mathrm{V}\left[\mathrm{E}\left(E^{LUC} \mid X_l\right)\right]$ is the expected amount of variance that would be removed from the total output variance, $\mathrm{V}\left(E^{LUC}\right)$, given a true value of variable X_l. The measure of the sensitivity index indicates the relative importance of an individual input variable in driving the uncertainty of the output (E_i^{LUC}).

3.3 Results

3.3.1 Net LUC Emissions

Baseline scenario estimates for each type of LUC emission, and aggregated iLUC and dLUC emissions are provided in Figure 3.2. Our estimate for iLUC emissions (13.5 Tg $PM_{2.5}$ emitted) is twelve times the estimated dLUC emissions (1.1Tg $PM_{2.5}$). Among LUC emissions, F2R (forest converted to rangeland) as iLUC is the dominant source because of the large area and large fuel loading for this LUC type relative to the other dLUC and iLUC types. While dLUC from rangelands to biomass (R2B) croplands accounted for large areas relative to other LUC types, the low fuel loadings of rangelands resulted in emissions (1 Tg $PM_{2.5}$) that were small relative to forest conversion.

The influences of each input parameter on the emission estimates are summarized in Table 3.5. Uncertainties in the fuel loading, emission factor, and combustion completeness cause the baseline scenario estimates to range from 6.7 to 26.4 Tg $PM_{2.5}$ emitted. Among three variables, the combustion completeness causes the widest range of estimates from 65% to 132% of the baseline. Fuel loading (F_{jk}) is the next most important source of uncertainty, with a range of 76% to 132% of the baseline. The emissions factor is much less significant than the other two variables with respect to uncertainties. Results of sensitivity analysis for each input variable are also shown in Table 3.5. These results suggest that improvement in estimates of combustion completeness should reduce the uncertainty of LUC emission estimates. Projections of LUC areas (A_{js}) are another potentially significant source of uncertainty [7]. However, it is hard to quantify its aggregated uncertainty due to the lack of uncertainty information for LUC associated

with Brazilian biofuels [4]. Further qualitative analysis on the uncertainty of A_{js} is discussed in section 3.4.

Estimates among the baseline case and scenarios of open burning control are compared in Figure 3.3. The open burning control scenario A reduces dLUC by nearly 10% but results in limited reduction in total LUC emissions. LUC emissions remain at a high level (7.4 Tg $PM_{2.5}$ emitted) even if burning practices are strictly controlled through scenario B.

In Figure 3.3 we also compare the emissions associated with biofuels LUC to current total open burning emissions in Brazil associated with drivers other than biofuels. Current Brazilian emissions are obtained from the GFEDv3 database. Biofuels LUC emissions under the three burning scenarios are found to be similar in magnitude to the cumulative Brazilian emissions from deforestation from years 2000 to 2009 and much larger than annual Brazilian emissions.

Table 3.5: Eight combinations of variables used to calculate a range of estimates of LUC emission and a sensitivity index for each input variable.

	Fuel Loading (F_{jk})	Emission Factor (EF_{ij})	Combustion Completeness (CF_{ijk})	LUC Emission (Tg $PM_{2.5}$ emitted)	Comparison with baseline case
Baseline	Medium	Medium	Medium	14.7	1
1.	High	High	High	26.4	1.80
2.	Medium	Medium	High	19.4	1.32
3.	Medium	Medium	Low	9.6	0.65
4.	High	Medium	Medium	19.4	1.32
5.	Low	Medium	Medium	11.1	0.76
6.	Medium	High	Medium	15.3	1.04
7.	Medium	Low	Medium	14.0	0.96
8.	Low	Low	Low	6.7	0.46
Sensitivity Index (S_l)	0.22	0.01	0.73	--	--

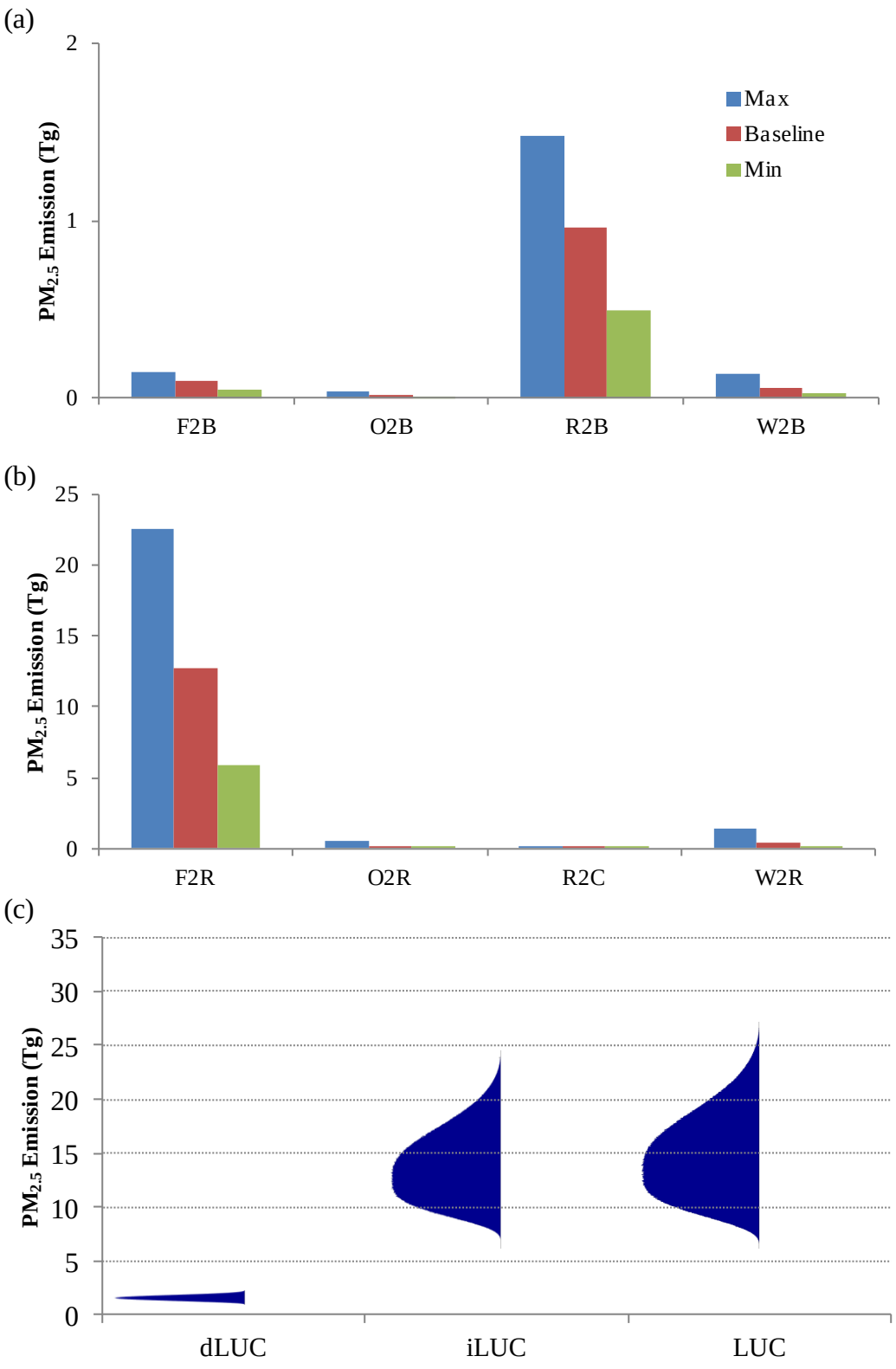
(a)
2
1
0
PM2.5 Emission (Tg)
Max
Baseline
Min
F2B
O2B
R2B
W2B
(b)
25
20
15
10
5
0
PM2.5 Emission (Tg)
F2R
O2R
R2C
W2R
(c)
35
30
25
20
15
10
5
0
PM2.5 Emission (Tg)
dLUC
iLUC
LUC

Figure 3.2: LUC emissions including maximum, baseline, and minimum values, and the distribution of estimates for dLUC, iLUC, and the total LUC emissions. (a) dLUC emissions include emissions from forest to biofuel (F2B), cropland to biofuel (C2B), ranchland to biofuel (R2B), woody savanna to biofuel (W2B), and other vegetation to biofuel. (O2B). (b) iLUC emissions include emissions from forest to rangeland (F2R), cropland to ranchland (C2R), wood savanna to ranchland (W2R), other vegetation to ranchland (O2R), and ranchland to cropland (R2C). (c) Aggregated estimates for dLUC, iLUC, and total LUC emissions with the shape of possible frequency distribution by Monte Carlo simulations (n = 106).

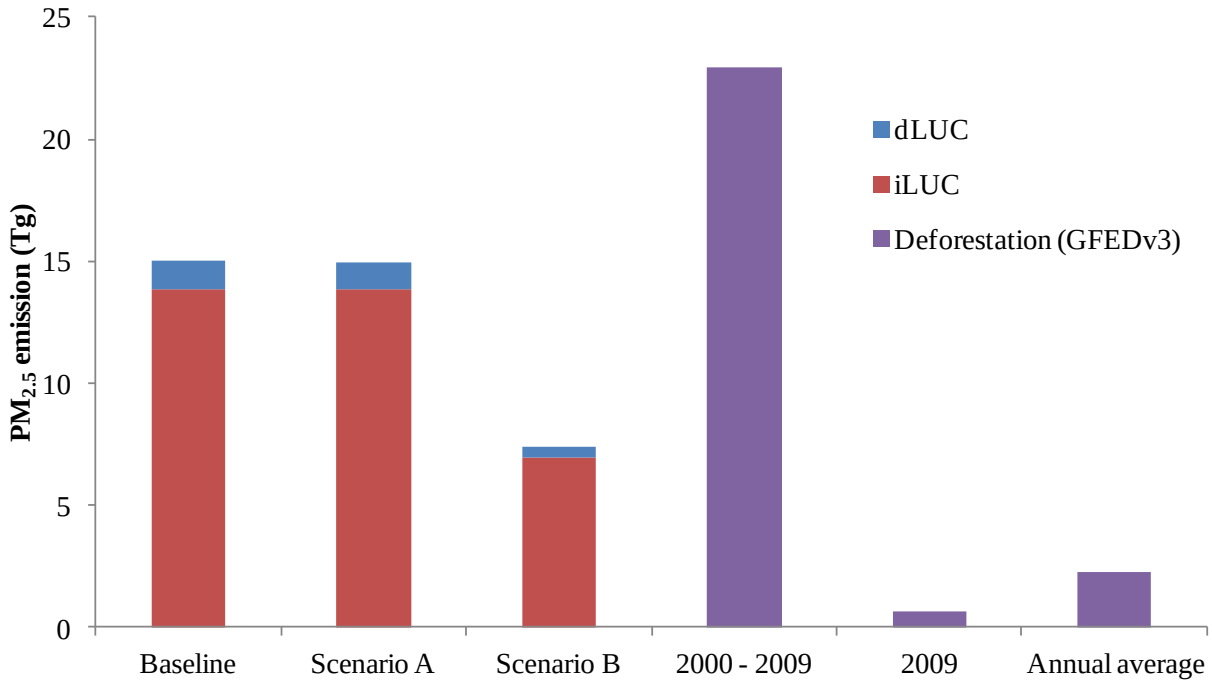

Figure 3.3: Baseline estimates of PM2.5 emission for LUC with two burning control scenarios: (A) 50% reduction of burning practices in São Paulo state and (B) banning open burning practices in São Paulo state and 50% reduction of burning practices in the else states. Estimates are compared with PM2.5 emission from total deforestation in Brazil based on GFEDv3.

3.3.2 Spatial Analysis of LUC emissions

Figure 3.4 shows the spatial distribution of LUC emissions for the baseline case. Our results show that dLUC emissions mostly occur in southern Mato Grosso, Goiás, Minas Gerais, Rio de Janeiro, São Paulo, Mato Grosso do Sul, and some areas in southern and northeastern regions. iLUC emissions, which are more significant than dLUC emission, are concentrated along the frontier of the Amazonia rainforest (Northern Mato Grosso, Rondônia, Amazonas, Acre, and Pará). The largest LUC emissions occur in Mato Grosso State where nearly three million residents live, suggesting the potential for public health impacts.

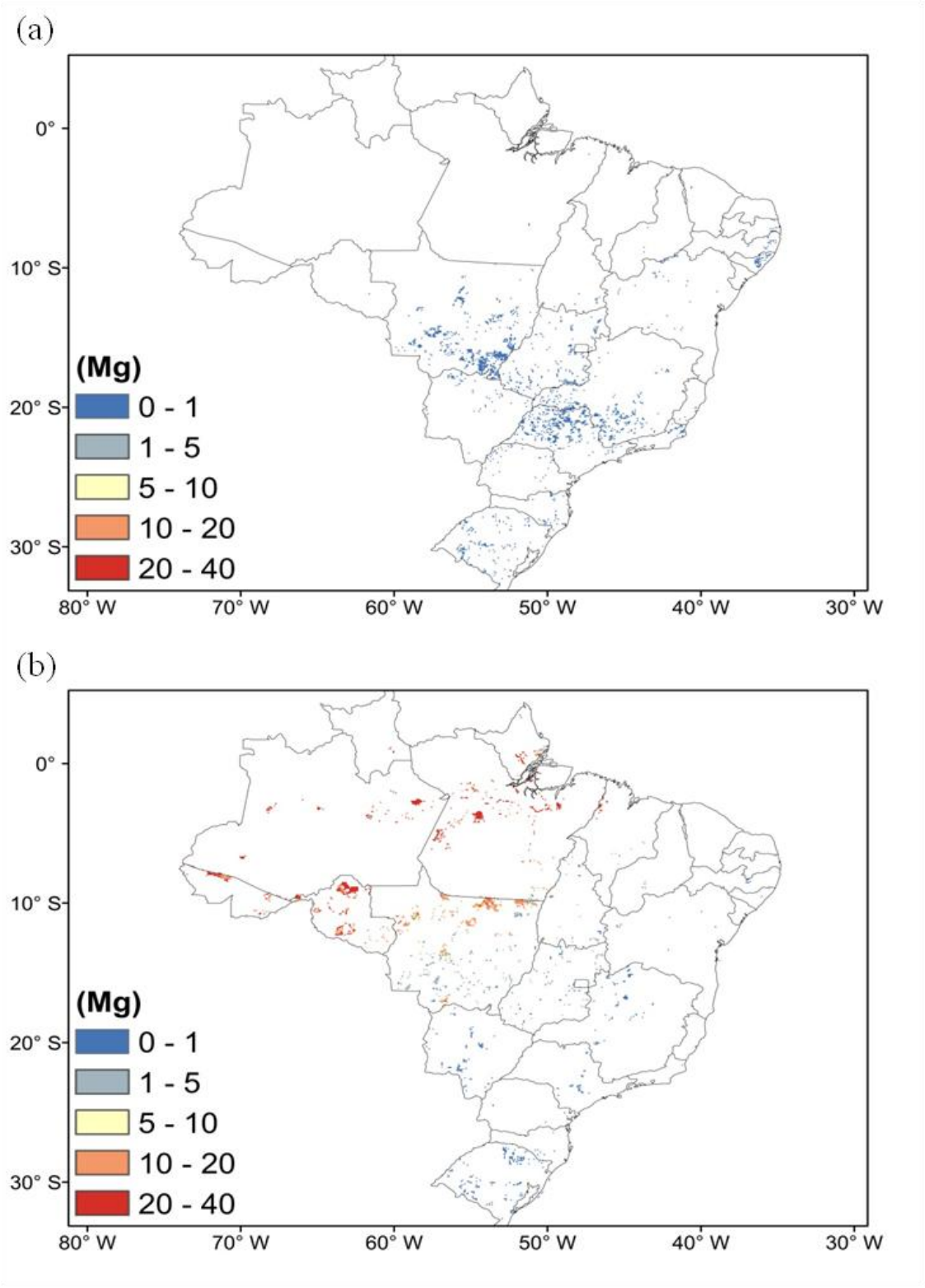

Figure 3.4: Spatial distribution of PM2.5 emission from LUC including (a) dLUC; (b) iLUC

3.3.3 Comparison of LUC and Life-cycle Emission for Fuels

Normalized LUC emissions on the basis of a functional unit (1 mmBTU fuel) are further compared with non-LUC life-cycle stages of Brazilian biofuels and with life-cycle emissions of gasoline and diesel (Figure 3.5). Life-cycle emissions are taken from the GREET model [38]. Normalized LUC emissions are based on three cases of production periods (15, 30, 45 years). LUC emissions (ranging from 247 to 740 g $PM_{2.5}$ emitted per mmBTU fuel) exceed the sum of emissions from the other life-cycle phases of sugarcane ethanol (299 g $PM_{2.5}$ emitted per mmBTU fuel). These non-LUC emissions are dominated by pre-harvesting burning of sugarcane fields. LUC emissions are 49 to 148 times higher than the life-cycle emissions of conventional fossil fuels (5 g $PM_{2.5}$ emitted per mmBTU fuel for both conventional gasoline and diesel). In general, including the LUC phase, Brazilian biofuels have much larger life-cycle emissions than conventional fossil fuels for all six regulated air pollutants. Even if sugarcane pre-harvesting burning is eliminated in the future, Brazilian biofuels are still likely to have higher air pollution impacts than conventional fossil fuels due to LUC effects.

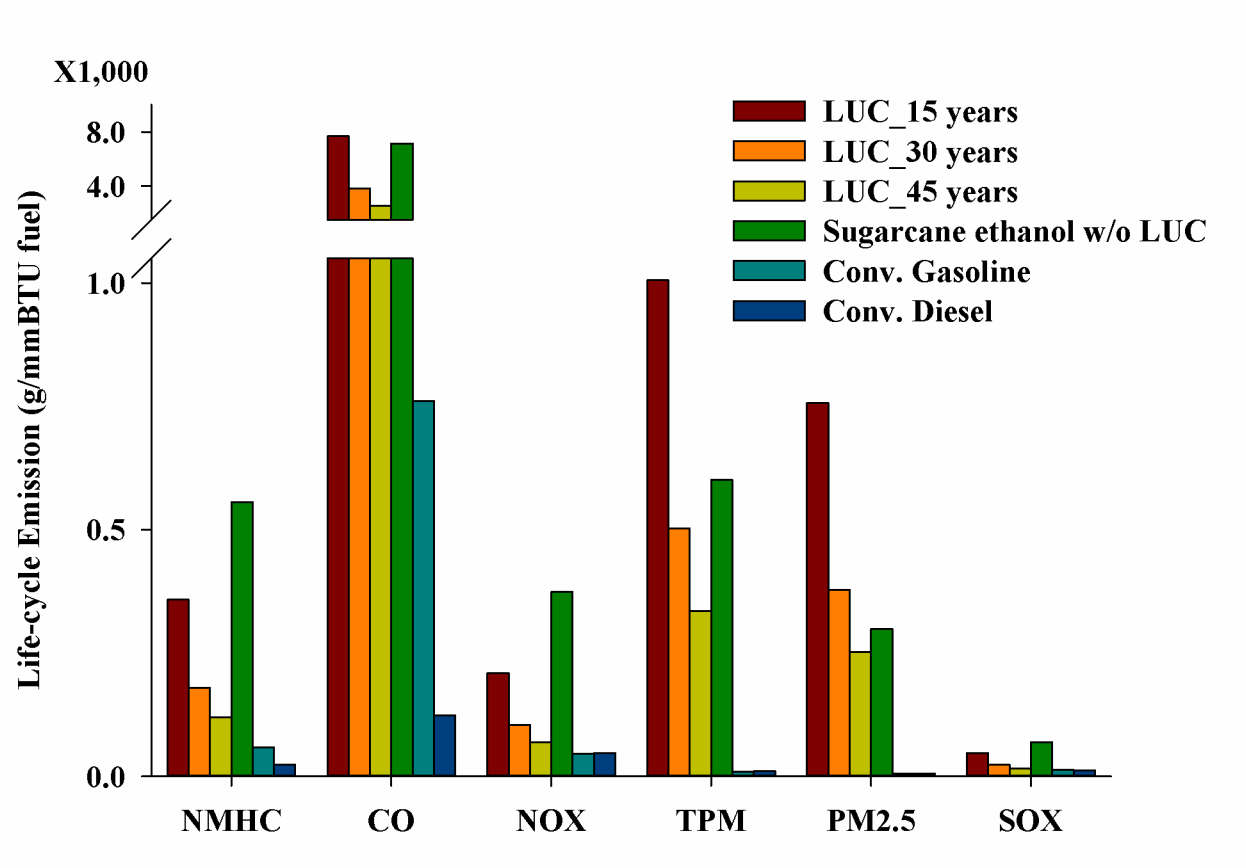

Figure 3.5: Comparisons of life-cycle emissions from LUC phase and other life-cycle phases of equivalent biofuels and fossil fuels.

3.4 Discussion and Conclusion

We found that LUC emissions, particularly iLUC (F2R), associated with an incremental increase in the supply of biofuels are expected to be significant under current burning practices. The planned reductions in pre-harvest burning will have positive impacts locally, but the LUC emissions will remain large unless burning practices for deforestation (F2R) are eliminated. The largest uncertainty in LUC emissions is from the CF for deforestation, ranging from 65% to 133% of baseline estimates. These LUC emissions may be underestimated as the CFs used in the analysis are measured from wild or prescribed fires [23, 30]. The practices for LUC, unlike wild or prescribed fire, involve slash-and-burn to remove biomass. In some cases, additional burns may occur two or three more times if the first fire has not removed enough slash [39].

Other important sources of uncertainty for LUC emissions are the magnitude and spatial distribution of the areas of LUC. The spatially explicit data of LUC expansion used in this study is derived via a modeling framework comprising a partial equilibrium model and a dynamic ecological model. The estimate of model uncertainties associated with these elements is not addressed in their work, although the projection of cropland area shows similarity to FAO (Food and Agriculture Organization) statistics [4]. Plevin et al. examined the uncertainty of iLUC emission (GHG) from US corn ethanol derived by the product of five parameters, i.e. average fuel yield, net displacement factor, ecosystem conversion fractions, land conversion CO_2 emission factors, and production period. The bounding values of three parameters associated with global LUC projection were determined from the average fuel yield (3500~ 4500 L $ha^{-1}yr^{-1}$), net displacement factor

(25%~80%), and ecosystem conversion fractions (45%~85%) [7]. These variables contribute to significant variation of global LUC emissions. Further work to determine the uncertainty and to improve the accuracy of LUC area projections is needed.

The emissions estimates presented here could provide valuable input to regional air quality models that are used to assess human health outcomes and regional climate impacts. However, the temporal allocation of LUC emissions, another major factor influencing health outcomes, remains to be determined. Burning practices for LUC in Brazil are usually concentrated in the end of dry season, August or September, depending on the location of LUC [40, 41]. Temporal concentration of emissions could exacerbate air quality impacts. These results suggest that careful management of LUC is essential for ensuring the sustainability of Brazilian biofuels and to prevent potential hazards from air pollution.

Reference

1. Farrell, A. E.; Plevin, R. J.; Turner, B. T.; Jones, A. D.; O'Hare, M.; Kammen, D. M., Ethanol can contribute to energy and environmental goals. *Science* **2006,** *311*, (5760), 506-508.
2. Field, C. B.; Campbell, J. E.; Lobell, D. B., Biomass energy: the scale of the potential resource. *Trends Ecol. Evol.* **2008,** *23*, (2), 65-72.
3. Schneider, U. A.; McCarl, B. A., Economic potential of biomass based fuels for greenhouse gas emission mitigation. *Environ. Resour. Econ.* **2003,** *24*, (4), 291-312.
4. Lapola, D. M.; Schaldach, R.; Alcamo, J.; Bondeau, A.; Koch, J.; Koelking, C.; Priess, J. A., Indirect land-use changes can overcome carbon savings from biofuels in Brazil. *Proc. Natl. Acad. Sci. U. S. A.* **2010,** *107*, (8), 3388-3393.
5. Pousa, G.; Santos, A. L. F.; Suarez, P. A. Z., History and policy of biodiesel in Brazil. *Energy Policy* **2007,** *35*, (11), 5393-5398.
6. Campbell, J. E.; Block, E., Land-use and alternative bioenergy pathways for waste biomass. *Environmental Science & Technology* **2010,** *44*, (22), 8665-8669.
7. Plevin, R. J.; O'Hare, M.; Jones, A. D.; Torn, M. S.; Gibbs, H. K., Greenhouse gas emissions from biofuels' indirect land use change are uncertain but may be much greater than previously estimated. *Environmental Science & Technology* **2010,** *44*, (21), 8015-8021.
8. Searchinger, T.; Heimlich, R.; Houghton, R. A.; Dong, F. X.; Elobeid, A.; Fabiosa, J.; Tokgoz, S.; Hayes, D.; Yu, T. H., Use of US croplands for biofuels increases greenhouse gases through emissions from land-use change. *Science* **2008,** *319*, (5867), 1238-1240.
9. Fargione, J.; Hill, J.; Tilman, D.; Polasky, S.; Hawthorne, P., Land clearing and the biofuel carbon debt. *Science* **2008,** *319*, (5867), 1235-1238.
10. Foley, J. A.; DeFries, R.; Asner, G. P.; Barford, C.; Bonan, G.; Carpenter, S. R.; Chapin, F. S.; Coe, M. T.; Daily, G. C.; Gibbs, H. K.; Helkowski, J. H.; Holloway, T.; Howard, E. A.; Kucharik, C. J.; Monfreda, C.; Patz, J. A.; Prentice, I. C.; Ramankutty, N.; Snyder, P. K., Global consequences of land use. *Science* **2005,** *309*, (5734), 570-574.
11. Fritsche, U. R.; Sims, R. E. H.; Monti, A., Direct and indirect land-use competition issues for energy crops and their sustainable production - an overview. *Biofuels Bioproducts & Biorefining-Biofpr* **2010,** *4*, (6), 692-704.
12. Phalan, B., The social and environmental impacts of biofuels in Asia: An overview. *Applied Energy* **2009,** *86*, S21-S29.
13. Ros, J.; Overmars, K. P.; Stehfest, E.; Prins, A. G.; Notenboom, J.; van Oorschot, M. *Identifying the indirect effects of bio-energy production*; Netherlands Environmental Assessment Agency (PBL): Bilthoven, February 2010, 2010.

14. van Oorschot, M.; Ros, J.; Notenboom, J. *Evaluation of the indirect effects of biofuel production on biodiversity: Assessment across spatial and temporal scales*; Netherlands Environmental Assessment Agency (PBL): Bilthoven, 2010.

15. Ward, D. E.; Susott, R. A.; Kauffman, J. B.; Babbitt, R. E.; Cummings, D. L.; Dias, B.; Holben, B. N.; Kaufman, Y. J.; Rasmussen, R. A.; Setzer, A. W., Smoke and fire characteristics for cerrado and deforestation burns in Brazil - Base-B experiment. *J. Geophys. Res.-Atmos.* **1992,** *97*, (D13), 14601-14619.

16. Macedo, I. C.; Seabra, J. E. A.; Silva, J., Green house gases emissions in the production and use of ethanol from sugarcane in Brazil: The 2005/2006 averages and a prediction for 2020. *Biomass & Bioenergy* **2008,** *32*, (7), 582-595.

17. Tsao, C. C.; Campbell, J. E.; Mena-Carrasco, M.; Spak, S. N.; Carmichael, G. R.; Chen, Y., Increased estimates of air-pollution emissions from Brazilian sugar-cane ethanol. *Nature Climate Change* **2012,** *2*, (1), 53-57.

18. van der Werf, G. R.; Randerson, J. T.; Giglio, L.; Collatz, G. J.; Mu, M.; Kasibhatla, P. S.; Morton, D. C.; DeFries, R. S.; Jin, Y.; van Leeuwen, T. T., Global fire emissions and the contribution of deforestation, savanna, forest, agricultural, and peat fires (1997-2009). *Atmos. Chem. Phys.* **2010,** *10*, (23), 11707-11735.

19. Loarie, S. R.; Asner, G. P.; Field, C. B., Boosted carbon emissions from Amazon deforestation. *Geophysical Research Letters* **2009,** *36*, (14), L14810 (5 pp.)-L14810 (5 pp.).

20. Carvalho, J. L. N.; Cerri, C. E. P.; Feigl, B. J.; Piccolo, M. D.; Godinho, V. D.; Herpin, U.; Cerri, C. C., Conversion of cerrado into agricultural land in the south-western amazon: Carbon stocks and soil fertility. *Sci. Agric.* **2009,** *66*, (2), 233-241.

21. Levine, J. S.; Cofer, W. R.; Cahoon, D. R.; Winstead, E. L., Biomass burning - A driver for global change. *Environmental Science & Technology* **1995,** *29*, (3), A120-A125.

22. OECD/FAO, *OECD-FAO Agricultural Outlook 2011-2020*. OECD Publishing and FAO: 2011.

23. Paustian, K.; Ravindranath, N. H.; Amstel, A. v. *2006 IPCC Guidelines for National Greenhouse Gas Inventories*; Intergovernmental Panel on Climate Change: Hayama, Japan, 2006.

24. Potter, C.; Klooster, S.; Genovese, V., Carbon emissions from deforestation in the Brazilian Amazon region. *Biogeosciences* **2009,** *6*, (11), 2369-2381.

25. Field, C. B.; Randerson, J. T.; Malmstrom, C. M., Global net primary production - Combining ecology and remote-sensing. *Remote Sens. Environ.* **1995,** *51*, (1), 74-88.

26. Saatchi, S. S.; Houghton, R. A.; Alvala, R.; Soares, J. V.; Yu, Y., Distribution of aboveground live biomass in the Amazon basin. *Global Change Biology* **2007,** *13*, (4), 816-837.

27. Potter, C. S.; Randerson, J. T.; Field, C. B.; Matson, P. A.; Vitousek, P. M.; Mooney, H. A.; Klooster, S. A., Terrestrial ecosystem production - A process model-based on

global satellite and surface data. *Global Biogeochemical Cycles* **1993,** *7*, (4), 811-841.

28. Wiedinmyer, C.; Akagi, S. K.; Yokelson, R. J.; Emmons, L. K.; Saadi, J. A.; Orlando, J. J.; Soja, A. J., The Fire INventory from NCAR (FINN) – a high resolution global model to estimate the emissions from open burning. *Geosci. Model Dev.* **2011,** *4*, (3), 625-641.
29. van der Werf, G. R.; Randerson, J. T.; Giglio, L.; Collatz, G. J.; Kasibhatla, P. S.; Arellano, A. F., Interannual variability in global biomass burning emissions from 1997 to 2004. *Atmos. Chem. Phys.* **2006,** *6*, 3423-3441.
30. Carvalho, J. A.; Higuchi, N.; Araujo, T. M.; Santos, J. C., Combustion completeness in a rainforest clearing experiment in Manaus, Brazil. *J. Geophys. Res.-Atmos.* **1998,** *103*, (D11), 13195-13199.
31. Houghton, R. A.; Skole, D. L.; Nobre, C. A.; Hackler, J. L.; Lawrence, K. T.; Chomentowski, W. H., Annual fluxes or carbon from deforestation and regrowth in the Brazilian Amazon. *Nature* **2000,** *403*, (6767), 301-304.
32. Moghaddas, E. E. Y.; Stephens, S. L., Thinning, burning, and thin-burn fuel treatment effects on soil properties in a Sierra Nevada mixed-conifer forest. *For. Ecol. Manage.* **2007,** *250*, (3), 156-166.
33. Rau, B. M.; Johnson, D. W.; Chambers, J. C.; Blank, R. R.; Lucchesi, A., Estimating root biomass and distribution after fire in a great basin woodland using cores and pits. *West. North Am. Naturalist* **2009,** *69*, (4), 459-468.
34. Tufekcioglu, A.; Kucuk, M.; Saglam, B.; Bilgili, E.; Altun, L., Soil properties and root biomass responses to prescribed burning in young corsican pine (Pinus nigra Arn.) stands. *J.Environ.Biol.* **2010,** *31*, (3), 369-373.
35. Reinhardt, T. E.; Ottmar, R. D.; Castilla, C., Smoke impacts from agricultural burning in a rural Brazilian town. *Journal of the Air & Waste Management Association* **2001,** *51*, (3), 443-450.
36. Rudorff, B. F. T.; Aguiar, D. A.; Silva, W. F.; Sugawara, L. M.; Adami, M.; Moreira, M. A., Studies on the rapid expansion of sugarcane for ethanol production in Sao Paulo State (Brazil) using Landsat data. *Remote Sensing* **2010,** *2*, (4), 1057-1076.
37. O'Hare, M.; Plevin, R. J.; Martin, J. I.; Jones, A. D.; Kendall, A.; Hopson, E., Proper accounting for time increases crop-based biofuels' greenhouse gas deficit versus petroleum. *Environ. Res. Lett.* **2009,** *4*, (2), 024001.
38. Wang, M.; Wu, M.; Huo, H.; Liu, J. H., Life-cycle energy use and greenhouse gas emission implications of Brazilian sugarcane ethanol simulated with the GREET model. *Int. Sugar J.* **2008,** *110*, (1317), 527-545.
39. Peters, W. J.; Neuenschwander, L. F., *Slash and Burn : Farming in the Third World Forest*. University of Idaho Press: Moscow, Idah, 1988; p 12.
40. Balch, J. K.; Nepstad, D. C.; Curran, L. M.; Brando, P. M.; Portela, O.; Guilherme, P.; Reuning-Scherer, J. D.; de Carvalho, O., Size, species, and fire behavior predict

tree and liana mortality from experimental burns in the Brazilian Amazon. *For. Ecol. Manage.* **2011,** *261*, (1), 68-77.

41. Guild, L. S.; Kauffman, J. B.; Ellingson, L. J.; Cummings, D. L.; Castro, E. A., Dynamics associated with total aboveground biomass, C, nutrient pools, and biomass burning of primary forest and pasture in Rondonia, Brazil during SCAR-B. *J. Geophys. Res.-Atmos.* **1998,** *103*, (D24), 32091-32100.

Chapter 4 Health Impacts Assessments of Brazilian Ethanol

4.1 Introduction

Each year, around a quarter of total world energy use, dominated by conventional fossil fuels, is consumed by transportation sector[1], which is responsible for 13% worldwide greenhouse gas (GHG) emissions [1]. The demand for transportation fuels expects to grow due to recent economic boost of developing countries. To maintain a stable fuel supply and avoid adverse consequence of global climate, finding affordable, renewable, and green alternatives is desperate.

Biomass-based liquid fuels as renewable energy sources can provide benefits that offset GHG emissions and reduce reliance on diminishing fossil fuels [2, 3]. The production and use of renewable transportation biofuels in the United States has been promoted through tax incentives and a mandated blending into vehicle fuel supply based on Energy Policy Act of 2005 (EPAct) and Energy Independence and Security Act of 2007 (EISA). However, the displacement of conventional fossil fuels with biofuels might bring a wide range of environmental and economic impacts. Recent research found that incremental use of biofuels might affect global food supply, water resources, and GHG reduction performance depending on pathways of production and land-use management[4-7]. Health impacts associated with air quality changes as a result of fuel substitution are also concerned by the public. The health consequences of mobile emissions due to a large-scale conversion from gasoline to E85 may result in enhanced health risks due to increased tropospheric ozone concentrations resulting from E85

[1] http://www.iea.org/stats/index.asp

vehicle emissions [8]. Monetizing the health impacts of life-cycle ethanol emissions (fuel production and vehicle emissions) of fine particulate matter emissions ($PM_{2.5}$) suggests that corn ethanol has higher health costs than gasoline while cellulosic ethanol may reduce costs [9].

Brazilian sugarcane ethanol, accounting for 25% global fuel ethanol production, is one of the most widely used biofuels[2]. Recent life-cycle assessments suggest that significant emissions of criteria air pollutants could occur, particularly during pre-harvest burning and indirect land-use phases, and much greater than other conventional liquid fuels [10, 11]. However, air-pollution-related health issues from the large-scale production and use of sugarcane ethanol have not been thoroughly examined. Herein, we established a framework combining life-cycle emission modeling, air quality simulation, and epidemiological models to examine the health impacts. A bottom-up model was first applied to estimate spatially and temporally explicit emissions through a life-cycle of sugarcane ethanol. We then simulated the changes of ambient concentration using the Weather Research and Forecasting model coupled with Chemistry (WRF-Chem). Health impacts were further quantified by epidemiological CRFs (concentration response functions) with the output of air quality changes and demographic data. Results were further compared with scenarios.

[2] http://ethanolrfa.org/pages/World-Fuel-Ethanol-Production

4.2 Methodology

4.2.1 Air Quality Model[3]

Air quality changes due to incremental sugarcane ethanol were examined using the Weather Research and Forecasting model coupled with Chemistry (WRF-Chem) [12].WRF-Chem is a widely used online coupled chemistry-climate model that has been routinely applied to study air quality in South America[13-15]. In this study, the model was run to simulate hourly $PM_{2.5}$ and ozone concentrations for 2008 at 20 km horizontal resolution, with vertical 35 layers. The study domain shown in Figure 4.1 covers the central part of South America including all of Brazil. The horizontal domain of 236 × 216 grid cells is centered at 52.4°W and 16.6°S. Gas-phase photochemistry was simulated using CBM-Z [16] and aerosols using 8 sectional bins in MOSAIC [17]. Biogenic emissions were estimated online at each time step from hourly meteorology using the Model of Emissions of Gases and Aerosols from Nature (MEGAN 2.04) [18], with daily forest fire emissions from FINN [19]. Other WRF-Chem configuration options used in these simulations are identical to those in Saide et al. [20] and given in Table 4.1.

[3] Air quality modeling and simulation is done by Dr. Macelo Mena from University of Andre Bello, Chile and Dr. Scott Spak from University of Iowa. Emission data as inputs in WRF-Chem is done by Chi-Chung Tsao.

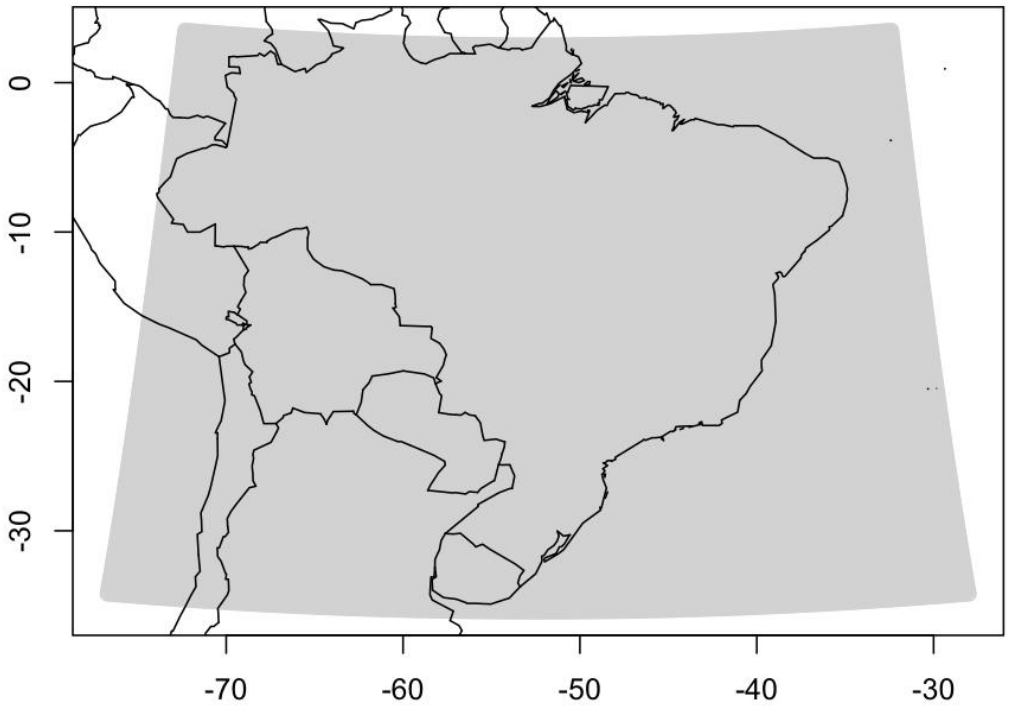

Figure 4.1: The study domain with the gridding of 20 km resolution

Table 4.1: Configurations of WRF-Chem model

Version	3.3.1
Microphysics	WSM 6-class [21]
Cumulus	Grell scheme
Planetary boundary layer	MYNN
Chemical mechanism	CBM-Z
Aerosol module	MOSAIC, 8 bins
Aerosol radiative effects	Direct, 1st & 2nd indirect, semi-direct
Biogenic emissions	MEGAN 2.04 [18]
Anthropogenic emissions	EDGAR 4.2 + Bond *et al.* [22]

4.2.2 Emission Estimations

4.2.2.1 Life-cycle Emissions of Sugarcane Ethanol

Spatially and temporally explicit emissions from Brazilian sugarcane ethanol were estimated by a bottom-up emission model based on Tsao et al.[11]. The model integrates emission factors and activity rates associated with emissions in different life-cycle phases. The annual emissions, E_{is}, of regulated pollutant *i* at location *s* is determined by aggregating the emissions from *p* phases, where *p* represents farming (*f*), field burning (*b*), refinery (*r*), transportation/distribution (T/D) (*t*), and vehicle use (*v*) phases as follows,

$$E_{is} = \sum_{p=f,b,r,t} \left[(Y_s \times CA_s \times CF_p) \times AR \times EF_{ip} \right] + \sum_{p=v} (POP_s \times ECC \times EF_{ip}) \quad (1)$$

where Y_s represents the spatial dataset of annual sugarcane yield (Mg/ha·yr), CA_s denotes the sugarcane crop area (ha) at location s, and CF_p denotes conversion factors. To improve the spatial accuracy of emissions in Tsao et al.[11], sugarcane cropland and pre-harvesting burning area (CA_s) data were obtained from high resolution Landsat images of CANASAT [23] instead of the data scaled from Monfreda et al's cropland data [24]. *AR* is the fraction of sugarcane production used for producing ethanol. EF_{ip} is the emission factor of pollutant *i* in the phase *p* from the Greenhouse Gases, Regulated Emissions, and Energy Use in Transportation (GREET) model. It was assumed that vehicle phase emissions are spatially related with population. POP_s denotes population at location s, and *ECC* denotes average ethanol consumption per capita (mmBTU/ca.). The spatial distribution of population was obtained from LandScan, a global population database with a resolution of 0.5 minute [25].

The annual life-cycle emissions for 2008 (B08) and incremental one billion gallon ethanol (BGE) were estimated by Equation (1). Assuming the same yield, sugarcane production for BGE was proportionally calculated by B08 level given 100% conversion from sugarcane to ethanol (AR = 100%). The fixed values for parameters in the life-cycle emission model are listed in Table 4.2. The emission product and its instructions for B08 and BGE can be accessed on the page: https://eng.ucmerced.edu/campbell.

Table 4.2: Parameters of the life-cycle emission model

	B08	BGE
Ethanol Production (Gal)	7×10^9	10^9
Yield (Mg sugarcane/ ha)	77.9	77.9
AR (%)	59	100
$CF_{f,b}$ (Mg/ Mg)	1	1
CF_r (Gal ethanol/ Mg sugarcane)	24	24
$CF_{t,v}$ (mmBTU ethanol/ Mg sugarcane)	1.824	1.824
ECC (mmBTU ethanol/ca.)	2.4	0.4

4.2.2.2 LUC Emissions

Spatially explicit emissions from LUC in Brazil due to incremental BGE were estimated by integrating predicted activities of LUC and emission factors [10]. Equation (2) formulates the LUC emissions,

$$E_i^{LUC} = \sum_{jks} \left[A_{js} \times F_{jks} \times CF_{jk} \times EF_{ijk} \right] \quad (2)$$

, where E_i^{LUC} (Mg emitted) is the LUC emissions of pollutant *i*. E_i^{LUC} is the aggregation of the emissions from different types (*j*) of LUC. A_{js} (ha) is the area for the *j* type LUC at location *s*. F_{jks} (Mg dried matter $\cdot$ ha^{-1}) is the removed biomass as the available fuel loading per area for burning practices due to the *j* type LUC and the *k* type biomass (i.e. aboveground or belowground biomass) at location *s*. CF_{jk} (%) is the fraction of fuel consumption relative to the total available fuel loading for the *j* type LUC and the *k* type biomass. EF_{ijk} (Mg emitted $\cdot$ Mg^{-1} dried matter) is the emission factor of the i^{th} pollutant for different types (i.e. *j* and *k*) of biomass burning.

The LUC area (A_{js}) for BGE case shown in Table 4.3 was calculated in a basis of LUC data estimated for incremental production of 35 billion liters sugarcane ethanol and 4 billion liter soybean biodiesel in a Brazilian study [7]. Firstly, LUC caused by incremental sugarcane ethanol was selected. Assuming the same spatial profile, LUC area was then scaled down by 0.1081 due to the shrinkage from 35 billion liters to 1 billion gallons ethanol.

Available fuel loading per area (F_{jks}) was derived from the difference of available aboveground and belowground biomass before and after LUC. We synthesized carbon stocks and fuel loading information from Saatchi et al. [26] and Fargione et al. [6] and

developed a spatially explicit dataset of potential fuel loadings for LUC. Emission factors (EF_{ij}) representing emission intensity per unit fuel burned (g kg dried matter burned^{-1}) were obtained from the van der Werf et al. [27] and Wiedinmyer et al. [19] studies of biomass fire emissions. We also assumed the emission factor for belowground biomass burning is the same as aboveground biomass. The fraction (CF) of fuel consumption relative to the total available fuel loading were synthesized from IPCC [28], Carvalho et al.[29], Tufekcioglu et al. [30], and Rau et al. [31]. The detail information for LUC emissions can be found at https://eng.ucmerced.edu/campbell.

Table 4.3: Summary of LUC area for BGE and data reported in Lapola et al.[7].

			dLUC					iLUC		
Type	**F2B**	**R2B**	**W2B**	**O2B**	**C2B**	**F2R**	**R2C**	**W2R**	**O2R**	**C2R**
LUC for ethanol and biodiesel (10^3 km^2)	2	146	2	1	14	122	16	20	26	2
LUC for ethanol (10^3 km^2)	0	53	0	0	4	52	6	8	11	1
LUC for BGE (10^3 km^2)	0	5.73	0	0	0.43	5.62	0.65	0.86	1.19	0.11
Fraction	0	39.3	0	0	2.9	38.5	4.5	5.9	8.2	0.8

4.2.2.3 Life-cycle Emissions of Conventional Gasoline

Life-cycle emissions for BGE equivalent convention gasoline (CG) including two phases, i.e. refinery and vehicle use phase, were modeled. We applied emission factors based on the GREET model for each phase. Information for Brazilian refineries was obtained from the Brazilian Institute of Geography and Statistics (IBGE), and the latitudes and longitudes of refineries were located via Google Earth©. We simply assumed that additional BGE equivalent conventional gasoline is produced proportionally to the production capacity of Brazilian refineries in 2008. Table 4.4 shows their location and emissions for six criteria air pollutants. Emissions for vehicle use phase which are related to population, fuel consumption, and emission factors were calculated through the same approach to the BGE case. The emission product and its instructions for CG can be accessed on the page: https://eng.ucmerced.edu/campbell.

Table 4.4: Location and emissions of refineries for conventional gasoline in Brazil

Refinery name	latitude	longitude	production (mmBTU)	NMHC (Mg/y)	CO (Mg/y)	NO_X (Mg/y)	PM_{10} (Mg/y)	PM_{25} (Mg/y)	SO_X (Mg/y)
Paulinia-São Paulo	-22.7299	-47.1353	1.40E+07	322.84	94.16	283.02	106.92	40.42	192.89
Mataripe-Bahia	-12.7077	-38.5717	1.17E+07	270.91	79.01	237.50	89.72	33.92	161.86
Duque de Caxias-Rio de Janeiro	-22.7217	-43.2602	9.29E+06	214.18	62.47	187.77	70.93	26.81	127.97
São Jose dos Campos-São Paulo	-23.1915	-45.821	9.66E+06	222.76	64.97	195.29	73.78	27.89	133.09
Canoas-Rio Grande do Sul	-29.8743	-51.1625	7.24E+06	166.86	48.67	146.28	55.26	20.89	99.70
Araucaria-Paraná	-25.5728	-49.3638	7.24E+06	166.86	48.67	146.28	55.26	20.89	99.70
Cubatao-São Paulo	-23.8712	-46.4323	6.52E+06	150.26	43.83	131.73	49.76	18.81	89.78
Betim Minas Gerais	-19.9732	-44.095	5.79E+06	133.56	38.96	117.09	44.23	16.72	79.80
Refinaria de Petróleo Ipiranga	-32.0443	-52.0884	2.42E+06	55.85	16.29	48.96	18.50	6.99	33.37
Manaus, Amazonas	-3.14677	-59.9532	2.42E+06	55.85	16.29	48.96	18.50	6.99	33.37

4.2.3 Scenarios and Emission Themes Preparation

Four emission themes associated with the production and uses of fuels were prepared for air quality simulation (via WRF-Chem) of scenarios in Brazil. In a background case, we used 2008 life-cycle emission dataset for Brazilian sugarcane ethanol (B08). To examine effects of incremental ethanol, additional three emission themes were set for life-cycle emissions of one billion gallon ethanol (1BGE) and emissions from land-use change (LUC) due to 1BGE, and life-cycle emissions of 1BGE equivalent conventional gasoline (CG). Table 4.5 summarizes emission themes and scenarios. Each emission theme was developed from annual emissions with proper temporal and vertical profiles and VOC speciation.

Monthly profiles for four emission themes are shown in Table 4.6. We applied monthly allocation factors which are derived from the monthly intensity of emission activities for each phase [11] in B08 and BGE emission themes. We also assumed a uniform monthly profile for refinery and vehicle use phase in CG emission theme due to year-round production and use of conventional gasoline. Because LUC emissions associated with biomass burning have similar monthly pattern of biomass fire emissions, we made the monthly profiles for LUC based on FINN emission data. Fire emissions from deforestation and savanna burning are considered in the calculation since the two type emissions contribute the most LUC emissions [7].

For diurnal profiles (Table 4.7), we assumed point source (refinery) and farming related emissions (farming and T/D) are constant. Diurnal cycle (as a % of total) for vehicle use phase and LUC emissions was assumed the same as area sources. Diurnal

cycle for sugarcane pre-harvesting burning emissions was based on the daily pattern of pre-harvesting burning in a Brazilian study [32].

Vertical profiles for each emission scheme were assigned. We assumed a fixed distribution that accounts for point sources (refinery phases) and area sources (the other phases). Table 4.8 shows the vertical profiles of emission themes.

VOC emissions were speciated by the information of emission characteristics from USEPA SPECIATE database and a literature [33]. The speciated organic species were further aggregated using RADM2 mechanism [34] with updates to the original mechanism [35]. Table 4.9 shows the fractions of VOC emissions in each species group.

Table 4.5: Scenarios and associated emission themes

Scenario	Scenario Description	Emission Themes [a]
B	Background	B08-b; B08-no-b
I1	Incremental 1 billion gallon ethanol	B08-b; B08-no-b; 1BGE-b; 1BGE-no-b
I2	Incremental1 billion gallon ethanol with LUC emissions	B08-b; B08-no-b; 1BGE-b; 1BGE-no-b; LUC
I3	Incremental1 billion gallon ethanol equivalent conventional gasoline	B08-b; B08-no-b; CG

[a]: B08-b: Field burning phase of 2008 life-cycle emission dataset for Brazilian sugarcane ethanol
B08-no-b: The other phases (farming, refinery, transportation and distribution, and vehicle use) of 2008 life-cycle emission dataset for Brazilian sugarcane ethanol
1BGE-b: Field burning phase of life-cycle emissions for one billion gallon ethanol
1BGE-no-b: The other phases (farming, refinery, transportation and distribution, and vehicle use) of life-cycle emissions for one billion gallon ethanol
LUC: LUC phase of life-cycle emissions for one billion gallon ethanol

Table 4.6: Monthly profiles for life-cycle emissions in different phases of an emission theme

Emission Theme	B08/BGE					CG		LUC
Phase [a]	F	B	R	T/D	V	R	V	LUC
Jan	9.4%	0.3%	0.3%	8.3%	8.3%	8.3%	8.3%	1.5%
Feb	10.0%	0.0%	0.0%	8.3%	8.3%	8.3%	8.3%	1.7%
Mar	10.0%	0.0%	0.0%	8.3%	8.3%	8.3%	8.3%	1.7%
Apr	9.6%	3.9%	3.9%	8.3%	8.3%	8.3%	8.3%	1.4%
May	8.5%	11.3%	11.3%	8.3%	8.3%	8.3%	8.3%	1.1%
Jun	7.6%	13.2%	13.2%	8.3%	8.3%	8.3%	8.3%	1.5%
Jul	7.2%	14.6%	14.6%	8.3%	8.3%	8.3%	8.3%	6.8%
Aug	7.2%	13.7%	13.7%	8.3%	8.3%	8.3%	8.3%	21.7%
Sep	7.3%	13.5%	13.5%	8.3%	8.3%	8.3%	8.3%	30.3%
Oct	7.4%	12.4%	12.4%	8.3%	8.3%	8.3%	8.3%	19.2%
Nov	7.6%	11.5%	11.5%	8.3%	8.3%	8.3%	8.3%	9.6%
Dec	8.3%	5.6%	5.6%	8.3%	8.3%	8.3%	8.3%	3.4%

Table 4.7: Diurnal profiles for life-cycle emissions in different phases of an emission theme

Emission Theme	B08/BGE					CG		LUC
Phase	F	B	R	T/D	V	R	V	LUC
00:00	4.2%	0.0%	4.2%	4.2%	3.9%	4.2%	3.9%	3.9%
01:00	4.2%	0.0%	4.2%	4.2%	3.0%	4.2%	3.0%	3.0%
02:00	4.2%	0.0%	4.2%	4.2%	2.8%	4.2%	2.8%	2.8%
03:00	4.2%	0.0%	4.2%	4.2%	2.8%	4.2%	2.8%	2.8%
04:00	4.2%	0.0%	4.2%	4.2%	2.8%	4.2%	2.8%	2.8%
05:00	4.2%	0.0%	4.2%	4.2%	2.8%	4.2%	2.8%	2.8%
06:00	4.2%	0.0%	4.2%	4.2%	3.9%	4.2%	3.9%	3.9%
07:00	4.2%	0.0%	4.2%	4.2%	4.8%	4.2%	4.8%	4.8%
08:00	4.2%	0.0%	4.2%	4.2%	5.8%	4.2%	5.8%	5.8%
09:00	4.2%	0.0%	4.2%	4.2%	4.3%	4.2%	4.3%	4.3%
10:00	4.2%	0.0%	4.2%	4.2%	3.9%	4.2%	3.9%	3.9%
11:00	4.2%	0.0%	4.2%	4.2%	3.9%	4.2%	3.9%	3.9%
12:00	4.2%	0.0%	4.2%	4.2%	4.3%	4.2%	4.3%	4.3%
13:00	4.2%	0.0%	4.2%	4.2%	4.3%	4.2%	4.3%	4.3%
14:00	4.2%	0.0%	4.2%	4.2%	3.9%	4.2%	3.9%	3.9%
15:00	4.2%	0.0%	4.2%	4.2%	3.9%	4.2%	3.9%	3.9%
16:00	4.2%	0.0%	4.2%	4.2%	4.5%	4.2%	4.5%	4.5%
17:00	4.2%	11.8%	4.2%	4.2%	5.4%	4.2%	5.4%	5.4%
18:00	4.2%	22.4%	4.2%	4.2%	5.8%	4.2%	5.8%	5.8%
19:00	4.2%	20.5%	4.2%	4.2%	5.2%	4.2%	5.2%	5.2%
20:00	4.2%	18.6%	4.2%	4.2%	4.8%	4.2%	4.8%	4.8%
21:00	4.2%	13.7%	4.2%	4.2%	4.8%	4.2%	4.8%	4.8%
22:00	4.2%	7.5%	4.2%	4.2%	4.1%	4.2%	4.1%	4.1%
23:00	4.2%	5.5%	4.2%	4.2%	3.9%	4.2%	3.9%	3.9%

Table 4.8: Vertical profiles for life-cycle emissions in different phases of an emission theme

Emission Theme	B08/BGE					CG		LUC
Phase	F	B	R	T/D	V	R	V	LUC
<30 m	70%	70%	0	70%	70%	0	70%	70%
30-80 m	30%	30%	30%	30%	30%	30%	30%	30%
80-120 m	0	0	50%	0	0	50%	0	0
120-250 m	0	0	20%	0	0	20%	0	0
>250 m	0	0	0	0	0	0	0	0

Table 4.9: VOC speciation for life-cycle emissions in different phases of an emission theme

Emission Theme	B08/BGE					CG		LUC
Phase	F [a]	B [b]	R [c]	T/D [d]	V [e]	R [f]	V [g]	LUC [h]
ETH	0.652%	0.000%	0.000%	2.713%	4.393%	32.801%	12.868%	9.480%
HC3	2.889%	0.000%	29.054%	6.948%	66.984%	18.744%	6.397%	8.586%
HC5	1.093%	0.000%	0.000%	6.240%	2.733%	12.553%	20.526%	0.852%
HC8	0.739%	0.000%	3.879%	1.767%	1.077%	7.308%	1.296%	1.161%
OL2	17.633%	0.000%	0.000%	32.174%	10.242%	2.861%	5.911%	16.866%
OLT	4.284%	0.000%	0.000%	8.594%	0.661%	6.674%	4.379%	4.442%
OLI	0.928%	0.000%	0.000%	5.836%	1.187%	2.107%	8.248%	1.538%
TOL	1.148%	0.481%	0.000%	1.576%	0.887%	2.889%	14.712%	1.243%
XYL	0.985%	0.257%	0.000%	0.995%	0.799%	2.564%	16.263%	2.511%
HCHO	16.852%	64.957%	21.306%	13.061%	2.210%	0.000%	0.000%	11.048%
ALD	8.555%	32.493%	17.473%	7.086%	12.830%	0.000%	0.000%	4.431%
KET	1.831%	0.000%	0.120%	1.834%	0.035%	0.000%	0.000%	2.256%
ISO	0.000%	0.000%	0.000%	0.099%	0.034%	0.051%	0.000%	0.064%
CSL	0.002%	0.000%	0.000%	0.000%	0.000%	0.043%	0.000%	0.016%
ORA1	0.000%	0.000%	5.749%	0.000%	0.000%	0.000%	0.000%	6.002%
ORA2	0.000%	0.000%	5.765%	0.000%	0.000%	0.000%	0.000%	8.760%
GLY	0.000%	0.000%	0.000%	0.562%	0.000%	0.000%	0.000%	0.000%
MGLY	0.000%	0.000%	1.218%	0.000%	0.000%	0.000%	0.000%	2.677%
MVK	0.001%	0.000%	0.000%	0.000%	0.000%	0.010%	0.000%	0.000%
NVOL	0.000%	0.001%	0.000%	0.000%	0.000%	0.000%	0.000%	0.000%

[a]: Diesel exhaust - farm equipment (USEPA SPECIATE v4.3)
[b]: VOC characteristics of sugarcane field burning from Hall et al. (2012)
[c]: Dry mill fuel ethanol production - whole facility (USEPA SPECIATE v4.3)
[d]: Diesel exhaust emissions from pre-2007 model year heavy-duty diesel trucks (USEPA SPECIATE v4.3)
[e]: Gasoline exhaust - E85 ethanol gasoline (USEPA SPECIATE v4.3)
[f]: Refinery - Chevron south - august 6-17, 1996 (USEPA SPECIATE v4.3)
[g]: Sao Paulo vehicle emission: http://www.abq.org.br/cbq/2008/trabalhos/5/5-502-4748.htm
[h]: Biomass burning - tropical forest and savanna & grassland (USEPA SPECIATE v4.3)

4.2.4 Health Impacts Assessment

Effects on individual health endpoints caused by air pollution from incremental liquid fuels were estimated via BenMAP (the Environmental Benefits Mapping and Analysis Program). BenMAP, as a tool of health benefit analysis, developed by the U.S. Environmental Protection Agency (U.S. EPA) estimates health impacts by integrating changes of air pollution exposure, health effect estimates, and baseline incidence [36]. The simple expression is shown as the following.

$$\begin{aligned}[\text{Health Effect}] = [\text{Air Quality Change}] \times [\text{Exposed Population}] \\ \times [\text{Health Effect Estimate}] \times [\text{Health Baseline Incidence}]\end{aligned} \quad (2)$$

A change in air quality is the difference of targeted pollution concentration between baseline and scenarios that was simulated by WRF-Chem in this study. We used concentration response functions (CRFs) for certain health endpoint to determine the percentage change in an adverse health incidence due to the change in ambient concentration of air pollution. CRFs can be derived from the relative risk of air pollution accessed by epidemiological studies. In a recent decade, at least seven studies found epidemiological relationship between ambient concentration of fine particles (PM_{10} and $PM_{2.5}$) [37-40] and ozone [41-45] and specific causes of mortality rate in different regions of the world. They also presented the relative risks with uncertainty associated with air quality changes for population in a certain range of ages. Other studies also find air pollution might increase the risk of asthma exacerbation [46], bronchitis [47, 48], acute myocardial infarction[49], hospital admissions [50, 51], and other health adverse outcomes [52, 53].

The exposed population is the residential population exposed in air pollution. We used different levels of population data (grouping by ages) including national population from World Health Organization (WHO)[4], state- and municipality-level data from IBGE[5], and gridded dataset from LandScan [25]. The incidence data for individual health endpoints in all levels (national, state-, and municipality- level) was obtained from WHO, unified health system (SUS)[6] maintained by Ministry of Health, Brazil. All levels of population and incidence data are shown in Figure 4.2. Limited by availability of incidence data, CRFs applied in this study were only focused on $PM_{2.5}$ and ozone-associated mortality and hospital admissions. Table 4.10 summaries the references of applied CRFs.

[4] http://www.who.int/gho/countries/bra/en/
[5] http://www.ibge.gov.br/english/#sub_populacao
[6] http://www2.datasus.gov.br/DATASUS/index.php?area=02

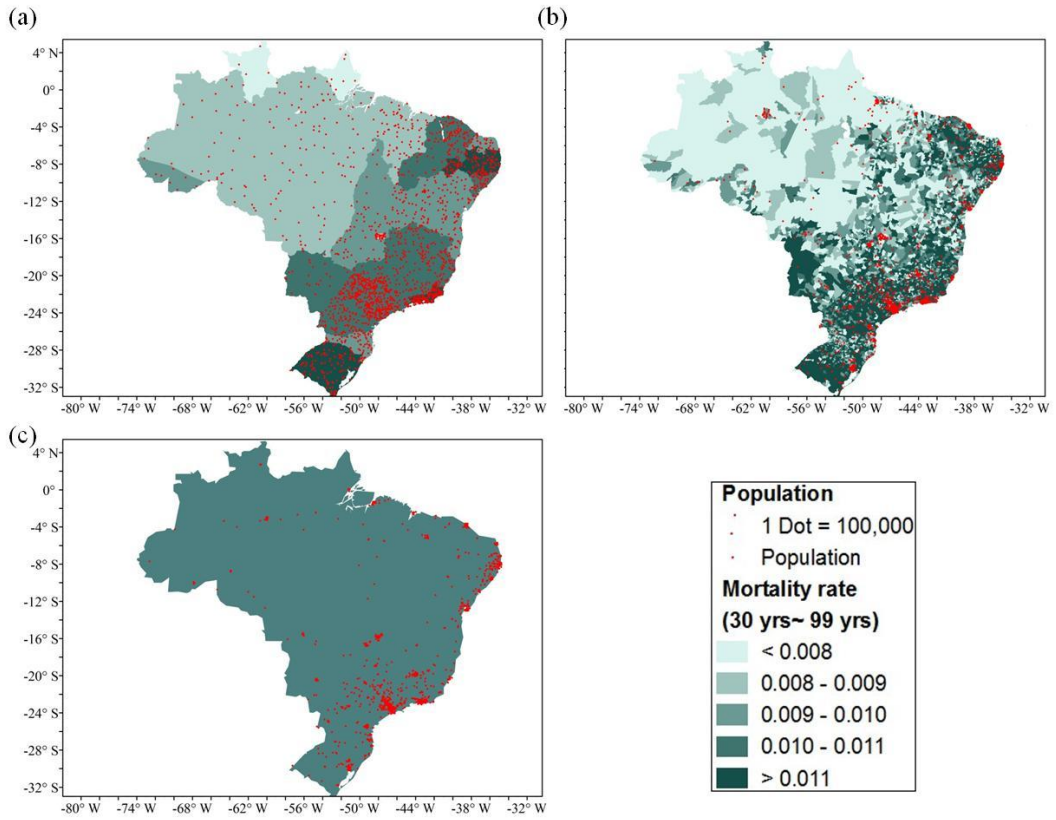

Figure 4.2: Population and mortality rate by different levels: (a) state-level; (b) municipality-level; (c) national mortality rate with LandScan population data.

Table 4.10: Summary of CRFs reference for $PM_{2.5}$ and ozone

Pollution	Health Endpoint	Study	Age Group	Relative risk (95% CI)	Function Form
$PM_{2.5}$	Premature mortality (long-term effect), all cause	Pope et al., 2002	30-99 yrs	1.06 (1.02–1.11) [a]	Log-linear
		Laden et al., 2006	25-99 yrs	1.16 (1.07-1.26) [a]	Log-linear
	Hospital admissions, All cardiovascular (less Myocardial Infarctions)	Moolgavkar, 2000	18-64 yrs	Estimated percent change of 1.4 (t-statistic of 4.1) [a]	Log-linear
		Moolgavkar, 2003	65-99 yrs	Estimated percent change of 1.58 (t-statistic of 4.59) [a]	Log-linear
Ozone	Premature mortality (short-term), all cause	Bell et al., 2005	0-99 yrs	1.008738 (1.0029-1.0056) [b]	Log-linear
		Levy et al. 2005	0-99 yrs	1.0043 (1.0055-1.0119) [b]	Log-linear
	Hospital admissions, All respiratory	Burnett et al. 2001	0-1 yr	Estimated percent change of 33 (t-statistic of 3.44) [c]	Log-linear

		Schwartz 1995	65-99 yrs	1.20 (1.06-1.37) [d]	Log-linear

[a]: with a change in annual mean exposure of 10.0 μg/m3
[b]: with a 10 ppb increase in daily average ozone
[c]: with a 45.2ppb increase in daily average ozone
[d]: with a 50 ppb increase in daily average ozone

4.3 Results

4.3.1 Emissions

Life-cycle emissions of eight species including $PM_{2.5}$, PM_{10}, NO_X, SO_X, VOC, CO, black carbon, and organic carbon were calculated in this study. Aggregated estimates for each emission theme and scenario in the Brazil domain are listed in Table 4.11. Estimates for B08 which accounts for nearly seven billion gallons ethanol in 2008 are seven times more than BGE estimates. LUC has the dominant emissions of particulate matter among four emission themes due to most of LUC emissions associated with uncontrolled field-burning practices. The emissions for CG comprising of refinery and vehicle use phases of conventional gasoline are relatively low due to controlled exhausts from refinery facilities and vehicle. In comparison of the background scenario, I1 scenario has around 14% increments of emissions for all species. The aggregated emissions for I2 scenario (B08+BGE+LUC) range from 2.3 to 7.5 times of the background scenario depending on species. I3 scenario (B08+CG) has the smallest increments of emissions among scenarios.

Maps of four emission themes for $PM_{2.5}$ including B08, BGE, CG, and LUC are shown in Figure 4.3. Other species in each emission theme have a similar distribution in space to $PM_{2.5}$ emission. B08 and BGE have dominant emissions from pre-harvesting burning practices concentrating in central- southern Brazil. For LUC, significant emissions occur around the rim of Amazonia area due to deforestation. In CG, only sparse peaks of emissions occur over oil refineries along the coast.

Table 4.11: Summary of emissions in Brazil domain for emission themes and scenarios

Theme/ Scenario	$PM_{2.5}$	PM_{10}	NO_X	SO_X	VOC	CO	BC	OC
B08	106,037	215,688	171,858	32,580	193,162	2,571,683	19,436	67,068
BGE	15,193	30,999	25,303	4,507	27,714	371,379	2,782	9,149
LUC	675,322	914,227	188,786	43,117	324,893	6,996,169	40,512	331,686
CG	452	1,030	3,745	1,148	4,572	59,015	--	--
B	106,037	215,688	171,858	32,580	193,162	2,571,683	19,436	67,068
I1	121,231	246,688	197,161	37,086	220,876	2,943,062	22,218	76,217
I2	796,553	1,160,915	385,947	80,203	545,768	9,939,230	62,731	407,903
I3	106,489	216,718	175,604	33,727	197,733	2,630,697	19,436	67,068

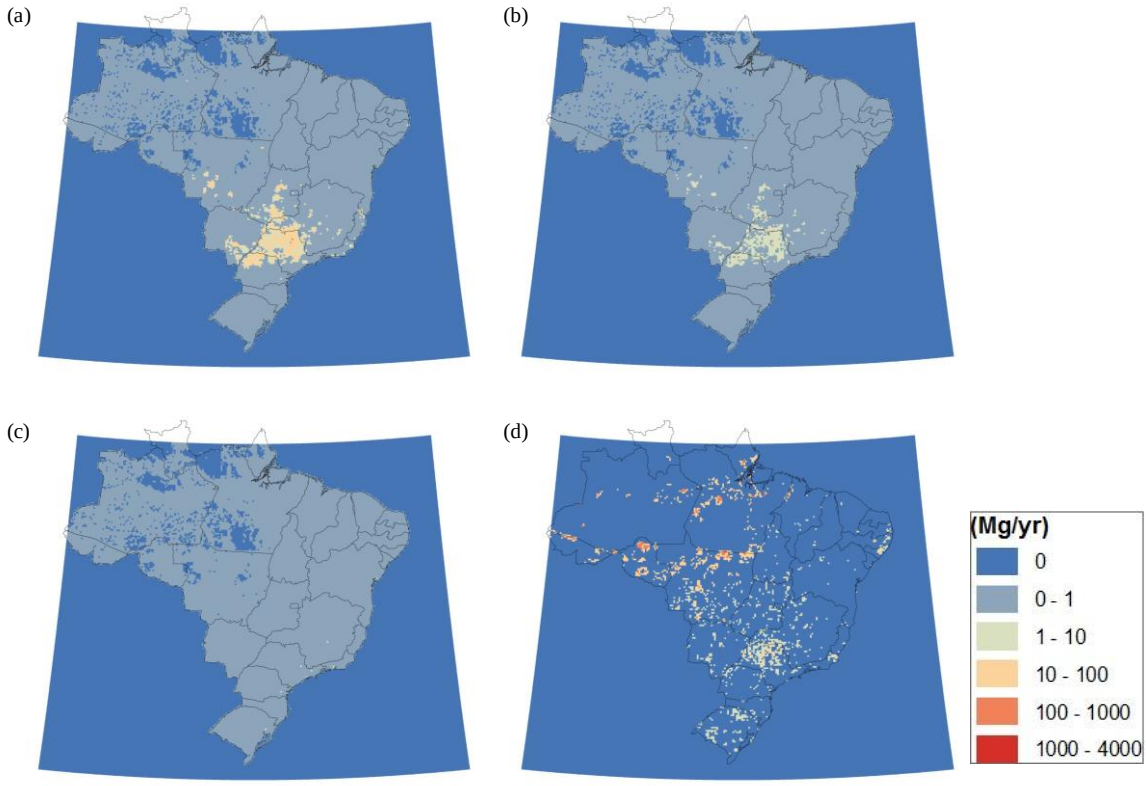

Figure 4.3: Maps of $PM_{2.5}$ emission for four themes: (a) B08; (b) BGE; (c) CG; (d) LUC.

4.3.2 Air Quality Changes

A two-week simulation for background and I1 scenario in July was run by the WRF-Chem. Maps of WRF-Chem output for $PM_{2.5}$ and ozone are shown in Figure 4.4. The ambient concentration of $PM_{2.5}$ for both scenarios stays at high level in the west part of the São Paulo state where most sugarcane crops are planted. The concentration then diffuses with effects of seasonal wind mostly from the south-east. This explains sugarcane pre-harvest burning contributes the dominant particulate air-pollution in the São Paulo state.

The formation of ground-level ozone, which involves a series of photochemical reactions, is driven by two major classes of directly emitted precursors, i.e. NO_X and VOC. From Figure 4.4, high level of ozone pollution occurs near populous areas along the coast because ozone pollution is often associated with the vehicle emissions and occurs near urban area [54].

The difference of concentration between background and I1 scenario was also calculated as Figure 4.4 (c). Significant increments of $PM_{2.5}$ concentration was found near the border among three states, Mato Grosso do Sul, Paraná, and São Paulo. The local impact is an increase in $PM_{2.5}$ due to primary aerosols, e.g. black carbon and organic carbon, and some secondary aerosols from nitrate and sulfate. The primary aerosols deposit out nearby while secondary aerosols remain in the atmosphere. The more acidic aerosols (i.e. nitrate and sulfate) would impede the formation of additional secondary organic aerosols and lead to lower aerosol mass downwind. The map for ozone (Figure 4.4 (c) right) shows the opposite consequence that the negative values center in the area

with an increase in $PM_{2.5}$. The decrease of ozone concentration is due to NO_X titration. The NO_X emissions form ozone during the day. The formed ozone may then be transported downwind. However, more NO_X emissions from pre-harvesting burning in evening would consume local ozone at night. The remaining NO_X will react with the abundant VOCs to form ozone in the morning, as conditions are NO_X-limited, and then be transported again. These simulation outcomes usually happen when the anthropogenic inventory are not included.

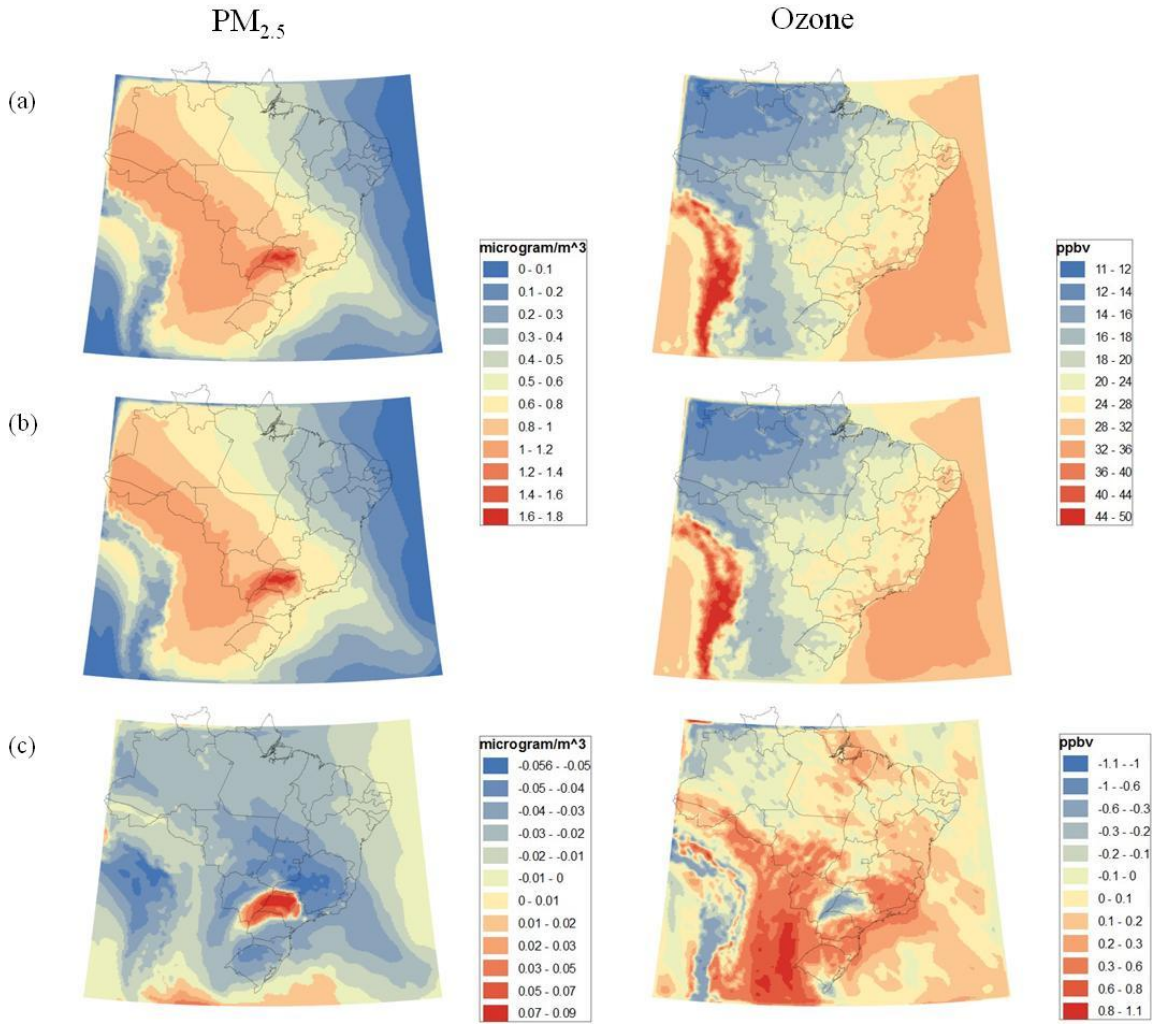

Figure 4.4: WRF-Chem output (July 1-13, 2008) for (a) B scenario (B08); (b) I1 scenario (B08+BGE); (c) the difference (I1- B scenario)

4.3.3 Health Impacts

Regional health impacts from air quality changes in I1 scenario were focused in this study because major changes (increments) of $PM_{2.5}$ occur locally in the area among Mato Grosso do Sul, Paraná, and São Paulo state. Changes outside the area are mostly minor and negative which is unrealistic. Simulation outcomes, particularly for minor changes, would be altered if inputting other anthropogenic emissions from biogenic, stationary, and mobile sources. Besides, ozone is sensitive to the composition of precursors in the atmosphere which is also largely affected by other anthropogenic emissions. Since those anthropogenic emissions were not included in the simulation, it reasonable to exclude the estimation of health impacts from ozone pollution in this study. However, the health impact estimates here would be conservative.

Figure 4.5 shows the spatial distribution of health impacts from incremental $PM_{2.5}$ pollution. Large health impacts occur in west and north parts of São Paulo state and some parts of north Paraná state where major sugarcane croplands exist. Table 4.12 and 4.13 summarize the estimates of mortality and hospital admission changes with 95% confident intervals in the top states and cities with significant $PM_{2.5}$ pollution. São Paulo state has the greatest estimates in both mortality and hospital admission changes among states nearby. Top 10 cities with largest health impacts are also within São Paulo state. The total estimate of mortality and hospital admission changes for I1 scenario ranges from 32 to 71 (deaths/ 1BGE) and 1,812 to 2,147 (extra admissions/ 1BGE) respectively depending on CRFs.

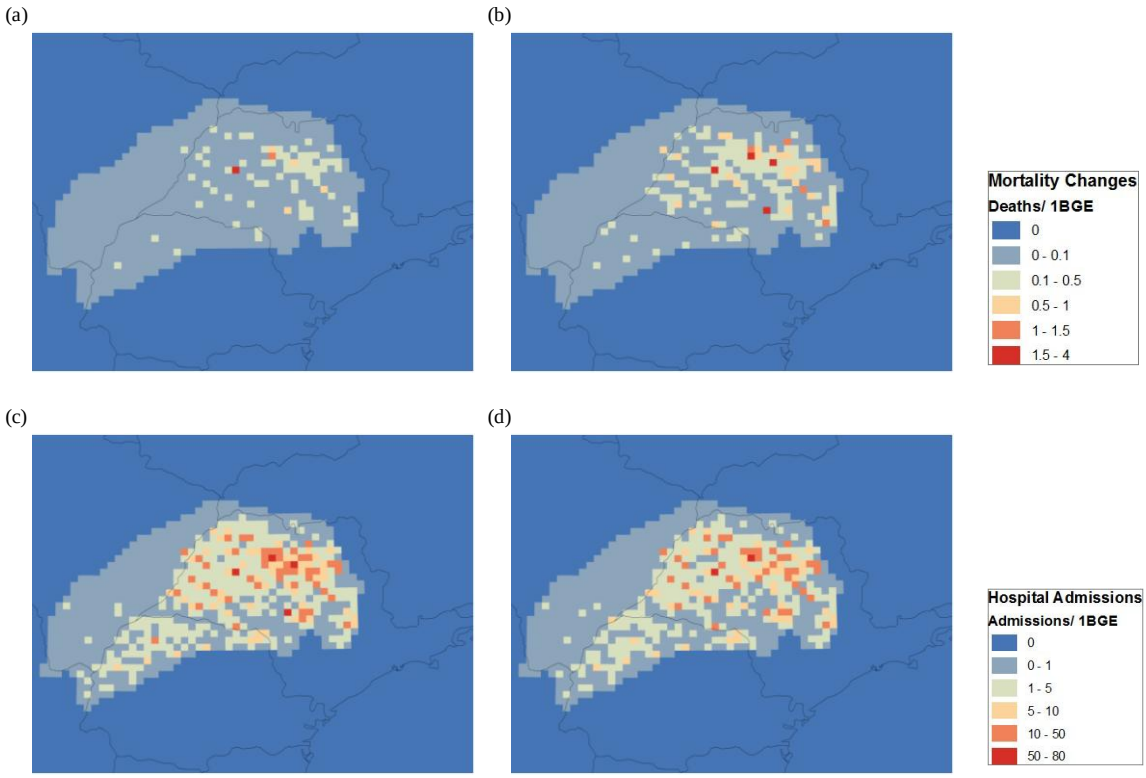

Figure 4.5: Maps of health impacts for I1 scenario: mortality changes based on (a) Pope et al. and (b) Laden et al.; hospital admission changes by cardiovascular cause based on (c) Moolgavkar (2000) and (d) Moolgavkar (2003).

Table 4.12: Health impacts changes (Mortality changes: deaths/ 1BGE) for I1 scenario (B08+BGE) in the top states and cities with significant impacts

Health Endpoint		Mortality, all cause				
Age Range		25-99 yrs			30-99 yrs	
Reference		Laden et al., 2006			Pope et al., 2002	
State/City	Population	Mean	(95% Confidence Intervals)	Population	Mean	(95% Confidence Intervals)
Mato Grosso do Sul	509,691	2.03	(1.09-2.97)	434,733	0.92	(0.36-1.48)
Paraná	1,892,148	5.63	(3.03-8.24)	1,613,878	2.48	(0.97-4.00)
São Paulo	6,127,089	63.80	(34.30-93.32)	5,226,003	28.26	(11.05-45.48)
Birigui, SP	105,575	2.47	(1.33-3.61)	90,049	1.08	(0.42-1.74)
Aracatuba, SP	66,462	1.58	(0.85-2.31)	56,688	0.69	(0.27-1.12)
Bauru, SP	146,122	1.48	(0.80-2.17)	124,633	0.67	(0.26-1.07)
São Jose do Rio Preto, SP	77,287	1.30	(0.70-1.91)	65,920	0.57	(0.22-0.92)
Araraquara, SP	135,765	1.25	(0.67-1.83)	115,799	0.56	(0.22-0.89)
Barretos, SP	65,577	1.13	(0.61-1.65)	55,933	0.50	(0.19-0.80)
Bebedouro, SP	51,080	1.11	(0.60-1.63)	43,568	0.50	(0.20-0.80)
Mirassol, SP	65,370	1.09	(0.58-1.59)	55,756	0.48	(0.19-0.77)
Piracicaba, SP	193,237	1.05	(0.57-1.54)	164,818	0.48	(0.19-0.77)
Ribeirao Preto, SP	223,251	1.05	(0.57-1.54)	190,418	0.48	(0.19-0.78)
Total	8,528,928	71.47	(38.43-104.53)	7,274,613	31.67	(12.38-50.96)

Table 4.13: Health impacts changes (Hospital admissions changes: extra admissions/ 1BGE) for I1 scenario (B08+BGE) in top significant states and cities in top states and cities with significant impacts

Health Endpoint	Hospital Admission, all cardiovascular cause					
Age Range	18-64 yrs			65-99 yrs		
Reference	Moolgavkar, 2000			Moolgavkar, 2003		
	Population	Mean (95% Confidence Intervals)		Population	Mean (95% Confidence Intervals)	
Mato Grosso do Sul	546,642	60.14	(36.01-84.26)	68,807	57.90	(37.15-78.65)
Paraná	2,029,321	202.18	(121.07-283.30)	255,436	184.48	(118.37-250.59)
São Paulo	6,571,276	1884.72	(1128.56-2640.92)	827,145	1569.19	(1006.82-2131.59)
Birigui, SP	113,229	53.72	(32.17-75.28)	14,252	54.56	(35.01-74.12)
São Jose do Rio Preto, SP	82,890	41.23	(24.69-57.78)	10,434	37.39	(23.99-50.79)
Mirassol, SP	70,109	36.62	(21.93-51.32)	8,825	36.26	(23.27-49.26)
Aracatuba, SP	71,280	34.39	(20.59-48.19)	8,972	33.88	(21.74-46.02)
Ribeirao Preto, SP	239,436	37.88	(22.68-53.08)	30,138	29.14	(18.70-39.59)
Bauru, SP	156,716	34.52	(20.67-48.37)	19,726	28.23	(18.11-38.35)
Bady Bassitt, SP	40,328	21.11	(12.64-29.57)	5,076	21.87	(14.03-29.71)
Andradina, SP	36,546	22.89	(13.70-32.07)	4,600	21.02	(13.49-28.56)
Barretos, SP	70,331	30.57	(18.31-42.84)	8,853	20.02	(12.85-27.20)
Jardinopolis, SP	98,208	23.60	(14.13-33.06)	12,362	19.32	(12.39-26.24)
Total	9,147,239	2147.04	(1285.64-3008.48)	1,151,389	1811.57	(1162.35-2460.83)

Sensitivity of parameters to health impacts estimation was also examined. Estimates based on population and incidence data in different levels including national, state-level, municipality-level, and LandScan (only for population data), were compared in Figure 4.6. Minor changes of estimates were observed among different levels of incidence data. However, different levels of population applied in estimation cause a significant variation of estimates. São Paulo state has the largest population among all Brazilian states, but an uneven distribution of population in space. Most of the population in state is concentrated in São Paulo city. Therefore, applying the state-level average for

the less populous areas in the west part of São Paulo state would lead larger estimates than other levels. We also found similar estimates based on municipality-level and LandScan population. Based on the analysis, it is suggested applying high resolution data of population, at least municipality-level, in health impact estimation is necessary to a more accurate outcome.

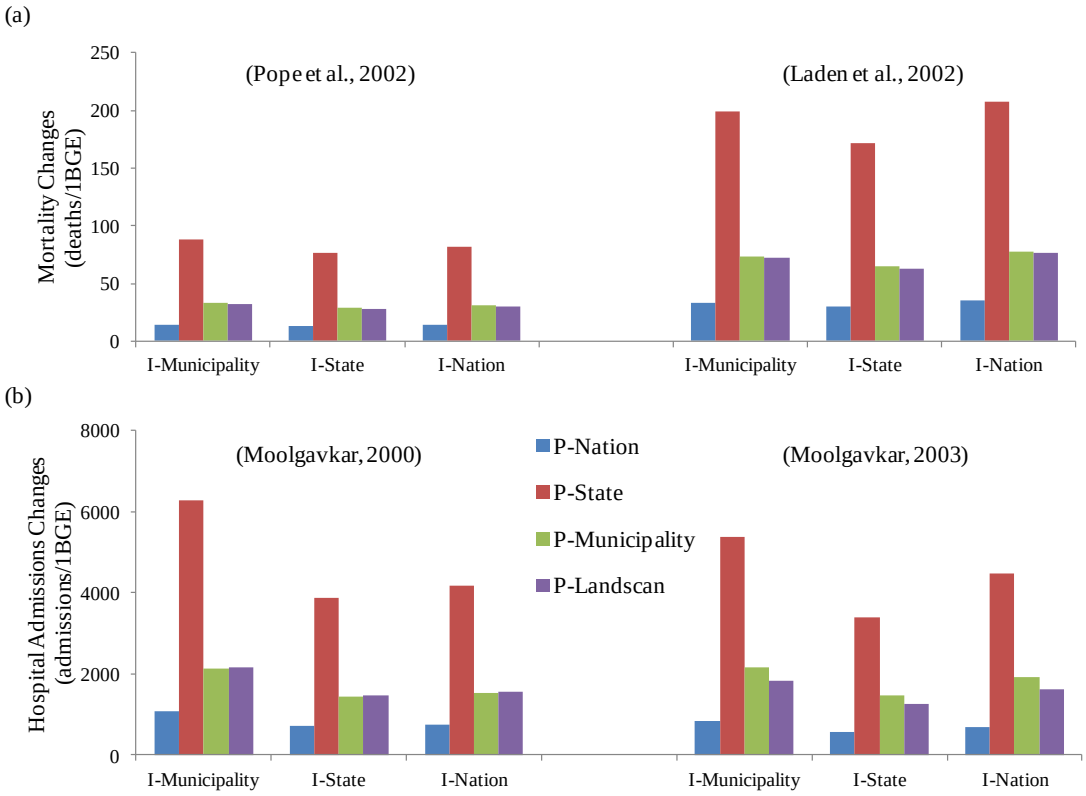

Figure 4.6: Sensitivity analysis on parameters of health impact estimation for two health endpoints affected by $PM_{2.5}$: (a) mortality changes and (b) hospital admissions changes. Results of I1 scenario are compared with CRFs and population (P) and incidence (I) data in different level (nation-level, state-level, municipality-level, and LandScan).

Health impact estimates of sugarcane ethanol were also compared with other equivalent fuels from previous study [9]. One billion gallons of sugarcane ethanol would cause mortality changes ranging from 32 to 71 more deaths with 95% confident intervals

(12 ~ 104). The estimate is mostly larger than cellulosic ethanol from switchgrass and prairie biomass, and conventional gasoline, but less than coal powered corn ethanol in US. Although sugarcane ethanol might offset greater GHG emissions, if without counting effects from land-use changes, its life-cycle air emissions from incremental uses might cause more health impacts than cellulosic ethanol and even gasoline.

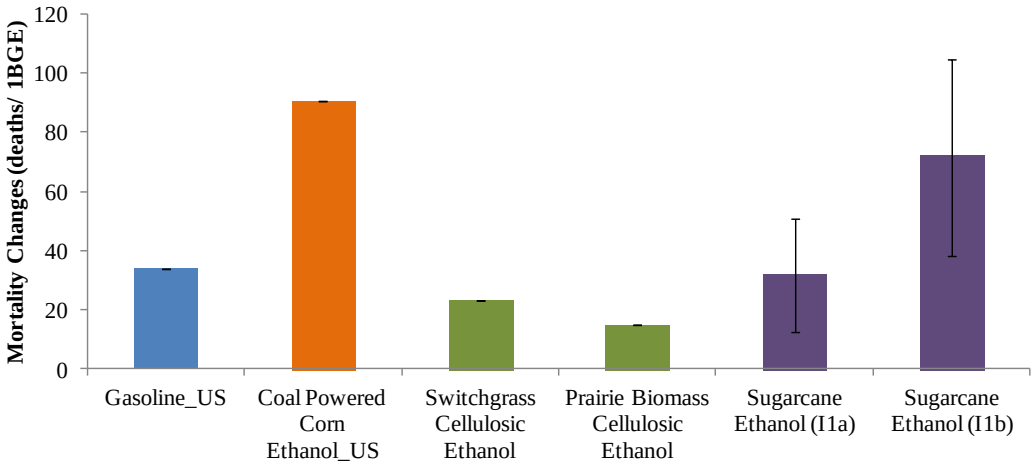

Figure 4.7: Comparisons of health impacts for equivalent bioethanols and conventional gasoline. (I1a) and (I1b) represent I1 scenario with the CRF from Pope et al. Laden et al. respectively.

4.4 Discussion and Conclusion

The life-cycle of transportation liquid fuels including production and combustion phases usually causes adverse emission impacts. For those fuels, although worldwide mainstream regards GHG emissions as one of the greatest concerns, health impacts from non-GHG air-pollution emissions remain an important issue of either energy or environmental policy.

Health impacts associated with life-cycle air pollution of sugarcane ethanol was thoroughly examined in this study. It was proven that the use and production of incremental one billion gallons may induce increments of ambient concentration for $PM_{2.5}$ and ozone. More global impacts may occur if considering effects from other anthropogenic emissions. The incremental air-pollution led health impacts, i.e. mortality and hospital admission changes, ranging from 32 to 72 extra deaths and from 1,812 to 2,147 extra admissions in 1BGE scenario. In comparison of equivalent liquid fuels, Brazilian sugarcane ethanol cause mostly greater health impacts than US conventional gasoline and cellulosic ethanol if current practices of sugarcane harvesting and land-use change management remain. Regional air quality might be improved by effective controls of sugarcane pre-harvesting burning, which is the dominant source of life-cycle emissions. Encouraging mechanical harvesting practices instead of manual ones might be a possible solution. However, the high initial cost, limitation of application in steep area (slope over 12%), and a decrease in job opportunity might be issues of future implementation [55]. Methods applied in this study and results would assist future researches to identify the sustainability of biofuels, particularly, in the aspect of air pollution and health impacts.

Reference

1. Kahn Ribeiro, S.; Kobayashi, S.; Beuthe, M.; Gasca, J.; Greene, D.; Lee, D. S.; Muromachi, Y.; Newton, P. J.; Plotkin, S.; Sperling, D.; Wit, R.; Zhou, P. J. *Transport and its infrastructure*; In Climate Change 2007: Mitigation. Contribution of Working Group III to the Fourth Assessment Report of the Intergovernmental Panel on Climate Change. Cambridge, United Kingdom and New York, NY, USA, 2007.
2. Farrell, A. E.; Plevin, R. J.; Turner, B. T.; Jones, A. D.; O'Hare, M.; Kammen, D. M., Ethanol can contribute to energy and environmental goals. *Science* **2006,** *311*, (5760), 506-508.
3. Schneider, U. A.; McCarl, B. A., Economic potential of biomass based fuels for greenhouse gas emission mitigation. *Environ. Resour. Econ.* **2003,** *24*, (4), 291-312.
4. Field, C. B.; Campbell, J. E.; Lobell, D. B., Biomass energy: the scale of the potential resource. *Trends Ecol. Evol.* **2008,** *23*, (2), 65-72.
5. Scown, C. D.; Horvath, A.; McKone, T. E., Water Footprint of U.S. Transportation Fuels. *Environmental Science & Technology* **2011,** *45*, (7), 2541-2553.
6. Fargione, J.; Hill, J.; Tilman, D.; Polasky, S.; Hawthorne, P., Land clearing and the biofuel carbon debt. *Science* **2008,** *319*, (5867), 1235-1238.
7. Lapola, D. M.; Schaldach, R.; Alcamo, J.; Bondeau, A.; Koch, J.; Koelking, C.; Priess, J. A., Indirect land-use changes can overcome carbon savings from biofuels in Brazil. *Proc. Natl. Acad. Sci. U. S. A.* **2010,** *107*, (8), 3388-3393.
8. Jacobson, M. Z., Effects of ethanol (E85) versus gasoline vehicles on cancer and mortality in the United States. *Environmental Science & Technology* **2007,** *41*, (11), 4150-4157.
9. Hill, J.; Polasky, S.; Nelson, E.; Tilman, D.; Huo, H.; Ludwig, L.; Neumann, J.; Zheng, H. C.; Bonta, D., Climate change and health costs of air emissions from biofuels and gasoline. *Proc. Natl. Acad. Sci. U. S. A.* **2009,** *106*, (6), 2077-2082.
10. Tsao, C.-C., Air pollution emissions from biofuels indirect land-Use change. *Environmental Science & Technology* **2012** (reviewing).
11. Tsao, C. C.; Campbell, J. E.; Mena-Carrasco, M.; Spak, S. N.; Carmichael, G. R.; Chen, Y., Increased estimates of air-pollution emissions from Brazilian sugar-cane ethanol. *Nature Climate Change* **2012,** *2*, (1), 53-57.
12. Grell, G. A.; Peckham, S. E.; Schmitz, R.; McKeen, S. A.; Frost, G.; Skamarock, W. C.; Eder, B., Fully coupled "online" chemistry within the WRF model. *Atmospheric Environment* **2005,** *39*, (37), 6957-6975.
13. Mena-Carrasco, M.; Oliva, E.; Saide, P.; Spak, S. N.; de la Maza, C.; Osses, M.; Tolvett, S.; Campbell, J. E.; Tsao, T. e. C.-C.; Molina, L. T., Estimating the health benefits from natural gas use in transport and heating in Santiago, Chile. *Science of The Total Environment* **2012,** *429*, (0), 257-265.

14. Saide, P. E.; Carmichael, G. R.; Spak, S. N.; Gallardo, L.; Osses, A. E.; Mena-Carrasco, M. A.; Pagowski, M., Forecasting urban PM10 and PM2.5 pollution episodes in very stable nocturnal conditions and complex terrain using WRF–Chem CO tracer model. *Atmospheric Environment* **2011,** *45*, 2769-2780.

15. Tie, X. X.; Madronich, S.; Li, G. H.; Ying, Z. M.; Zhang, R. Y.; Garcia, A. R.; Lee-Taylor, J.; Liu, Y. B., Characterizations of chemical oxidants in Mexico City: A regional chemical dynamical model (WRF-Chem) study. *Atmospheric Environment* **2007,** *41*, (9), 1989-2008.

16. Zaveri, R. A.; Peters, L. K., A new lumped structure photochemical mechanism for large-scale applications. *J. Geophys. Res.-Atmos.* **1999,** *104*, (D23), 30387-30415.

17. Zaveri, R. A.; Easter, R. C.; Fast, J. D.; Peters, L. K., Model for Simulating Aerosol Interactions and Chemistry (MOSAIC). *J. Geophys. Res.-Atmos.* **2008,** *113*, (D13).

18. Guenther, A.; Karl, T.; Harley, P.; Wiedinmyer, C.; Palmer, P. I.; Geron, C., Estimates of global terrestrial isoprene emissions using MEGAN (Model of Emissions of Gases and Aerosols from Nature). *Atmos. Chem. Phys.* **2006,** *6*, 3181-3210.

19. Wiedinmyer, C.; Akagi, S. K.; Yokelson, R. J.; Emmons, L. K.; Saadi, J. A.; Orlando, J. J.; Soja, A. J., The Fire INventory from NCAR (FINN) – a high resolution global model to estimate the emissions from open burning. *Geosci. Model Dev.* **2011,** *4*, (3), 625-641.

20. Saide, P. E.; Spak, S. N.; Carmichael, G. R.; Mena-Carrasco, M. A.; Yang, Q.; Howell, S.; Leon, D. C.; Snider, J. R.; Bandy, A. R.; Collett, J. L.; Benedict, K. B.; de Szoeke, S. P.; Hawkins, L. N.; Allen, G.; Crawford, I.; Crosier, J.; Springston, S. R., Evaluating WRF-Chem aerosol indirect effects in Southeast Pacific marine stratocumulus during VOCALS-REx. *Atmos. Chem. Phys.* **2012,** *12*, (6), 3045-3064.

21. Hong, S.-Y.; Lim, J.-O. J., The WRF single-moment 6-class microphysics scheme (WSM6). *Journal of the Korean Meteorological Society* **2006,** *42*, (2), 129-151.

22. Bond, T. C.; Streets, D. G.; Yarber, K. F.; Nelson, S. M.; Woo, J.-H.; Klimont, Z., A technology-based global inventory of black and organic carbon emissions from combustion. *J. Geophys. Res.* **2004,** *109*, (D14), D14203.

23. Rudorff, B. F. T.; Aguiar, D. A.; Silva, W. F.; Sugawara, L. M.; Adami, M.; Moreira, M. A., Studies on the rapid expansion of sugarcane for ethanol production in Sao Paulo State (Brazil) using Landsat data. *Remote Sensing* **2010,** *2*, (4), 1057-1076.

24. Monfreda, C.; Ramankutty, N.; Foley, J. A., Farming the planet: 2. Geographic distribution of crop areas, yields, physiological types, and net primary production in the year 2000. *Global Biogeochemical Cycles* **2008,** *22*, (1), GB1022.

25. LandScan™ Global Population Database. In Oak Ridge National Laboratory: Oak Ridge, TN, 2008.

26. Saatchi, S. S.; Houghton, R. A.; Alvala, R.; Soares, J. V.; Yu, Y., Distribution of aboveground live biomass in the Amazon basin. *Global Change Biology* **2007,** *13*, (4), 816-837.

27. van der Werf, G. R.; Randerson, J. T.; Giglio, L.; Collatz, G. J.; Mu, M.; Kasibhatla, P. S.; Morton, D. C.; DeFries, R. S.; Jin, Y.; van Leeuwen, T. T., Global fire emissions and the contribution of deforestation, savanna, forest, agricultural, and peat fires (1997-2009). *Atmos. Chem. Phys.* **2010,** *10*, (23), 11707-11735.

28. Paustian, K.; Ravindranath, N. H.; Amstel, A. v. *2006 IPCC Guidelines for National Greenhouse Gas Inventories*; Intergovernmental Panel on Climate Change: Hayama, Japan, 2006.

29. Carvalho, J. A.; Higuchi, N.; Araujo, T. M.; Santos, J. C., Combustion completeness in a rainforest clearing experiment in Manaus, Brazil. *J. Geophys. Res.-Atmos.* **1998,** *103*, (D11), 13195-13199.

30. Tufekcioglu, A.; Kucuk, M.; Saglam, B.; Bilgili, E.; Altun, L., Soil properties and root biomass responses to prescribed burning in young corsican pine (Pinus nigra Arn.) stands. *J.Environ.Biol.* **2010,** *31*, (3), 369-373.

31. Rau, B. M.; Johnson, D. W.; Chambers, J. C.; Blank, R. R.; Lucchesi, A., Estimating root biomass and distribution after fire in a great basin woodland using cores and pits. *West. North Am. Naturalist* **2009,** *69*, (4), 459-468.

32. Lara, L. L.; Artaxo, P.; Martinelli, L. A.; Camargo, P. B.; Victoria, R. L.; Ferraz, E. S. B., Properties of aerosols from sugar-cane burning emissions in Southeastern Brazil. *Atmospheric Environment* **2005,** *39*, (26), 4627-4637.

33. Hall, D.; Wu, C.-Y.; Hsu, Y.-M.; Stormer, J.; Engling, G.; Capeto, K.; Wang, J.; Brown, S.; Li, H.-W.; Yu, K.-M., PAHs, carbonyls, VOCs and PM2.5 emission factors for pre-harvest burning of Florida sugarcane. *Atmospheric Environment* **2012,** *55*, (0), 164-172.

34. Stockwell, W. R.; Middleton, P.; Chang, J. S.; Tang, X. Y., The 2nd generation regional acid deposition model chemical mechanism for regional air-quality modeling. *J. Geophys. Res.-Atmos.* **1990,** *95*, (D10), 16343-16367.

35. Stockwell, W. R.; Kirchner, F.; Kuhn, M.; Seefeld, S., A new mechanism for regional atmospheric chemistry modeling. *J. Geophys. Res.-Atmos.* **1997,** *102*, (D22), 25847-25879.

36. Davidson, K.; Hallberg, A.; McCubbin, D.; Hubbell, B., Analysis of PM2.5 using the Environmental Benefits Mapping and Analysis Program (BenMAP). *J. Toxicol. Env. Health Part A* **2007,** *70*, (3-4), 332-346.

37. Pope, C. A.; Burnett, R. T.; Thun, M. J.; Calle, E. E.; Krewski, D.; Ito, K.; Thurston, G. D., Lung cancer, cardiopulmonary mortality, and long-term exposure to fine particulate air pollution. *Jama-Journal of the American Medical Association* **2002,** *287*, (9), 1132-1141.

38. Laden, F.; Schwartz, J.; Speizer, F. E.; Dockery, D. W., Reduction in fine particulate air pollution and mortality - Extended follow-up of the Harvard six cities study. *American Journal of Respiratory and Critical Care Medicine* **2006,** *173*, (6), 667-672.

39. Woodruff, T. J.; Parker, J. D.; Schoendorf, K. C., Fine particulate matter (PM2.5) air pollution and selected causes of postneonatal infant mortality in California. *Environmental Health Perspectives* **2006,** *114*, (5), 786-790.

40. Martins, M. C. H.; Fatigati, F. L.; Vespoli, T. C.; Martins, L. C.; Pereira, L. A. A.; Martins, M. A.; Saldiva, P. H. N.; Braga, A. L. F., Influence of socioeconomic conditions on air pollution adverse health effects in elderly people: an analysis of six regions in Sao Paulo, Brazil. *Journal of Epidemiology and Community Health* **2004,** *58*, (1), 41-46.

41. Bell, M. L.; Dominici, F.; Samet, J. M., A meta-analysis of time-series studies of ozone and mortality with comparison to the national morbidity, mortality, and air pollution study. *Epidemiology* **2005,** *16*, (4), 436-445.

42. Levy, J. I.; Chemerynski, S. M.; Sarnat, J. A., Ozone exposure and mortality - An empiric Bayes metaregression analysis. *Epidemiology* **2005,** *16*, (4), 458-468.

43. Ito, K.; De Leon, S. F.; Lippmann, M., Associations between ozone and daily mortality - Analysis and meta-analysis. *Epidemiology* **2005,** *16*, (4), 446-457.

44. Jerrett, M.; Burnett, R. T.; Pope, C. A., II; Ito, K.; Thurston, G.; Krewski, D.; Shi, Y.; Calle, E.; Thun, M., Long-Term ozone exposure and mortality. *New England Journal of Medicine* **2009,** *360*, (11), 1085-1095.

45. Schwartz, J., How sensitive is the association between ozone and daily deaths to control for temperature? *American Journal of Respiratory and Critical Care Medicine* **2005,** *171*, (6), 627-631.

46. Ostro, B.; Lipsett, M.; Mann, J.; Braxton-Owens, H.; White, M., Air pollution and exacerbation of asthma in African-American children in Los Angeles. *Epidemiology* **2001,** *12*, (2), 200-208.

47. Abbey, D. E.; Ostro, B. E.; Petersen, F.; Burchette, R. J., Chronic respiratory symtoms associated with estimated long-term ambient concentrations of fine particulates less-than 2.5 microns in aerodynamic diameter ($PM_{2.5}$) and other air-pollutants. *Journal of Exposure Analysis and Environmental Epidemiology* **1995,** *5*, (2), 137-159.

48. Dockery, D. W.; Cunningham, J.; Damokosh, A. I.; Neas, L. M.; Spengler, J. D.; Koutrakis, P.; Ware, J. H.; Raizenne, M.; Speizer, F. E., Health effects of acid aerosols on North American children: Respiratory symptoms. *Environmental Health Perspectives* **1996,** *104*, (5), 500-505.

49. Peters, A.; Dockery, D. W.; Muller, J. E.; Mittleman, M. A., Increased particulate air pollution and the triggering of myocardial infarction. *Circulation* **2001,** *103*, (23), 2810-2815.

50. Moolgavkar, S. H., Air pollution and daily mortality in two U. S. counties: Season-specific analyses and exposure-response relationships. *Inhalation Toxicology* **2003,** *15*, (9), 877-907.

51. Moolgavkar, S. H., Air pollution and hospital admissions for diseases of the circulatory system in three US metropolitan areas. *Journal of the Air & Waste Management Association* **2000,** *50*, (7), 1199-1206.

52. Chen, L.; Jennison, B. L.; Yang, W.; Omaye, S. T., Elementary school absenteeism and air pollution. *Inhalation Toxicology* **2000,** *12*, (11), 997-1016.

53. Ostro, B. D., Air-pollution and morbidity revisited – a specification test. *Journal of Environmental Economics and Management* **1987,** *14*, (1), 87-98.

54. Sillman, S., The relation between ozone, NOx and hydrocarbons in urban and polluted rural environments. *Atmospheric Environment* **1999,** *33*, (12), 1821-1845.

55. Smeets, E.; Junginger, M.; Faaij, A.; Walter, A.; Dolzan, P.; Turkenburg, W., The sustainability of Brazilian ethanol—An assessment of the possibilities of certified production. *Biomass and Bioenergy* **2008,** *32*, (8), 781-813.

Chapter 5 Summary and Recommendations

5.1 Summary

As recent boost of worldwide utilization of liquid-biofuels, identifying potential effects on environment and human economics becomes essential. With regard to bio-ethanol, air-pollution emission is one of its several environmental aspects. In this dissertation, a systematic framework including emission modeling, air quality simulation, and health impact assessment was developed to quantify direct and indirect air-pollution impacts throughout the life-cycle of Brazilian biofuels.

In Chapter 2, life-cycle air-pollution emissions were quantified in space and time from production to consumption phases of sugarcane ethanol with the dominant emissions associated with the pre-harvest burning of sugarcane. Even in regions where burning has been eliminated on 50% of the farms, burning continue to be the dominant life-cycle stage for emissions and emissions continue to grow in time due to expanding sugarcane areas. It was also found that current satellite-based approaches may not account for sugarcane burning emissions due to the small scale of these fires relative to satellite resolution and assumptions regarding fuel loadings.

In Chapter 3, indirect air pollution from land-use change caused by the anticipated expansion of biofuels production was examined. Air pollution estimation was developed by a spatially explicit approach with synthesized information of fuel loading, combustion completeness, and emission factors. It was found that Brazilian biofuels with land-use change effects have much larger life-cycle emissions than conventional fossil fuels for all six regulated air pollutants. While biofuels cropland burning policies in Brazil may have

positive impacts on air pollution reductions, these policies do not address the much larger emissions caused by indirect land-use change.

In Chapter 4, health impacts from air quality changes due to incremental use of sugarcane ethanol was quantified by an integrated approach combining epidemiological models and air quality simulation. The spatially and temporally explicit emission data were estimated by approaches mentioned in previous chapters. Impact information was also compared with other types of transportation liquid fuels. Results indicated that Brazilian sugarcane ethanol with dominant effects of pre-harvesting burning and land-use change has larger health impacts than US gasoline and coal-powered corn ethanol.

5.2 Recommendations

This study provides a robust framework integrating air pollution and health impacts assessments to examine the sustainability of biofuels. The use of emission modeling based on a bottom-up approach with spatially and temporally agronomic information improves the accuracy of life-cycle impact assessments for Brazilian sugarcane ethanol. The research framework may assist the future determination on the sustainability of other advanced fuels.

Results in this study reveal that the production and uses of Brazilian sugarcane ethanol, relative to other fossil fuels and conventional ethanol, would cause significant air pollution and health impacts with dominant effects from current practices of harvesting and land-use management. Although local government puts efforts to eliminate pre-harvesting burning, direct and indirect land-use changes driven by incremental demands of ethanol still contribute a big portion of air-pollution emissions. To improve life-cycle environmental performance of Brazilian ethanol and avoid adverse effects of air emissions, several points are suggested as the following.

1. Better management of open burning practices. Burning practices may not be a cost-effective approach for sugarcane harvesting and other land-use management if counting in external costs from air pollution. São Paulo state government plans to regulate practices of pre-harvesting burning in the daytime and gradually substitute burning practices with mechanical harvesting. Expanding the measure of fire-control to other types of burning practices, e.g. slash-and-burn, and better scheduling prescribed fires in time and location may assist to alleviate regional air pollution.

2. Better control of deforestation. Expansion of sugarcane cropland would indirectly induce rainforest deforestation in Amazonia and cause dominant iLUC emissions. Measures to reduce deforestation, e.g. raising subsidies for forest conservation, may inhibit the land-use changes of forest and avoid abundant emissions from deforestation.

3. Utilization of agricultural wastes. Ample agricultural residues are left after sugarcane harvesting and land-use changes. Utilizing the abundant biomass as sources of cellulosic ethanol instead of burning would not only reduce air pollution but also support the supply of ethanol.

Appendix A: A Scientific Paper of Energy Policy Analysis

Energy Policy ▮ (▮▮▮▮) ▮▮▮–▮▮▮

Contents lists available at ScienceDirect

Energy Policy

journal homepage: www.elsevier.com/locate/enpol

When renewable portfolio standards meet cap-and-trade regulations in the electricity sector: Market interactions, profits implications, and policy redundancy

C.-C. Tsao [a,b], J.E. Campbell [a,b], Yihsu Chen [a,b,c,*]

[a] School of engineering, University of California Merced, Merced, CA 95343, United States
[b] Sierra Nevada Research Institute, University of California Merced, Merced, CA 95343, United States
[c] School of social sciences, humanities, and art, University of California Merced, Merced, CA 95343, United States

ARTICLE INFO

Article history:
Received 4 November 2010
Accepted 12 January 2011

Keywords:
Renewable portfolio standard
Emission trading
Power market

ABSTRACT

Emission trading programs (C&T) and renewable portfolio standards (RPS) are two common tools used by policymakers to control GHG emissions in the energy and other energy-intensive sectors. Little is known, however, as to the policy implications resulting from these concurrent regulations, especially given that their underlying policy goals and regulatory schemes are distinct. This paper applies both an analytical model and a computational model to examine the short-run implications of market interactions and policy redundancy. The analytical model is used to generate contestable hypotheses, while the numerical model is applied to consider more realistic market conditions. We have two central findings. First, lowering the CO_2 C&T cap might penalize renewable units, and increasing the RPS level could sometimes benefit coal and oil and make natural gas units worse off. Second, making one policy more stringent would weaken the market incentive, which the other policy relies upon to attain its intended policy target.

1. Introduction

In order to reduce greenhouse gas (GHG) emissions and promote renewable energy, ongoing efforts at various levels employ a suite of instruments. The purpose of these instruments is to level the playing field of less polluting-intensive facilities (e.g. renewable) by either direct subsidy or tax on polluting resources (e.g. coal). For example, the European Union (EU) launched the Emission Trading Scheme (EU ETS) in 2005. California Assembly Bill 32 (AB 32) or the Global Warming Solution Act stipulates a cap-and-trade (C&T) program as the main policy to control GHG emission from the power sector. Another common tool is the renewable portfolio standard (RPS), which requires a certain percentage of electricity to be generated from renewable sources. In the United States, 34 states and the District of Columbia have established an RPS (Doris et al., 2009). Most states allow producers to use renewable energy certificates (RECs) to meet their obligation. Surplus RECs can be traded for extra revenue in the market. In other words, RECs are essentially the analogue of tradable permits in C&T programs. In Europe, the European Commission (EC) proposed national renewable targets for each member state. The EC allows member states to achieve the targets through feed-in tariffs or transferable tradable green certificates (TGC) (Nielsen and Jeppesen, 2003). TGCs are equivalent to RECs in USA. Several other countries, including Australia, Brazil, China, Japan, South Korea, and Taiwan, also planned or had established similar programs to promote renewable energy (IEA, 2004).

Currently, two proposed energy policies in the USA, i.e. the American Clean Energy and Security Act of 2009 (ACES) and the Clean Energy Jobs and American Power Act, both have language about using C&T and RPS as the main mechanisms to control GHG emissions in the energy and other energy-intensive sectors. One emerging question that remains unanswered, however, is the implication on policy efficiency resulting from the interactions of these potentially overlapping schemes, especially given that their underlying policy goals and regulatory schemes are somehow distinct. Whereas C&T aims to reduce GHG emissions, the RPS mandates a certain level of renewable energy generation but lacks explicitness in emissions abatement.

A number of studies qualitatively discuss the RECs market and its interactions with the C&T program. Mozumder and Marathe (2004) give an overview of RPS and examine the implications of an integrated RECs market. They also address other RPS-related issues, including the fluctuating availability of renewable resources, time lags in capacity development, and the harmonized level on RPS setting in the short and long run. Gillenwater (2008a, 2008b)

* Corresponding author at: School of Engineering, Sierra Nevada Research Institute, University of California Merced, Merced, CA 95343, United States.
E-mail addresses: cctsao3@ucmerced.edu (C.-C. Tsao), ecampbell3@ucmerced.edu (J.E. Campbell), yihsu.chen@ucmerced.edu (Y. Chen).

0301-4215/$ - see front matter © 2011 Published by Elsevier Ltd.
doi:10.1016/j.enpol.2011.01.030

explains the challenges when using voluntary market RECs for offsetting pollution emissions. The study concludes that the offset credits from renewable energy can be identified by fully addressing additionality, ownership of credits on emission reduction, and quantification of emission reduction. Bird et al. (2008) discuss the key issues of how renewable energy markets might intervene with carbon regulation, including the implications for emissions benefits claims, voluntary market demand, and the use of RECs in co-existing markets. They also stress the importance that policymakers need to be aware of the policy interaction with new and emerging policies.

Other studies have analyzed the market interaction under different energy regulations quantitatively. Amundsen and Mortensen (2001) apply a static equilibrium model to investigate both long and short-term interactions between the RECs market and C&T for the Danish power sector. The model considers price ceilings and floors of RECs, CO_2 prices, and electricity imports. Their results show that under the condition of autarchy, tightening the CO_2 emission together with a fixed RPS requirement may lead to a reduction in green producers profit and the RECs price. On the other hand, an increasing RPS with a fixed CO_2 emission cap suggests that the effects on the capacity expansion of renewables are ambiguous, depending on the price elasticity of demand. Jensen and Skytte (2002) model a regional electricity market under RPS. They also find that the effect of RPS on the electricity price is ambiguous. This is because raising RPS might induce a greater electricity output, thereby pushing down the price of electricity; on the other hand, it might also increase the RECs demand simultaneously, effectively raising the electricity price. Another study examines the long run implications of the co-existence of the C&T and RECs markets in the Baltic Sea region (Hindsberger et al., 2003). It shows that two policies can effectively increase renewable deployment. However, they did not consider the mechanism under which the permit price interacts with the RECs markets. Linares et al. (2008) examine the interactions of C&T and RPS in the context of the Spanish electricity market using conceptually graphic and simulation approaches. They conclude that the co-existing policies could lower consumer costs if policies are well coordinated because the RPS somehow attenuates the effect of the CO_2 emission cap. Bohringer and Rosendahl (2010), based on a theoretical analysis, examine the consequence of overlapping regulations (i.e. C&T and RPS with feed-in tariff). They conclude that overlapping regulations might promote dirty fossil technology because it will reduce the permit price, thereby benefiting emission-intensive technologies. Fischer (2010) also finds that the RPS program might increase or lower the electricity price, depending on two factors: the elasticity of renewable/non-renewable electricity supply and the stringency of the RPS target. Two European studies which examine the implication of co-existence of C&T and RPS in the energy market using numerical models also reach a similar conclusion (De Jonghe et al., 2009; Unger and Ahgren, 2005). In summary, these studies find that tightening the CO_2 emission cap while subject to a fixed RPS would hurt renewable producers yet the effect of RPS with a fixed CO_2 cap is ambiguous.

Some of these studies examine the market by applying theoretical models that allow market equilibria to be solved analytically. However, these models lack market details that might misrepresent supply and demand. For example, supply curves in these models are usually assumed as smooth functions that require an interior solution assumption when deriving first-order optimality conditions. In reality, the marginal cost function likely is a stepwise or piecewise function. The marginal emission rate, which differs by each unit/technology, is likely non-monotonic and non-differentiable if ordered in commensurate with production costs, can be appropriately represented by this approach. Therefore, they cannot be properly represented in theoretical models. Although some other studies examine market interactions using numerical approaches, intermittence of renewable output (e.g. wind) is generally overlooked, and the results tend to overstate the benefit of renewables. Moreover, the effect of policies on profitability by fuel types and emission intensity is not addressed thoroughly. These are crucial pieces of information in steering firms for their long run investment decision and evaluating efficiency of policies for promoting renewables and CO_2 emissions reduction.

This paper applies both an analytical model and a computational model to study the interaction of RPS and C&T policies. Practically, obtaining permits for new facilities could be a lengthy process, in which RPS or CO_2 requirement might change without any progress being made to bring new capacity to the market. We thus focus on short-run analysis because we are interested in the effects of overlapping policies on generators profits as well as the RECs and C&T permit prices in general. The analytical model is used to generate contestable hypotheses. The numerical model with California data is applied to consider more realistic market conditions. In particular, uncertain wind output is modeled by its empirical cumulative density function. A spinning reserve market is incorporated in order to compensate unavailable wind. Otherwise, its cost is grossly underestimated, and its output is then overstated. We then apply a Monte Carlo simulation in order to examine the distribution of the potential market outcomes. We have three central findings in this paper. First, making one policy more stringent would weaken the market signal created by the other policy. Second, the C&T and RPS policies affect fuel-specific profit differently. More specifically, while lowering the CO_2 cap benefits natural gas units, it also penalizes renewables (in additions to coal and oil) by reducing subsidies received through REC sales. On the other hand, increasing the RPS requirement could sometimes benefit coal and oil units and make natural gas units worse off. These are consistent with other studies (Amundsen and Mortensen, 2001; Bohringer and Rosendahl, 2010; Linares et al., 2008). Third, the CO_2 emission intensity could increase when the authority increases the RPS requirement.

The remainder of this paper is organized such that the theoretical analysis on the co-existence of RPS and C&T is given in Section 2. In Section 3, we introduce the method of numerical simulation including the model formulations, parameter inputs, and assumptions. Then in Section 4, we report our results of simulation and discuss the intuitions behind the market interaction. They include the effects of co-existing policies on the sale-weighed electricity price, the CO_2 emission permit and RECs prices, per MWh profits by fuel types, and emission intensity and policy redundancy.

2. Theoretical analysis

A theoretical economic model is built in this section to overview the interaction of markets in the co-existence of the C&T and RPS policies. We consider three types of power producer, i.e. coal, natural gas, and renewable producers, who face price-responsive electricity demands. Three producers are assumed to be price-takers in the electricity, the spinning reserve, the RECs, and the CO_2 permit markets.

The overall market model is expressed in Eqs. (1)–(6).[1] The indices (either superscript or subscript) c, n, and r denote the coal,

[1] The equivalence of Eqs. (1)–(6) is by formulating the model as a social welfare maximization problem—a nonlinear program (NLP). Their resulting first-order conditions will be the same. In this paper, we use the NLP formulation in Section 3 for numeric simulations. Yet, the formulation here allows us to understand the optimization problem faced by each producer.

Please cite this article as: Tsao, C.-C., et al., When renewable portfolio standards meet cap-and-trade regulations in the electricity sector: Market interactions, profits implications, and policy redundancy. Energy Policy (2011), doi:10.1016/j.enpol.2011.01.030

the natural gas, and the renewable producers, respectively. Variables p, p^{REC}, and p^{CO_2} are the electricity price ($/MWh), the RECs price ($/MWh), and the CO_2 emission permit price ($/MT), respectively. Output in MW is denoted by q_f, where the subscript f is fuel type. Likewise the functions C_f are the total cost functions ($) by fuel type f. Parameter RPS denotes RPS (%), and CAP is the CO_2 emission cap (MT). E_f gives the CO_2 emission rates (MT/MWh) for fuel f. We also assume that renewables emit no emission.

In Eqs. (1)–(3), producers maximize their profits, π_f, which are equal to the total revenue (from the electricity or the RECs sales) minus the production cost and the payments for RECs and the CO_2 emission permits. The third term in Eqs. (1)–(3) represents the revenue from the RECs sales for renewable producers. Consumers demand for electricity is represented by an inverse linear demand function as Eq. (4) where the parameters a and b are the intercept and slope, respectively. Since we are interested in the interaction of markets while the CO_2 emission cap and RPS constraints are binding, the equality condition is assumed for two market clearing conditions in Eqs. (5) and (6).[2] Eq. (5) expresses that the total CO_2 emission (by summing emission from coal and natural gas producers) is equal to the CO_2 emission cap. Eq. (6) indicates that the output from renewable producers should meet RPS:

$$\underset{q_c}{\text{maximize}} \quad \pi_c = p(Q)q_c - C_c(q_c) - RPSp^{REC}q_c - p^{CO_2}E_c q_c \tag{1}$$

$$\underset{q_n}{\text{maximize}} \quad \pi_n = p(Q)q_n - C_n(q_n) - RPSp^{REC}q_n - p^{CO_2}E_n q_n \tag{2}$$

$$\underset{q_r}{\text{maximize}} \quad \pi_r = p(Q)q_r - C_r(q_r) - (RPS-1)p^{REC}q_r \tag{3}$$

$$p = a - b \times \sum_f q_f \tag{4}$$

$$\sum_f E_f \times q_f = CAP \tag{5}$$

$$\sum_{f \in F^R} q_f = \sum_f q_f \times RPS \tag{6}$$

The market equilibrium (defined by the CO_2 permit, the RECs, the electricity prices, and the output from three producers) is calculated by deriving the first-order conditions from Eqs. (1)–(3) together with the market clearing conditions in Eqs. (4)–(6). In the following analyses, we assume linear marginal cost functions with intercepts (c_f) and slopes (d_f). These conditions constitute a square system with six unknowns (q_f, p, p^{REC} and p^{CO_2}) and six equations. If we assume the determinant is non-zero, it then has a single unique solution.

Given the market equilibrium conditions, we are interested in the comparative statics on two policy parameters: CAP and RPS. Comparative statics measures the marginal effect on the market outcomes associated with these two policy parameters. The results of the comparative statics based upon linear marginal cost are summarized in Table 1, where "+", "−", and "+/−" indicates the effect is positive, negative, and undetermined, respectively. The first row in Table 1 shows the impact of the parameter CAP on several variables. It implies that increasing the emissions level would lower the electricity (p), the permit prices (p^{CO_2}), and output from natural gas units, and raise the RECs price (p^{REC}), accompanied with an increase of coal and renewable outputs. This is consistent with findings elsewhere (Amundsen and Mortensen, 2001).

[2] Otherwise, a complementary condition ($0 \le x \perp F(x) \ge 0$), one for each variable, will be replaced if the models allow for corner solutions. These conditions state that both x and $F(x)$ are non-negative, and their product is equal to zero. The NLP formulation in Section 3 would allow corner solutions (e.g. $p^{CO_2}=0$).

Table 1
Summary of comparative statics with a linear marginal cost function.

Variables\parameters	p	p^{CO_2}	p^{REC}	q_c	q_r	q_n
CAP	−	−	+	+	+	−
RPS	+/−	+/−	+/−	+/−	+/−	+/−

Table 1 shows that the impact of the parameter RPS on the electricity prices and the outputs by different fuels is ambiguous, depending on the supply and demand parameters. Other studies also indicate a similar finding (Amundsen and Mortensen, 2001; Bohringer and Rosendahl, 2010; Fischer, 2010). For instance, Amundsen and Mortensen (2001) find ambiguous effects of RPS on the renewable capacity expansion under a fixed CO_2 emission cap. Bohringer and Rosendahl (2010) find that increasing electricity prices might occur if the elasticity of the renewable supply curve is greater than the natural gas one. Fischer (2010) also has a similar conclusion that the elasticity of supply from renewables relative to non-renewables ones and the effective stringency of RPS are the two factors that determine the impact on the electricity price.

3. Numerical analysis

This section summarizes the approach associated with numerical analysis based on the California electricity market. The content includes the development of simulation models in Section 3.1, the derivation of electricity inverse demand function in Section 3.2, the assumptions and the parameter inputs in Section 3.3.

3.1. Simulation models

This section summarizes the models that examine the interaction of electricity market with the RPS and emission cap. This consists of three modules that are solved in a sequence. We describe them in the following sections.

3.1.1. Module A: short-run dispatch model with spinning reserve market

The first module is constructed to determine the availability of the operating reserves in each period. In this module, consumers willingness-to-pay (WTP) for electricity is represented by the inverse linear demand function which is discussed later in Section 3.2. The short-run dispatch model is displayed as follows:

$$\begin{aligned} \underset{x_{ift}, r_{ift}}{\text{maximize}} \quad & W = \sum_t \left[\int_0^{Q_t} p_t^E\left(\sum_{i,f} x_{ift}\right) dQ_t - \sum_{i,f} \int_0^{x} C_{if}(x_{ift})\, dx \right] B_t \\ \text{subject to :} \quad & x_{ift} \le X_{ift} \\ & r_{ift} \le R_{if} \\ & x_{ift} + r_{ift} \le X_{ift} \\ & \sum_{i,f,t} r_{ift} \ge RR \sum_{i,f,t} x_{ift} \\ & \forall r_{ift}, x_{ift} \ge 0. \end{aligned} \tag{7}$$

The objective function in Module A (Eq. (7)) maximizes the social welfare, which is equal to the aggregated consumers WTP for electricity (integral under the demand curve) minus the total production cost, where B_t is the duration (hours) of each period t, and C_{if} is the marginal cost ($/MWh) where i is the generation unit, and f is the fuel type. Four constraints are associated with Module A. We describe them in the order of their appearance. First, the output of generator (x_{ift} in MW) is constrained by its maximum capacity (X_{ift} in MW). All generating units, except wind

Please cite this article as: Tsao, C.-C., et al., When renewable portfolio standards meet cap-and-trade regulations in the electricity sector: Market interactions, profits implications, and policy redundancy. Energy Policy (2011), doi:10.1016/j.enpol.2011.01.030

and solar, have the same capacity in all periods. Second, the operating reserve (r_{ift} in MW) is limited by the reserving capacity (R_{if} in MW), which is defined by a fraction of the generating capacity. This fraction depends on the type of generation technologies. Third, the total output (power output plus operating reserve) of each generating unit should be less than its capacity (X_{ift}). Fourth, the sum of the operating reserves needs meet a reserve requirement (RR). All variables (i.e. q_{ift} and r_{ift}) are non-negative in period t. As wind is an intermittent resource, we set the right hand side of the capacity constraint (X_{ift}) for wind as the average over hours in a given period t using the historical data from the California Independent System Operator (CAISO, 2009). The output from Module A produces the spinning reserve supply curves for period t, which will be used as inputs (RM_{ift}) in Module B.

3.1.2. Module B: identification of must-run units

Once we have the spinning reserve supply from Module A, the purpose of Module B is to determine the set of units that will be used to compensate unavailable wind in each period. In this module, we take into account the stochasticity of wind output using the historical hourly wind output data:

$$\begin{aligned} \underset{rw_{ift}}{\text{minimize}} \quad & Cost = \sum_{i,f,t} rw_{ift} C_{if} B_t \\ \text{subject to}: \quad & rw_{ift} \le RM^*_{ift} \\ & \sum_{i,f,t} rw_{ift} \ge \max(0, \overline{W_t} - \tilde{W}_t) \\ & \forall rw_{ift} \ge 0. \end{aligned} \tag{8}$$

The objective function in Module B (Eq. (8)) minimizes the total cost associated with these units that provide the reserving services for supplying or compensating unavailable wind. We assume that these units incur zero cost as long as they are not selected to compensate wind. In addition to non-negativity constraints, two constraints are associated with Module B. First, the must-run reserves for wind generation (rw_{ift}) should be constrained by its reserve capacity (RM^*_{ift} in MW) which is the solutions of variables r_{ift} from Module A. Second, the sum of the must-run reserve has to cover the shortage between the committed level (the average historical output in period t, $\overline{W_t}$) and the real-time wind output ($\tilde{W}_t$) in each period. The shortage is defined either as 0 while the real-time output level is greater than the committed level, or the difference between the committed and the real-time level. That is, the extra energy will be spilled at no cost when it is greater than average. The term $\tilde{W}_t$ is defined by a function of a uniform random variable using an empirical cumulative density function (or CDF) of wind output. The CDF for each period is derived from historical California wind output using regressions with 4-order polynomials. The detail is described in Section 3.3. The output of this module (rw_{ift}) gives the must-run levels of these reserve units to compensate unavailable wind.

3.1.3. Module C: short-run dispatch model with rps and emission cap constraints

Module C is a typical short-run dispatch model. Combined with the solution with the must-run levels of the reserve units from Module B, it simulates the operation of an electricity market that is subject to the RPS and C&T policies. As Module C is a variant of Module A, we slightly abuse the presentation of the notation by using the same notation for the electricity output (x_{ift}), and the spinning reserve (r_{ift}). As Modules A and C have the same objective function, we explain as follows how we modify the constraints to account for the RPS and C&T policies, and other output limitations:

$$\sum_{i,f,t} x_{ift} B_t E_{if} \le CAP \tag{9}$$

$$\sum_{f \in F^R} x_{ift} B_t \ge \left(\sum_{i,f,t} x_{ift} B_t \right) RPS \tag{10}$$

$$\sum_{i,f,t} r_{ift} \ge RR \sum_{i,f,t} x_{ift} - \sum_{i,f,t} rw_{ift} \tag{11}$$

$$x_{wind,t} = \min(\tilde{W}_t, \overline{W_t}). \tag{12}$$

Two constraints are added to represent the RPS and C&T policies (Eqs. (9) and (10)), where E_{if} is the emission rate for generators (MT CO_2 emitted/MWh), and CAP is the emission cap (MT CO_2 emitted). We also modify the reserve requirement contrasted to the fourth constraint in Module A by subtracting the must-run level of the reserve units from Module B (Eq. (8)). Eq. (11) requires that the reserve units produce at least at their must-run level determined by Module B. We also add a constraint to set the output of wind generation equal to its real-time output ($\tilde{W}_t$) or the average historical output ($\overline{W_t}$) if $\tilde{W}_t$ is greater than $\overline{W_t}$ (Eq. (12)).

3.2. Inverse demand function

The demand of electricity is represented by the price-responding linear inverse demand function. Although the short-run electricity demand is nearly inelastic, the residual demand faced by producers is price-response if there exists competitive imports or fringes. By the same spirit, we apply a similar approach as in reference (Bushnell, 2007) to construct the residual demand curve. Our empirical strategy involves estimating two parameters associated with the demand curves for each hour. The residual demand is estimated by subtracting the market historical demand ($Load_h$) from the imports ($Import_h$) and the hydro ($Hydro_h$)-outputs. So, the output from the in-state generators, except the hydrofacilities, is equal to $Q_h (= Load_h - Import_h - Hydro_h)$. We assume that the hydroproduction is uniformly distributed in each hour.[3] The estimating equation of the import and the hydro-output for hour h ($Q_h^{IMP} = Import_h + Hydro_h$) is as follows:

$$Q_h^{IMP} = \beta p_h + \boldsymbol{f}(month_{mh}, Day_{dh}, Hour_{th}) + \boldsymbol{g}(Temp_{sh}) + \varepsilon_h, \tag{13}$$

where m denotes month, d for day, t for hour, and s for state, respectively. In addition to monthly, weekly, and hourly fixed effects (function $\boldsymbol{f}$), we also include a quadratic function $\boldsymbol{g}$ to control for nonlinear demand shifters in the neighboring states (e.g. Arizona, Oregon and Nevada) using hourly temperature. As the electricity price is likely endogenous to the output, we apply a two-stage-least-square (2SLS) approach using the hourly quantities demanded as the instrument variables. As alluded to in Bushnell (2007), the derived demand is likely fixed for the majority of customer because they face a fixed electricity rate. We believe this is a valid instrument. For a given β, we then can obtain the inverse residual demand function for hour h accordingly:

$$p_h^E = \left(P_h^{Actual} + \frac{Q_h}{\beta} \right) - \frac{1}{\beta} Q_h = A_h - \frac{1}{\beta} \sum_f q_{fh}, \tag{14}$$

where A_h is the vertical intercept of the residual demand function in hour h, and P_h^{Actual} is the actual electricity price. The term Q_h is

[3] The extent to which the hydroproduction is positively (negatively) correlated with the loads levels we might underestimate (overestimate) the demand elasticity.

Please cite this article as: Tsao, C.-C., et al., When renewable portfolio standards meet cap-and-trade regulations in the electricity sector: Market interactions, profits implications, and policy redundancy. Energy Policy (2011), doi:10.1016/j.enpol.2011.01.030

the electricity quantity demanded, which equals the total power output ($\sum_f q_{fh}$) in the equilibrium. To facilitate the simulation, we further group the hourly data from a load duration curve into ten blocks (periods).

3.3. Parameter input and scenario assumptions

We rely on the USEPA eGRID as the main source for the information on unit marginal cost, generating capacity, CO_2 emission rate, and technology type. For those units that lack marginal cost information in eGRID, we assign them the average marginal cost of the same type technology. The capacity of units for providing the operating reserve depends on its generation technology. We assume that a generator with a combustion turbine (CT), a gas turbine (GT), or combined cycle (CC) can provide 70% of its generating capacity as the operating reserve, and a steam turbine (ST) and internal combustion (IC) can provide at most 20% and 100%, respectively. Such assumptions are consistent with previous study (Chen and Hobbs, 2005). The required operating reserve (*RR*) for the electricity market is assumed to be 10% of the total load which is broadly consistent with the CAISO requirement (FERC, 2010).

To facilitate our simulation, we categorize all renewable units into five groups: solar, geothermal, biomass, MSW/landfill gas, and wind. The hydropower is regarded as the baseload and subtracted from the fixed load when deriving the price-responding inverse demand functions. The marginal cost of renewable units is obtained from the National Renewable Energy Laboratory (NREL, 2010). We include the annual fixed and the variable operation and the maintenance (O&M) costs when calculating the marginal cost. We levelize the annual fixed O&M cost by its expected annual output. Renewable capacity is retrieved from the California Energy Commission (CEC, 2010) and the US Energy Information Administration (EIA, 2010). Renewable outputs from geothermal, biomass, and MSW/landfill gas are relatively constant, and are assumed to be fixed in each period based on their historical data in 2008 (CEC, 2010). The output of solar energy is calibrated by the historical solar irradiance (which varies by hour of a day and season) from NREL (2007). The historical data (2007) of the hourly output from wind generation, which was used to construct the CDFs, is obtained from CAISO (2009). We also assume that the renewable units cannot provide any operating reserve due to their uncertain output. The parameters RPS and Cap represent the policy requirement of RPS and C&T. In our baseline scenario, we simulate an electricity market in absence of the RPS and C&T policy. In addition to the baseline scenario, we perform a total of 1800 scenarios, varying RPS from 15% to 21% by an increment of 0.1%, and Cap from 0% to 30% with an increment of 1% reduction from the baseline emission. We repeat each scenario by 100 times using the Monte Carlo simulations in order to consider stochastic wind output.

4. Results

This section summarizes the results of our simulation based on the California electricity market. Those results include the effects of the RPS and C&T policies on sale-weighted electricity price, RECs price, CO_2 emission permit price, per MWh profit by fuel types, and emission intensity. We further discuss the policy redundancy and the intuitions behind market interaction when the RPS and C&T policies are co-existed.

4.1. Empirical cumulative density functions of wind output

We derived CDFs using regressions with four-order polynomials. For each period, the regression equation fits well the empirical wind outputs (all R^2 values greater than 0.97). For instance, Fig. 1 shows the cumulative probability (*y*-axis) and the wind outputs (*x*-axis) in the sixth period. It implies that a four-order polynomials function is a good approximation of the data except when wind output is high. For a random variable *x* between 0 and 1, the expected wind output is *W* (*x*).

4.2. Supply of must-run spinning reserve

By Module B (Eq. (8)), we determine the set of units from the reserve market that will be used to compensate unavailable wind in each period. The aggregated marginal costs of those units can be seen as the marginal cost function of wind when its output cannot achieve the committed level. We illustrate in Fig. 2 the supply curve of spinning reserves in the sixth period.

4.3. Sale-weighted electricity price

Fig. 3 shows the sale-weighted electricity prices under different levels of the RPS (Fig. 3, left) and CO_2 reduction requirements (Fig. 3, right). Sale-weighted electricity price in each scenario is calculated by dividing the total revenue ($) with the total output (MWh) over ten periods. The portion of the lines with marks

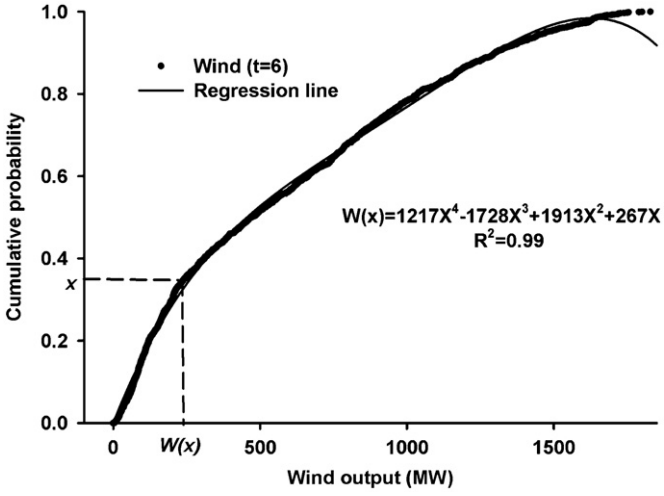

Fig. 1. The regression of the empirical wind outputs in the sixth period.

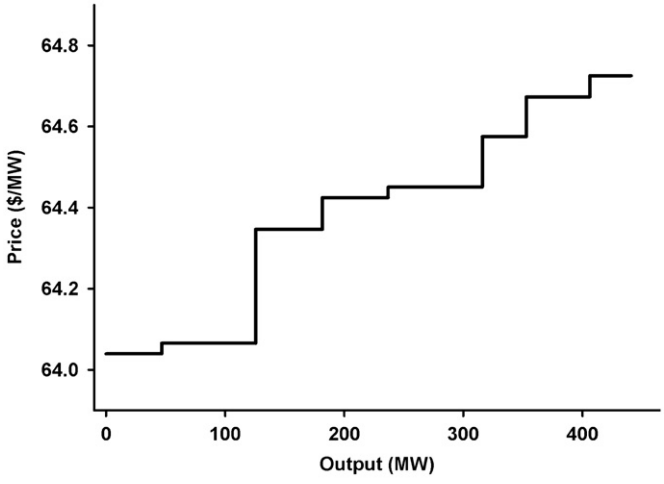

Fig. 2. The supply curve of the spinning reserves in the sixth period.

Please cite this article as: Tsao, C.-C., et al., When renewable portfolio standards meet cap-and-trade regulations in the electricity sector: Market interactions, profits implications, and policy redundancy. Energy Policy (2011), doi:10.1016/j.enpol.2011.01.030

displays the outcomes of the scenarios if both RPS and CO_2 cap constraints are binding. We also show their 95% confidence intervals (CI) based on 100 runs of the Monte Carlo simulation with uncertain wind outputs. The portion of lines without CI indicates either C&T or RPS is not binding. For a better presentation, we do not plot the CI for the scenarios when either C&T or RPS is not binding. Each curve in Fig. 3 represents the sale-weighted electricity prices by altering the RPS (left) or CO_2 cap (right) requirement in *x*-axis when fixing the CO_2 cap (left) or RPS (right) at a certain level. For example, the CO_2 reduction is fixed at 10%, 20%, and 30% when plotting Fig. 3 (left). The legend of the plots is arranged by the order of curves from top to bottom when possible. The lines representing the fixed RPS level of 15.5% and 16% in Fig. 3 (right) are almost overlapped.

In general, the sale-weighted electricity price increases when RPS (Fig. 3, left) and CO_2 (Fig. 3, right) become more stringent (i.e. move to the right along the *x*-axis.) This consequence is consistent with the results in Section 2, which conclude that (1) the effect of lowering CO_2 cap on the electricity price is positive and (2) the effects of RPS level on the electricity price is ambiguous. The sale-weighted electricity price then increases significantly when one of the constraints becomes non-binding (i.e. cap constraint in Fig. 3 (left) and RPS constraint in Fig. 3 (right)). A relatively large band of the confidence interval exists in the scenarios when altering RPS levels (Fig. 3, left). This suggests that the uncertain wind output affects the sale-weighted electricity price significantly by altering the RECs prices. However, the impact of CO_2 cap on the sale-weighted electricity price is smoothed out possibly by fuel switch in order to maintain the CO_2 cap when wind is not available.

4.4. CO_2 emission permit and RECs prices

Fig. 4 plots the CO_2 permit price (left) and REC price (right) when changing the RPS and CO_2 cap, respectively. As before, the portion of the curves without marks indicates the market outcomes when either RPS (left) or CO_2 (right) policy is not binding. As expected, the price of RECs and CO_2 emission permits generally increases with the rise of RPS and CO_2 reduction requirements. However, the effect of one policy is attenuated when the other policy is in effect (or binding). That is, the RECs price declines with the increasing CO_2 reduction requirement. Likewise, the CO_2 emission permit price declines as RPS rises. For example, Fig. 4 (left) shows the drops of the CO_2 permit price given four levels of CO_2 reduction requirements (i.e. 10%, 20%, and 30%) while increasing the RPS level from 15% to 21%. This is because the raising RPS will induce displacement of fossil outputs by renewable outputs, which in turn puts a downward pressure on the CO_2 permit demand, thereby driving down the permit price. Likewise, tightening the requirement of CO_2 reduction will first encourage output from less CO_2-intensive units and drive up the electricity price. This effectively pushes down the quantities demanded and lowers the amount of renewable needed for the RPS requirement, thereby resulting in a lower RECs price. This consequence is consistent with the conclusion in Section 2 that a lower emission cap will have a positive (negative) impact on the CO_2 permit price (RECs price).

The changes of the CO_2 permit and RECs prices would also affect the sale-weighted electricity price. Increasing the RPS requirement (the RECs price goes up accompanied by a decrease of CO_2 permit price) might change the sale-weighted electricity

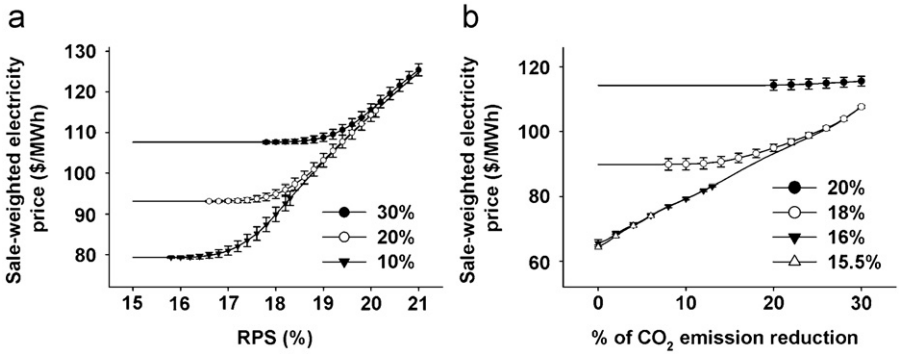

Fig. 3. The sale-weighted electricity prices with 95% confidence intervals when altering the RPS levels (left) and the CO_2 reduction levels (right). (a) RPS and (b) CO_2 emissions cap.

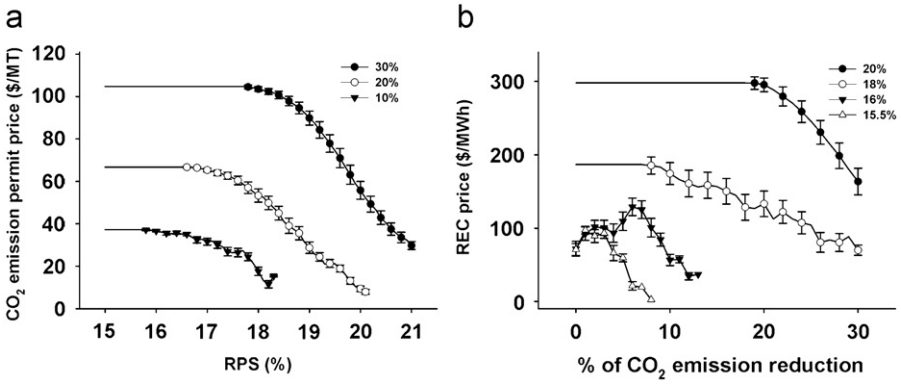

Fig. 4. The CO_2 emission permit and RECs prices with 95% confidence interval when altering the RPS levels (left) and the CO_2 reduction levels (right). (a) RPS and (b) CO_2 emissions cap.

Please cite this article as: Tsao, C.-C., et al., When renewable portfolio standards meet cap-and-trade regulations in the electricity sector: Market interactions, profits implications, and policy redundancy. Energy Policy (2011), doi:10.1016/j.enpol.2011.01.030

price in either direction. This is because the sale-weighted electricity price (a function of marginal production cost, RECs, and CO_2 emission permit prices) would be driven up by increasing the RECs price and partially offset by the drop of CO_2 permit price. When RPS becomes the only binding constraint (i.e. RPS is sufficiently high that it results in non-binding cap constraint), the sale-weighted electricity price continues increasing with the RECs level as the RPS becomes higher. That might explain why the sale-weighted electricity price slightly increases in the scenarios that the RPS constraint becomes binding at low levels of the RPS requirement and then accelerates when RPS becomes the only binding constraint (Fig. 3, left).

4.5. Per MWh profits by fuel types

In this section, we compare the profit per MWh by fuel types under the C&T and RPS policies. Per MWh profits by fuel types are calculated by dividing Eqs. (1)–(3) with x (the output for each type): the electricity price net of the marginal average cost, the emission cost (permit price × average emission rate), the REC cost or subsidy plus the revenue from the reserve market. Per MWh profits give producers an indication how profitable each fuel type or technology is under two policies. As the CO_2 cap penalizes CO_2-intensive technologies, per MWh profits should therefore decline for these units. On the other hand, RPS effectively subsidizes renewables (see Eq. (3)). Therefore, its per MWh profit would expect to increase.

Overall, we observe that the per MWh profits decline for coal, oil, and renewable types and increase for the natural gas type while gradually tightening up the CO_2 emission cap. The changes in per MWh profit are also consistent with our conclusions in Section 2 that outputs from coal and renewable would decline when lowering the CO_2 cap. The reverse is expected for natural gas. Interestingly, the impact of changing the RPS level on the per MWh profits suggests an entirely different picture. Figs. 5 and 6 display the per MWh profits with increasing RPS levels for four fuel types: coal and oil (Fig. 5) as well as natural gas and renewables (Fig. 6). In the low level of emission reduction (e.g. 10% and 20%), the per MWh profit of coal increases with the RPS level until the CO_2 cap becomes non-binding. When emission is capped by a 30% reduction, the per MWh profit of coal drops first and then increases subsequently. This is because increasing the RPS results in two counteracting effects. It increases the RECs price since the right hand side of the RPS constraint in Eq. (12) becomes large. In the meantime, it leads to a decline of permit price as discussed previously. The second effect overwhelms the first effect at low levels of emission reduction (e.g. 10% and 20%), and the impact is reversed for the RPS requirements between 18% and 20% when the market is subject to the 30% emission reduction. For the oil type, the emission rate is greater than that of coal, and its per MWh profit continues increasing as the RPS requirement elevates. This is because the second effect dominates the first effect for CO_2-intensive units. For the natural gas type, its per MWh profit continuously drops as the RPS increases. By the same spirit, the first effect (i.e. an increase in the RECs price) outweighs the second effect since natural gas has a relatively low emission rate. Finally, the per MWh profit of the renewable type increases with the RPS levels. This is because there are no emission costs associated with renewables (so the second effect vanishes). The aforementioned observations are consistent with our conclusions in Section 2 that changes in output by fuel types are ambiguous when altering the RPS level.

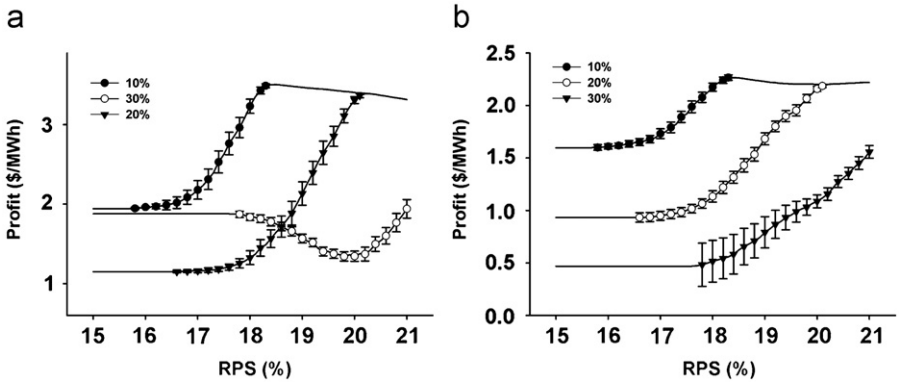

Fig. 5. Per MWh profits of coal (left) and oil (right) when altering the RPS levels. (a) Coal and (b) oil.

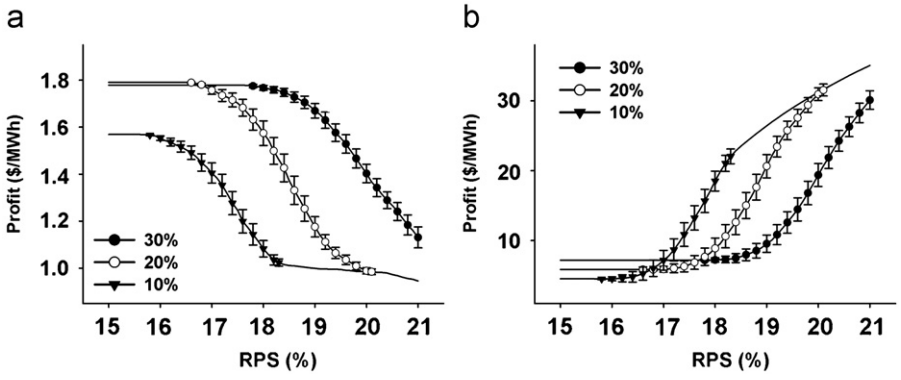

Fig. 6. Per MWh profits of natural gas (left) and renewables (right) when altering the RPS levels. (a) Natural gas and (b) renewables.

Please cite this article as: Tsao, C.-C., et al., When renewable portfolio standards meet cap-and-trade regulations in the electricity sector: Market interactions, profits implications, and policy redundancy. Energy Policy (2011), doi:10.1016/j.enpol.2011.01.030

A surprising result is the effect of the CO_2 reduction requirement on the per MWh profits of renewables. Fig. 7 suggests that the per MWh profit decreases as lowering the emission cap (i.e. a greater reduction requirement). This is because the high power price suppresses the electricity demand, thereby lowering the per MWh subsidy received by renewables through RECs. Clearly, demand elasticity might play an important role in determining the impact. Our empirical estimate of demand elasticity in Section 3 is approximately 0.02. Had demand been more price-responsive, the downward trend of the per MWh profit in Fig. 7 would be amplified.

4.6. Emission intensity

Fig. 8 plots the emission intensity when changing the levels of RPS (left) and CO_2 cap (right) holding the other policy at fixed levels, respectively. The emission intensity (MT/MWh) is calculated by dividing the total CO_2 emission (MT) by the total output of electricity (MWh) over ten periods. Overall, we observe a declining trend of the emission intensity as the CO_2 reduction requirement grows. This is because a lower cap (a higher reduction requirement) penalizes CO_2-intensive units by higher permit prices. This effectively reduces their output level and lower the overall emission intensity. However, the emission intensity surprisingly increases with the RPS levels in the range we simulate. This is because increasing the RPS levels penalizes natural gas more than coal and oil, resulting in shrinking outputs from natural gas units and increases in the emission intensity.

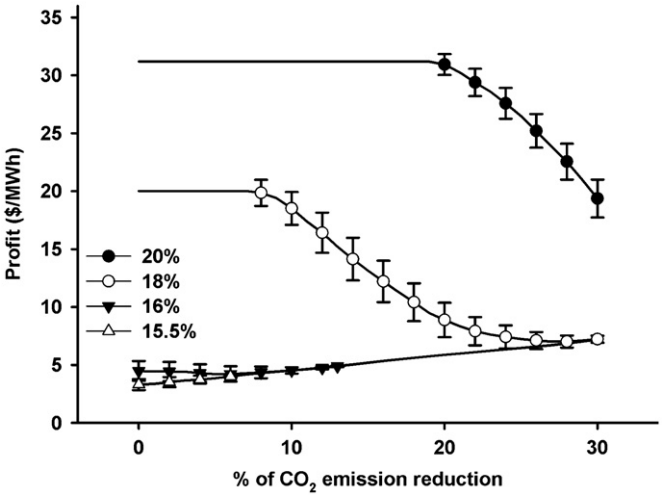

Fig. 7. Per MWh profits of renewables when altering the CO_2 requirements.

4.7. Policy redundancy

While there might be various definitions of policy redundancy, we refer in the current context as the implementation of or tightening in one policy will weaken the underlying mechanisms of the other policies to meet their intended policy targets. The numerical results suggest that the co-existence of the RPS and C&T policies would lead to such phenomena. In particular, a ramp-up of the RPS level would effectively subsidize renewable producers and penalize fossil fuel producers. The changes in the relative cost structure will result in a different generation mixture, reducing the total emission, and lowering the permit prices. To the extreme, even if the intended emissions reduction is attained, the C&T emission policy could be so ineffective that results in a zero permit price. For example, Fig. 4 (left) shows that the CO_2 permit prices continuously plunge as RPS percentage increases. When the RPS is greater than 23% (not shown) for the CO_2 reduction equal to 30%, the permit price crashes to zero. The reverse could be true for the REC price when lowering the C&T emission cap.

5. Conclusion and discussion

Choices of policy instruments on emissions reduction have a profound impact on regulated industries and the environment. This paper explores the policy implications in a situation at which two policies—the renewable portfolio standards (RPS) and the emissions trading (C&T)—co-exist in a competitive electricity market. We apply a theoretical analysis to obtain general results. A case analysis based upon the California electricity market in 2007 is used to illustrate the main findings. We take advantage of the available data, and model uncertain wind output using its empirical cumulative density functions. We find that making either the RPS or the C&T policies more stringent would weaken the market incentives created by the other policy. Therefore, one policy may become redundant. Changes of the policy parameters associated with the RPS and C&T impact the profits earned by various fuel types differently. More specifically, lowering the CO_2 cap, while benefiting natural gas units, it may unintentionally penalize renewable producers by reducing the subsidies they receive from RECs sales. On the other hand, increasing the RPS requirement could sometimes benefit coal and oil units and hurt natural gas units.

Although this study advances the methodology by modeling uncertain wind output with a spinning reserve market, it has a few limitations worth noting. First, we ignore transmission network. Transmission congestion might greatly alter producers outputs and profits because the equilibrium electricity prices

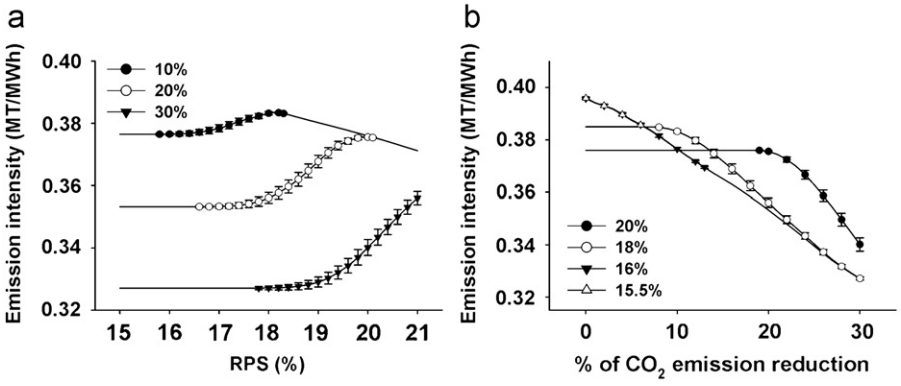

Fig. 8. Average emission intensity when altering the RPS levels (left) and the CO_2 reduction levels (right). (a) RPS and (b) CO_2 emissions cap.

Please cite this article as: Tsao, C.-C., et al., When renewable portfolio standards meet cap-and-trade regulations in the electricity sector: Market interactions, profits implications, and policy redundancy. Energy Policy (2011), doi:10.1016/j.enpol.2011.01.030

might change. Second, the ability to bank or borrow emissions permits or other price-containment provisions such as price ceiling or floor might effectively soften or even reverse the impacts. Finally, if the industry can quickly respond to the price signals, e.g. permit or REC prices, by introducing new generating capacity, it might either amplify or diminish the impacts. We leave consideration of these factors to our future research.

References

Amundsen, E.S., Mortensen, J.B., 2001. The danish green certificate system: some simple analytical results. Energy Economics 23, 489–509.

Bird, L.A., Holt, E., Carroll, G.L., 2008. Implications of carbon cap-and-trade for US voluntary renewable energy markets. Energy Policy 36, 2063–2073.

Bohringer, C., Rosendahl, K.E., 2010. Green promotes the dirtiest: on the interaction between black and green quotas in energy markets. Journal of Regulatory Economics 37, 316–325.

Bushnell, J., 2007. Oligopoly equilibria in electricity contract markets. Journal of Regulatory Economics 32, 225–245.

California Independent System Operator (CAISO), 2009. ISO Balancing Authority Area Hourly Wind Generation Data for 2009, CAISO, Folsom, CA. 〈www.caiso.com/2747/274778eb12970ex.html〉.

California Energy Commission (CEC), 2010. California Electrical Energy Generation. CEC, Sacramento, CA. 〈energyalmanac.ca.gov/electricity/electricitygeneration.html〉.

Chen, Y., Hobbs, B.F., 2005. An oligopolistic power market model with tradable NOx permits. IEEE Transactions on Power System 20, 119–129.

De Jonghe, C., Delarue, E., Belmans, R., D'Haeseleer, W., 2009. Interactions between measures for the support of electricity from renewable energy sources and CO_2 mitigation. Energy Policy 37, 4743–4752.

Doris, E., McLaren, J., Healey, V., Hockett, S., 2009. State of the States 2009: Renewable Energy Development and the Role of Policy. NREL, Golden, CO.

Energy Information Administration (EIA), 2010. California Renewable Electricity Profile. EIA, Washington, DC. 〈www.eia.gov/cneaf/solar.renewables/page/stateprofiles/california.html〉.

Federal Energy Regulatory Commission (FERC), 2010. California Electric Market: Overview and Focal Points. FERC, Washington, DC. 〈www.ferc.gov/market-oversight/mkt-electric/california.asp〉.

Fischer, C., 2010. Renewable portfolio standards: when do they lower energy prices? Energy Journal 31, 101–119.

Gillenwater, M., 2008a. Redefining RECs — part 1: untangling attributes and offsets. Energy Policy 36, 2109–2119.

Gillenwater, M., 2008b. Redefining RECs — part 2: untangling certificates and emission markets. Energy Policy 36, 2120–2129.

Hindsberger, M., Nybroe, M.H., Ravn, H.F., Schmidt, R., 2003. Co-existence of electricity TEP and TGC markets in the Baltic sea region. Energy Policy 31, 85–96.

International Energy Agency (IEA), 2004. Renewable Energy — Market and Policy Trends in IEA Countries. Head of Publications Service, OECD, Paris. 〈www.iea.org/textbase/nppdf/free/2004/renewable1.pdf〉.

Jensen, S.G., Skytte, K., 2002. Interactions between the power and green certificate markets. Energy Policy 30, 425–435.

Linares, P., Santos, F.J., Ventosa, M., 2008. Coordination of carbon reduction and renewable energy support policies. Climate Policy 8, 377–394.

Mozumder, P., Marathe, A., 2004. Gains from an integrated market for tradable renewable energy credits. Ecological Economics 49, 259–272.

Nielsen, L., Jeppesen, T., 2003. Tradable green certificates in selected european countries — overview and assessment. Energy Policy 31, 3–14.

National Renewable Energy Laboratory (NREL), 2007. National Solar Radiation Database 1991–2005 Update: Users Manual NREL, Golden, CO. 〈rredc.nrel.gov/solar/olddata/nsrdb/1991-2005/〉.

National Renewable Energy Laboratory (NREL), 2010. Energy Technology Cost and Performance Data. NREL, Golden, CO. 〈www.nrel.gov/analysis/techcosts.html〉.

Unger, T., Ahgren, E.O., 2005. Impacts of a common green certificate market on electricity and CO_2-emission markets in the nordic countries. Energy Policy 33, 2152–2163.

Please cite this article as: Tsao, C.-C., et al., When renewable portfolio standards meet cap-and-trade regulations in the electricity sector: Market interactions, profits implications, and policy redundancy. Energy Policy (2011), doi:10.1016/j.enpol.2011.01.030